DANMARKS OG GRØNLANDS GEOLOGISKE UNDERSØGELSE **RAPPORT 2020/22**

Thermo-tectonic history of northern East Greenland (Wandel Sea Basin), Svalbard and the Barents Sea

Final report to Equinor

Paul F. Green & Peter Japsen

GEOLOGICAL SURVEY OF DENMARK AND GREENLAND
DANISH MINISTRY OF CLIMATE, ENERGY AND UTILITIES

G E U S

Thermo-tectonic history of northern East Greenland (Wandel Sea Basin), Svalbard and the Barents Sea

Final report to Equinor

Paul F. Green[1] & Peter Japsen[2]

[1]Geotrack International, Australia

[2]Geological Survey of Denmark and Greenland (GEUS)

Confidential report

Copy No.

Released 01.09.2025

GEOLOGICAL SURVEY OF DENMARK AND GREENLAND
DANISH MINISTRY OF CLIMATE, ENERGY AND UTILITIES

G E U S

Contents

Summary

Here we present a study of the thermo-tectonic evolution of the Wandel Sea Basin (North Greenland) and Svalbard and the implications for the development of the Barents Sea (Fig. *i*). Apatite fission-track analysis (AFTA) data reveal a long history of burial and exhumation across the study area since the late Palaeozoic: Six episodes of cooling were identified in overlapping time intervals, while one episode was only identified in the Wandel Sea Basin and one only on Svalbard (Figs *ii*, *iii*). As the cooling episodes correlate with unconformities, we conclude that they represent periods of exhumation.

Mid-Carboniferous cooling (onset 326–320 Ma) correlates with the unconformities between the Billefjorden and Gipsdalen Groups at ~325 Ma in Svalbard and between the Sortebakker and Kap Jungersen Formations in North Greenland.
Late Triassic cooling (onset 234–229 Ma) correlates with base-Carnian (~235 Ma) unconformities in Svalbard and North Greenland. In Svalbard, that timing corresponds to the transition between the Sassendalen and Kap Toscana Groups. In North Greenland, it corresponds to a marked erosional, base-Carnian unconformity within the Storekløft Formation on Peary Land.
Jurassic cooling (onset 173–150 Ma) overlaps with a well-defined hiatus in the stratigraphic record in both regions. On Svalbard, it corresponds to stratigraphic gap of Aalenian–Bajocian age, near the top of the Kapp Toscana Group. In North Greenland, it corresponds to the gap at the base of the Ladegårdsåen Formation in Peary Land. We interpret the Jurassic cooling to represent denudation that began at the Early – Middle Jurassic transition, at ~175 Ma.
Mid-Cretaceous cooling (onset 118–95 Ma) overlaps with the late Albian – Maastrichtian gap in the stratigraphic record on Svalbard and with the Aptian – mid-Turonian gap in North Greenland below the Herlufsholm Stand Formation on Peary Land. The stratigraphic record thus indicates that the exhumation in both parts of the study area took place during the late Albian – mid-Turonian (about 105 – 92 Ma).
Maastrichtian cooling (onset 72–65 Ma), recognized in AFTA data from samples across a wide part of Svalbard, corresponds to the base-Paleocene unconformity in the Central Tertiary Basin (Fig. *iv*). Late Maastrichtian uplift and erosion followed by Paleocene subsidence and burial was also widespread across the Canadian Arctic. The data from North Greenland do not resolve definite evidence of Maastrichtian cooling. However, a significant hiatus separates the youngest, well-dated Upper Cretaceous sediments of Santonian age from late Paleocene deposits in Kronprins Christian Land.
Mid-Paleocene cooling (onset 60–57 Ma) is documented by the AFTA data from the Wandel Sea Basin, based on samples that are localised within the fault zones in a belt along the coastline (Fig. *iv*). Integration of AFTA and VR data along these fault zones indicate that exhumation in this episode defines the timing of the compressional event that caused folding and thrusting of Upper Cretaceous and older sediments within these fault zones.
End-Eocene cooling (onset ~35 Ma) is documented by the AFTA data from the Palaeogene successions on Svalbard and in North Greenland as well as in older units (Fig. *v*), and it correlates with the post-Eocene unconformity in both areas. This phase of exhumation thus constrains the age of the youngest Palaeogene sediments on Svalbard (e.g. the Aspelintoppen Formation) to be Priabonian or older.

Late Miocene cooling (~10 Ma) corresponds to the wide hiatus between Palaeogene and glacial sedimentary units exposed in both parts of the study area. This cooling episode correlates closely with the age of the late Miocene basalts (Seidfjellet Formation) that occur on northern Spitsbergen, possibly an indicator of tectonic activity.

The Paleocene–Eocene convergence between Greenland, the Canadian Arctic and Svalbard resulted in the compressional tectonics in the High Arctic, collectively known as the **Eurekan Orogeny** (Kronprins Christian Land Orogeny in North Greenland and the West Spitsbergen Fold Belt on Svalbard). The mid-Paleocene inversion of the major fault zones of the Wandel Sea Basin began after the onset of seafloor spreading west of Greenland that led to the convergence between Greenland and the High Arctic and thus represents the first phase of the Eurekan Orogeny. Regional end-Eocene exhumation took place after the cessation of sea-floor spreading west of Greenland and thus represents post-Eurekan tectonics. This episode also coincides with an important phase of plate reorganization in North-East Atlantic and with episodes of uplift and erosion that affected East and West Greenland, far from the Eurekan Orogen. How the regional Maastrichtian exhumation relates to the Eurekan Orogeny is not clear, but since it pre-dates the onset of break-up west of Greenland it clearly pre-dates the onset of the Eurekan Orogeny proper. There is, however, an overlap between the Arctic areas affected by the Maastrichtian event and those affected by the Eurekan Orogeny, even though the Maastrichtian event appears to have affected a much wider region. It is thus possible that it may represent a precursor event prior to the onset of the more focused effects of the Eurekan Orogeny.

AFTA data in samples from the **Sysselmannbreen** and **Reindalspasset** boreholes on Spitsbergen define three episodes of cooling which correlate closely with the Maastrichtian, end-Eocene and late Miocene episodes defined in the outcrop samples in this study. In the **Sysselmannbreen** borehole, the Maastrichtian episode is recorded in samples of Palaeogene depositional ages and is interpreted to represent pre-depositional cooling in sedimentary provenance terrains, while Eocene and Miocene cooling episodes are post-depositional. Maximum post-depositional palaeotemperatures derived from VR data are consistent with the Eocene palaeotemperatures derived from AFTA data at similar depths, and the combined dataset can be described by a linear profile, sub-parallel to the present-day temperature profile but offset to higher temperatures by 80–90°C. Miocene palaeotemperatures defined by AFTA can also be described by a similar profile but offset by ~50°C from the present-day temperature profile. In samples of Carboniferous to Early Cretaceous depositional ages analysed from the **Reindalspasset** borehole the Maastrichtian, Eocene and Miocene cooling episodes are all post-depositional. The maximum post-depositional palaeotemperatures derived from VR data are consistent with the Maastrichtian palaeotemperatures derived from AFTA data at similar depths, and again, the combined dataset can be described by a linear profile, sub-parallel to the present-day temperature profile but offset to higher temperatures by ~120°C. Eocene and Miocene palaeotemperatures defined by AFTA can also be described by similar profiles but offset by ~70°C and ~45°C, respectively, from the present-day temperature profile. For both boreholes, these profiles suggest an explanation in terms of heating and cooling largely by deeper burial and exhumation.
Analysis of the palaeotemperature profiles defined from AFTA and VR data in these boreholes, indicate that the range of allowed palaeo-gradients in each episode encompasses the present-day thermal gradient (30°C/km for Sysselmannbreen, 28°C/km for

Reindalspasset). This suggests that an interpretation involving heating due to deeper burial and subsequent cooling due to exhumation provides an acceptable explanation of the palaeotemperature constraints. Based on the analysis of the palaeogeothermal gradients in the boreholes, the amount of additional burial in the Syssellmannbreen borehole is estimated to be 2.1 and 1.5 km, for the end-Eocene and late Miocene episodes, respectively, and in the Reindalspasset borehole to 4.1, 2.1 and 1.2 km, for Maastrichtian, end-Eocene and late Miocene episodes, respectively. Reconstructed burial/uplift histories for these boreholes, are illustrated in Figure *vi* for a scenario that involves an arbitrary amount of re-burial between the three exhumation events.

Figure *vii* compares the timing of the episodes of cooling defined in this study with similar events in **North-East Greenland** and **southern Scandinavia** that were also defined by AFTA data in previous studies. In southern Scandinavia, **Late Carboniferous, Middle Triassic and mid-Jurassic** events of uplift and erosion were important for the development of the southern Baltic Shield and beyond that region and were interpreted as epeirogenic uplifts accompanying fragmentation of Pangaea (Japsen *et al.* 2016). In North-East Greenland, three episodes of uplift and erosion were recently defined that are almost synchronous with those in Scandinavia. The observations from North-East Greenland and southern Scandinavia thus point to common tectonic events in late Paleozoic and early Mesozoic, beginning at ~310, 245 and 175 Ma.

In North Greenland and Svalbard, the timing of late Paleozoic and early Mesozoic episodes of uplift and erosion show broad similarities with those defined further south, but with some variation in timing; i.e. the mid-Carboniferous, Late Triassic and Jurassic episodes. Evidence from the stratigraphic record indicate that these episodes most likely began at ~325, 235 and 175 Ma. Whereas the mid-Jurassic episode thus appears to have affected the entire region from Svalbard to southern Sweden simultaneously, there are time lags for the two earlier episodes across the region. Mid-Carboniferous exhumation affected the northern part of the region about 15 Myr earlier than the late Carboniferous episode in the south, and Late Triassic exhumation affected the northern region about 10 Myr later than the Middle Triassic episode further south. It is not clear whether the time lag from north to south between these episodes reflect propagation of the underlying processes or a manifestation of different tectonic processes.

The onset of the **mid-Cretaceous** episode in this study area correlates closely with episodes in North-East Greenland and southern Scandinavia, indicating that they all reflect a common episode, earliest Late Cretaceous, around 95 Ma (Cenomanian–Turonian). In North-East Greenland, this episode corresponds to an important phase of basin reorganization, and in southern Scandinavia, it represents the inversion of the Sorgenfrei-Tornquist Zone. It is possible that these events are related to a global-scale, mid-Cretaceous phase of plate reorganization.

Late Miocene uplift and erosion affected both parts of our study area as well as West and East Greenland, but a similar phase has not been identified in southern Scandinavia. Both in Greenland and on Svalbard, the late Miocene tectonic phase is manifest in the landscape. Elevated plateaus at 1 km above sea level characterize much of the landscape on Svalbard, representing erosion surfaces which cut across sedimentary rocks of Palaeogene and older age as well as across metamorphic rocks. Remnants of late Miocene lavas (the Seidfjellet Fm) rest on these plateaus. The configuration of these plateaus on Svalbard thus appears to be comparable to that in East Greenland, where mid-Miocene basalts rest on

the regional peneplain, the Upper Planation Surface. This indicates that this surface had been formed by mid-Miocene times, after it had been graded to the baselevel of the Atlantic Ocean following end-Eocene uplift and erosion, and subsequently raised to its present elevation after uplift that began in the late Miocene. Given the synchroneity of uplift episodes in North and East Greenland and Svalbard at 35 and 10 Ma, it therefore seems likely that a similar sequence of events shaped the basalt-covered plateau in northern Svalbard.

The continental outliers at the **Morris Jesup Rise and the Yermak Plateau** most likely experienced the phase of exhumation that affected Peary Land at ~35 Ma as they were located north of Peary Land at that time. As the Fram Strait most likely opened in the early Miocene, it is therefore possible that an erosion surface developed across these continental outliers after end-Eocene exhumation, similar to the elevated plateaus in North-East Greenland and on Svalbard. Such a scenario may explain the flat topography across these features, with the notable difference that the erosion surface across Morris Jesup Rise and the Yermak Plateau subsided below sea level after its formation, whereas the correlative surfaces in Greenland and Svalbard were uplifted after 10 Ma.

The timing of the three phases of exhumation defined from AFTA in **Barents Sea** wells are very similar to the phases of exhumation defined in North Greenland and Svalbard in this study. Exhumation beginning at 40–30 Ma and between 10 and 5 Ma closely match the end-Eocene (~35 Ma) and Miocene (11–9 Ma) episodes. Recognition of these three episodes highlights the limitations of attempting to define the timing of exhumation from geological evidence alone, because the sediment packages from earlier episodes will have been disrupted and possibly removed during later phases.
In previous studies, we have assumed that the earliest of the three Cenozoic episodes of exhumation in the Barents Sea represented a similar regional event at ~60 Ma, synchronous with other events around this time in other areas (Green & Duddy 2010). However, based on the results of this study it seems more likely that this episode in the Barents Sea was slightly earlier, representing the effects of the event responsible for the base-Paleocene unconformity on Svalbard, attributed to regional Maastrichtian exhumation.
The scale of all three events defined across Svalbard and the Barents Sea suggests that they are controlled by plate tectonic forces. This is important to consider in basin modelling studies and attempts to predict patterns of hydrocarbon prospectivity because such studies often tend to seek local influences on the thermal history related to well-understood processes (e.g. localized inversion), which drastically underestimate the amount of heating and cooling which have affected the section. This problem is further compounded by the realization that prior to the onset of exhumation, the section that was removed must previously have been deposited. Thus, the controlling processes produce both positive and negative vertical motions, and this aspect is rarely considered in such studies.

In this study, we have defined a series of distinct palaeo-thermal episodes, of both local and regional extent across North Greenland and Svalbard. The magnitude of each episode varies significantly from place to place, resulting in a complex variation in thermal history across the study area, and this is likely to also apply to adjacent areas. Some effects can be interpreted in terms of inversion related to compression during the onset of the Eurekan Orogeny, but other events are recognized over vast areas, and the mechanisms responsible are as yet little understood.

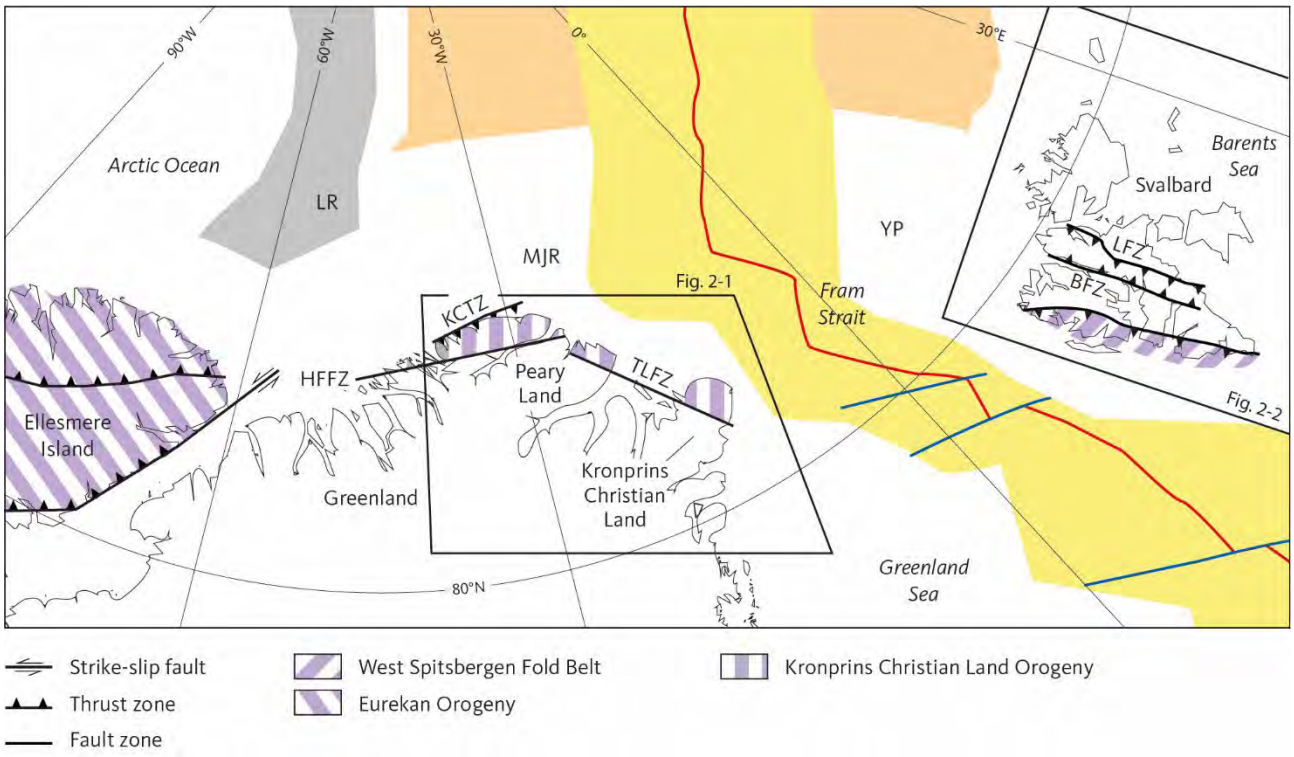

Figure *i*. Present-day outline of the High Arctic around northern Greenland. Based on Japsen *et al.* (2020a) with modifications from von Gosen & Piepjohn (2003), Oakey & Chalmers (2012) and Piepjohn *et al.* (2015). Outline of the Kronprins Christian Land Orogeny after Håkansson & Pedersen (2001) and Japsen *et al.* (2020a). Orange: Oceanic crust, 55–35 Ma. Yellow: Oceanic crust, younger than 35 Ma. **BFZ:** Billefjorden Fault Zone. **HFFZ**: Harder Fjord Fault Zone. **KCTZ**: Kap Cannon Thrust Zone. **LFZ**: Lomfjorden Fault Zone. **LR**: Lomonosov Ridge. **MJR**: Morris Jesup Rise. **TLFZ**: Trolle Land Fault Zone. **YP**: Yermak Plateau.

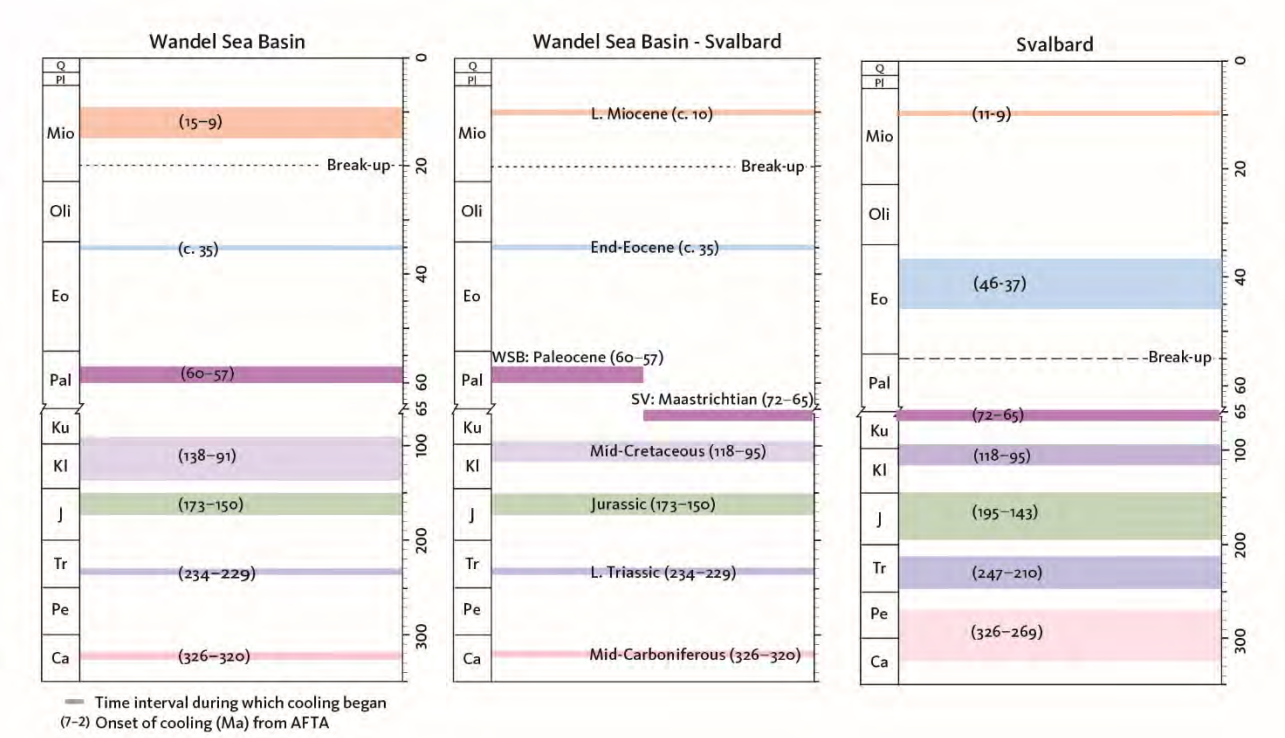

Figure *ii*. Onset of cooling episodes defined from AFTA. **Left**: Wandel Sea Basin (WSB). **Centre**: Overlap between the Wandel Sea Basin and Svalbard, **Right**: Svalbard (SV).

Figure *iii*. Comparison between the regional cooling episodes from AFTA and the stratigraphy for the Wandel Sea Basin and Svalbard. The vertical extent of the horizontal, coloured bars indicates the uncertainty for the onset of the cooling episode.
(Next page)

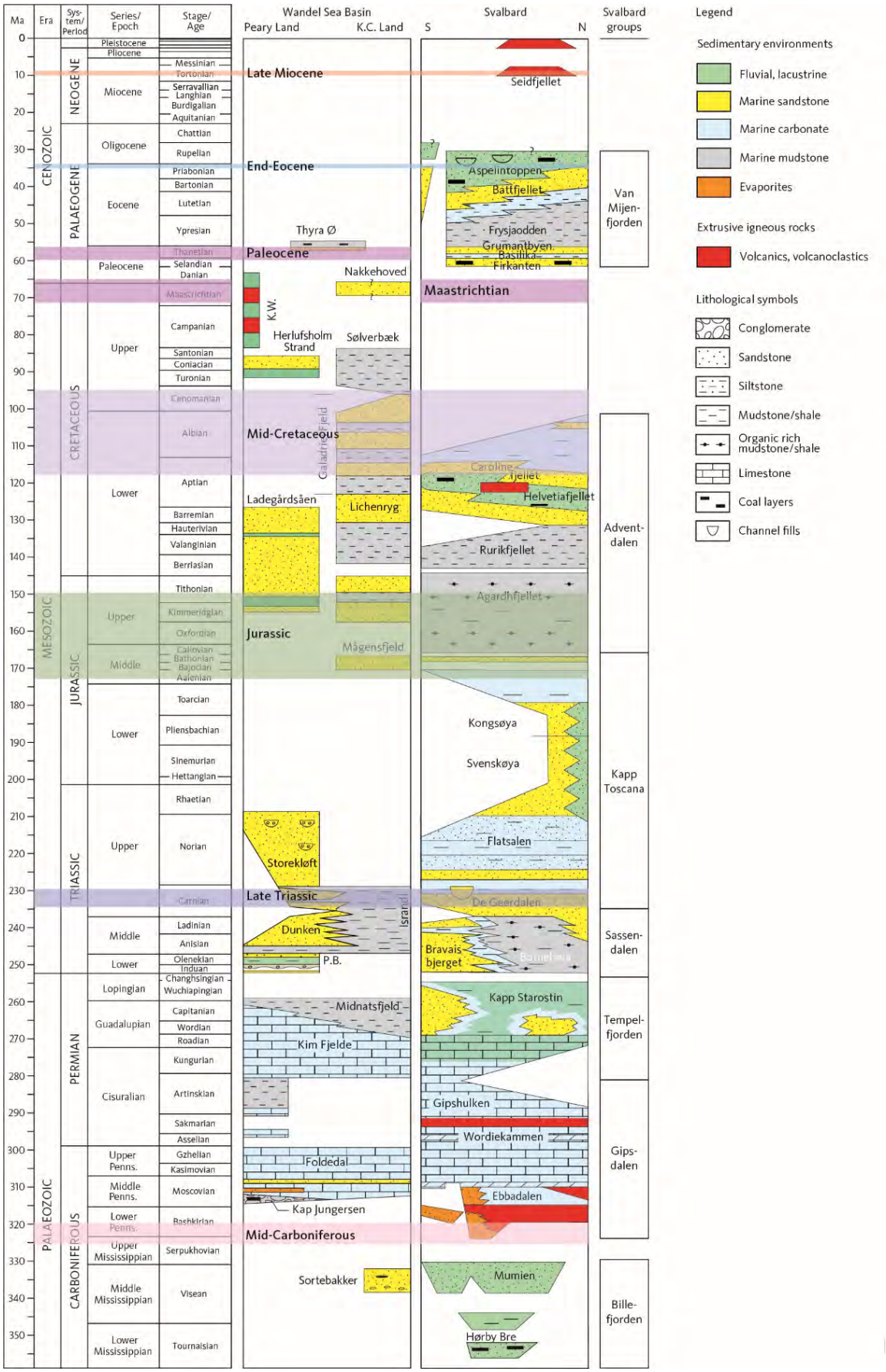
Ma
Era
System/ Period
Series/ Epoch
Stage/ Age
Wandel Sea Basin
Peary Land
K.C. Land
Svalbard
S
N
Svalbard groups
Legend
Sedimentary environments
Fluvial, lacustrine
Marine sandstone
Marine carbonate
Marine mudstone
Evaporites
Extrusive igneous rocks
Volcanics, volcanoclastics
Lithological symbols
Conglomerate
Sandstone
Siltstone
Mudstone/shale
Organic rich mudstone/shale
Limestone
Coal layers
Channel fills
CENOZOIC
MESOZOIC
PALAEOZOIC
NEOGENE
PALAEOGENE
CRETACEOUS
JURASSIC
TRIASSIC
PERMIAN
CARBONIFEROUS
Pleistocene
Pliocene
Miocene
Oligocene
Eocene
Paleocene
Upper
Lower
Middle
Messinian
Tortonian
Serravallian
Langhian
Burdigalian
Aquitanian
Chattian
Rupelian
Priabonian
Bartonian
Lutetian
Ypresian
Thanetian
Selandian
Danian
Maastrichtian
Campanian
Santonian
Coniacian
Turonian
Cenomanian
Albian
Aptian
Barremian
Hauterivian
Valanginian
Berriasian
Tithonian
Kimmeridgian
Oxfordian
Callovian
Bathonian
Bajocian
Aalenian
Toarcian
Pliensbachian
Sinemurian
Hettangian
Rhaetian
Norian
Carnian
Ladinian
Anisian
Olenekian
Induan
Lopingian
Guadalupian
Cisuralian
Changhsingian
Wuchiapingian
Capitanian
Wordian
Roadian
Kungurian
Artinskian
Sakmarian
Asselian
Upper Penns.
Middle Penns.
Lower Penns.
Gzhelian
Kasimovian
Moscovian
Bashkirian
Serpukhovian
Visean
Tournaisian
Upper Mississippian
Middle Mississippian
Lower Mississippian
Late Miocene
End-Eocene
Paleocene
Maastrichtian
Mid-Cretaceous
Jurassic
Late Triassic
Mid-Carboniferous
Thyra Ø
Nakkehoved
K.W.
Herlufsholm Strand
Sølverbæk
Galadriefjeld
Ladegårdsåen
Lichenryg
Mågensfjeld
Storekløft
Dunken
P.B.
Israndl
Midnatsfjeld
Kim Fjelde
Foldedal
Kap Jungersen
Sortebakker
Seidfjellet
Aspelintoppen
Battfjellet
Frysjaodden
Grumantbyen
Basilika
Firkanten
Caroline fjellet
Helvetiafjellet
Rurikfjellet
Agardhfjellet
Kongsøya
Svenskøya
Flatsalen
De Geerdalen
Bravais bjerget
Kapp Starostin
Gipshulken
Wordiekammen
Ebbadalen
Mumien
Hørby Bre
Van Mijen-fjorden
Advent-dalen
Kapp Toscana
Sassen-dalen
Tempel-fjorden
Gips-dalen
Bille-fjorden

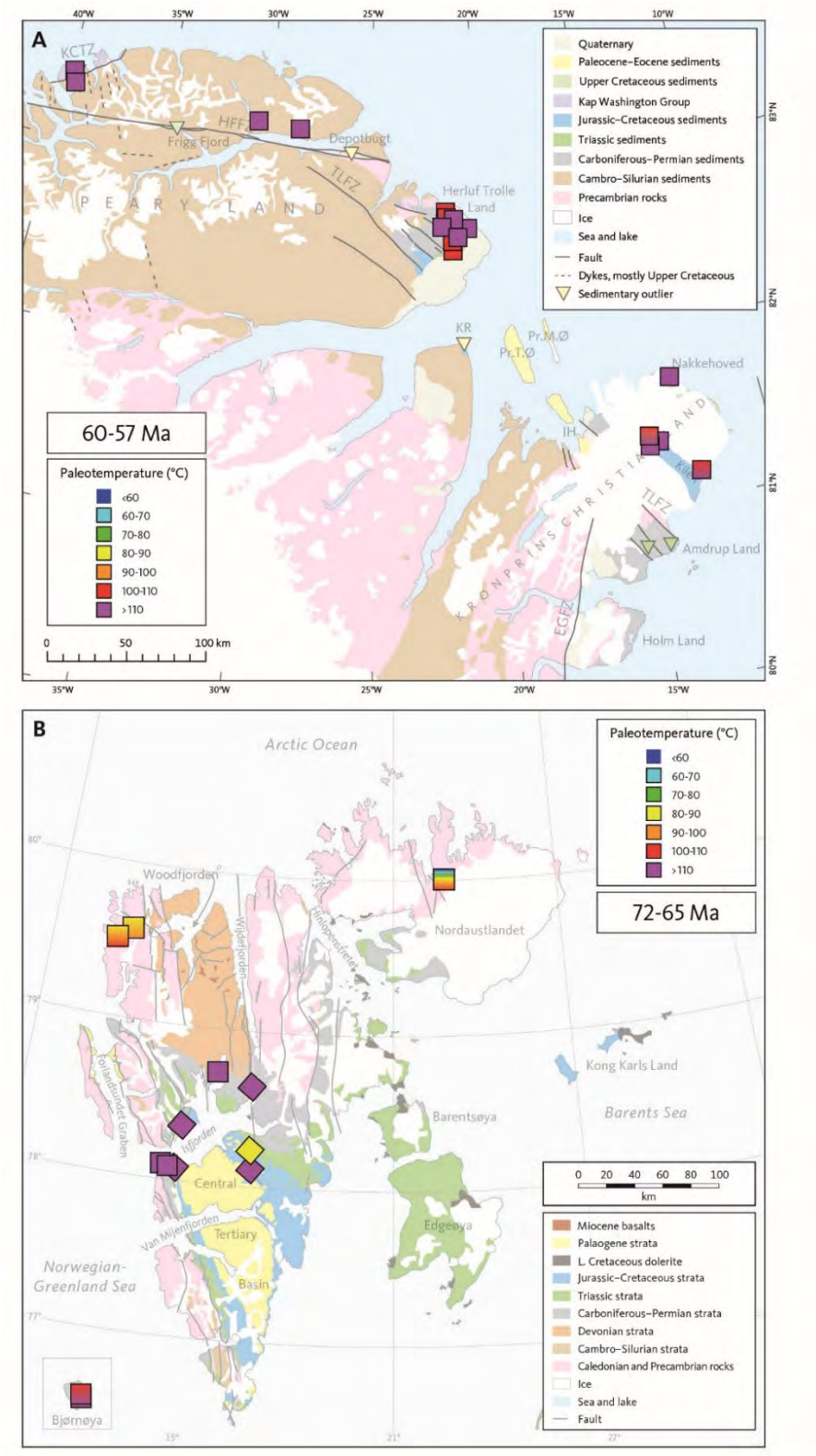

Figure *iv*. Paleotemperatures derived from AFTA data in outcrop samples. **A**. North Greenland, mid-Paleocene (60–57 Ma). **B**. Svalbard, Maastrichtian (72–65 Ma). Note that these time intervals do not overlap, thus indicating cooling during two different episodes. **Squares**: Values from AFTA. **Diamonds**: values from VR.

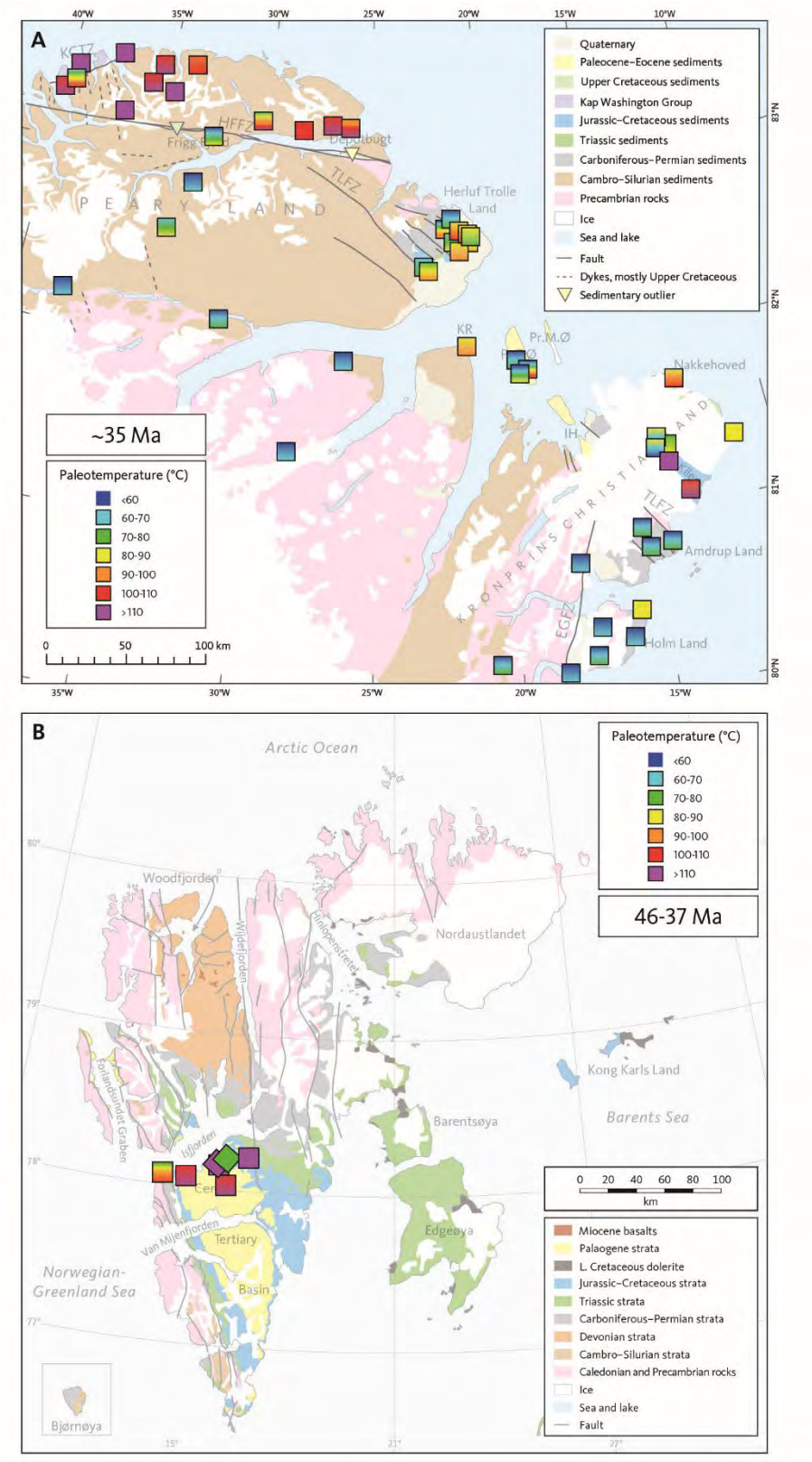

Figure. *v*. **End-Eocene (~35 Ma)** palaeotemperatures derived from AFTA data in outcrop samples. **A**. North Greenland. **B**. Svalbard. The timing constraint in one Svalbard sample regarded as a statistical outlier. **Squares**: Values from AFTA. **Diamonds**: Values from VR.

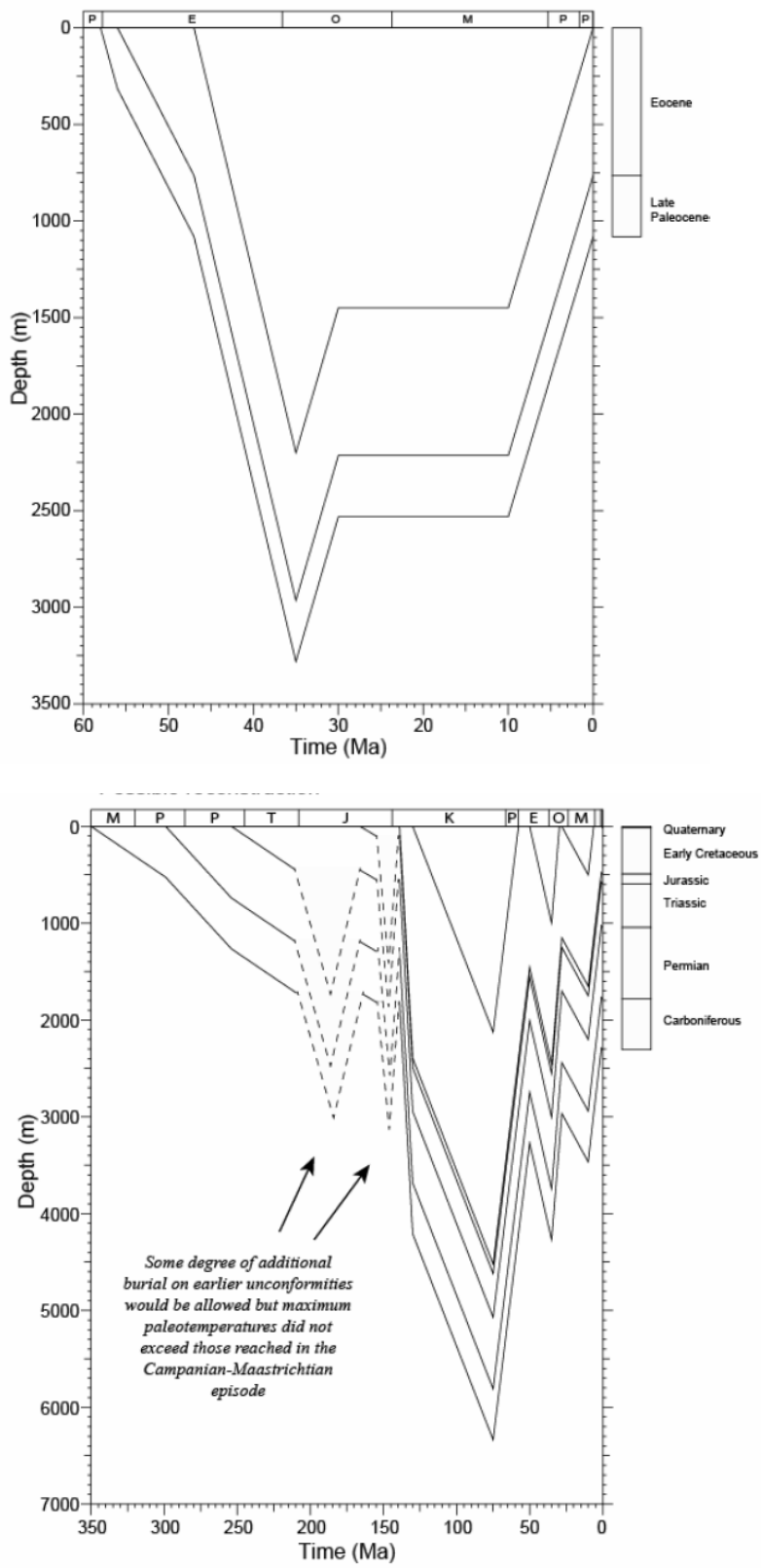

Figure *vi*. Reconstructed burial/uplift histories **Upper**: Syssellmannbreen. Additional burial 2.1 and 1.5 km, end-Eocene and late Miocene, respectively. **Lower**: Reindalspasset. Additional burial 4.1, 2.1 and 1.2 km, Maastrichtian, end-Eocene and late Miocene, respectively

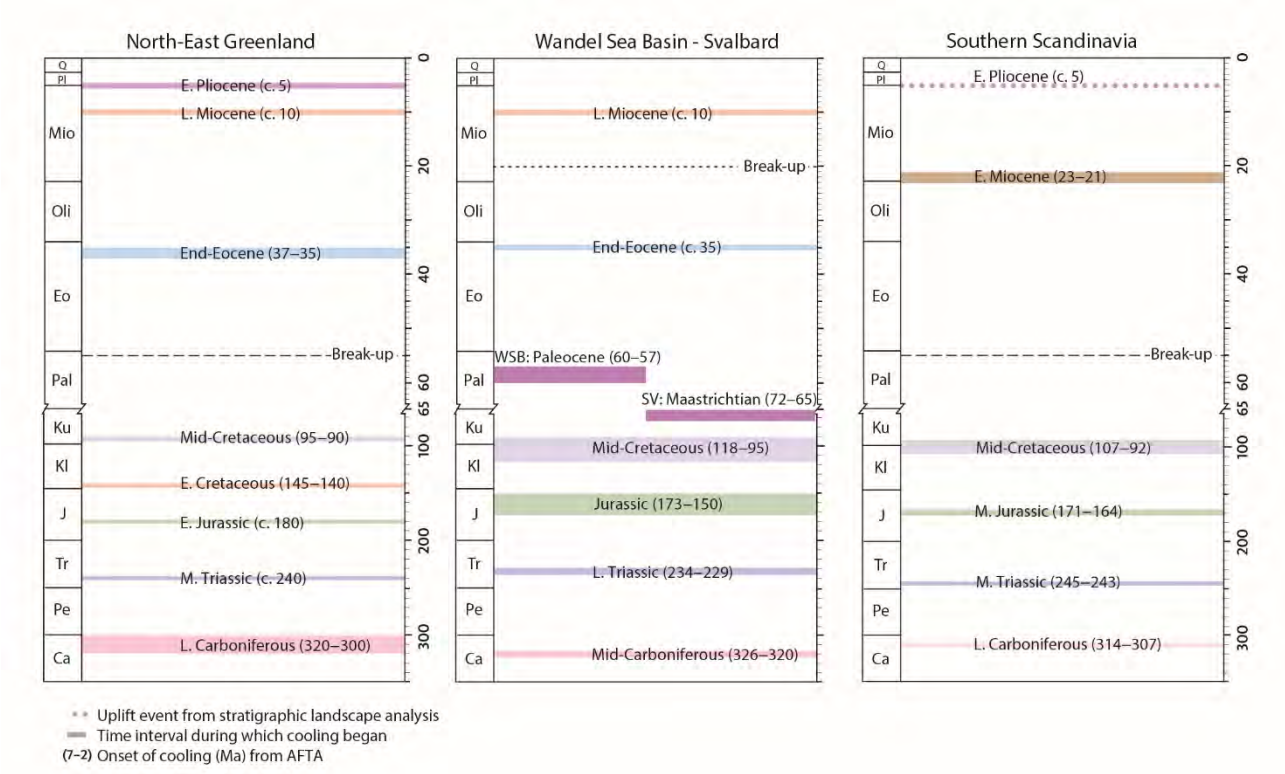

Figure *vii*. Comparison of the timing of regional, post-Devonian episodes of uplift and erosion estimated from AFTA data. **Left**: North-East Greenland (Japsen *et al.* 2020b). **Centre**: Wandel Sea Basin and Svalbard (Fig. *iii*). **Right**: Southern Scandinavia (Japsen *et al.* 2007, 2016, 2018). Break-up west of Greenland took place in mid-Paleocene (~62 Ma), but seafloor spreading ceased there by the end of the Eocene in contrast to the opening of the NE Atlantic, east of Greenland, which began at the Paleocene–Eocene transition (~56 Ma) and is still ongoing (Chalmers and Pulvertaft 2001; Oakey and Chalmers 2012; Gaina *et al.* 2017). The Fram Strait between Greenland and Svalbard opened in early Miocene (~20 Ma; Jokat *et al.* 2016; Dumais *et al.* (2020). **L**: Late. **E**: Early. **M**: Mid. **C**: Carboniferous. **Pe**: Permian. **Tr**: Triassic. **J**: Jurassic. **Kl**: Lower Cretaceous. **Ku**: Upper Cretaceous. **Pal**: Paleocene. **Eo**: Eocene. **Oli**: Oligocene. **Mio**: Miocene. **Pl**: Pliocene. **Q**: Quaternary. **SV**: Svalbard. **WSB**: Wandel Sea Basin.

1. Introduction

The Carboniferous to Palaeogene basins in Svalbard and North Greenland (the Wandel Sea Basin) are important pieces in the larger puzzle of Arctic geology (Fig. 1-1). The basins record sedimentation across North Greenland, on the north-western flank of the Danmarkshavn Basin (offshore North-East Greenland), along the north-western part of the Barents Sea, and south of the Cenozoic seafloor spreading in the Eurasian Basin.

Insights into the development of these basins are important for providing a better understanding of the relation between (1) the mid-Paleocene to Eocene movement of Greenland relative to both North America (Oakey & Chalmers 2012) and Eurasia (Gaina *et al.* 2017) and (2) the compressional tectonics in the Wandel Sea Basin (the Kronprins Christian Land Orogeny; Håkansson & Pedersen 2001; 2015), on Svalbard (the West Spitsbergen Fold Belt; Steer *et al.* 1985; Dallmann *et al.* 2015; Jones *et al.* 2017) and in the Carboniferous–Palaeogene Sverdrup Basin in Arctic Canada (the Eurekan Orogeny; Okulitch & Trettin 1991; Embry & Beauchamp 2019).

It is widely accepted that these compressional events, that we will refer to collectively as the Eurekan Orogeny, record the Palaeogene convergence between Greenland, the Canadian Arctic and Svalbard (Fig. 1-2; Steel *et al.* 1985; De Paor *et al.* 1989; Harrison 2008; Oakey & Chalmers 2012; Embry & Beauchamp 2019; Gion *et al.* 2017; Jones *et al.* 2017; Japsen *et al.* 2020a). Some restrict the term “Eurekan Orogeny” to the time span in the Eocene during which Greenland behaved as a separate plate that was able to move independently with respect to both North America and Europe (e.g. Tessensohn & Piepjohn 2000; Piepjohn *et al.* 2016). This definition, however, fails to include the deformations caused by the movement of Greenland during the late Paleocene. Whatever definition is preferred, the precise timing of the Eurekan Orogeny and related events remains a matter of debate. Did tectonism begin around the Cretaceous–Palaeogene boundary (Håkansson & Pedersen 1982, 2001, 2015) in the Paleocene (Gaina *et al.* 2017; Jones *et al.* 2017; Japsen *et al.* 2020a) or in the Eocene (Tessensohn & Piepjohn 2000; von Gosen & Piepjohn 2003; Piepjohn *et al.* 2016.

The timing and magnitude of exhumation on Svalbard and in the Barents Sea has been extensively studied over the years, with particular emphasis on the Cenozoic history (Manum & Throndsen 1978; Vorren *et al.* 1991; Nyland *et al.* 1992; Riis & Fjeldskaar 1992; Vågnes *et al.* 1992; Løseth *et al.* 1993; Richardsen *et al.* 1993; Blythe & Kleinspehn 1998; Dimakis *et al.* 1998; Skilbrei 1998; Ohm *et al.* 2008; Green & Duddy 2010; Henriksen *et al.* 2011; Dörr *et al.* 2012. 2019, 2019; Marshall *et al.* 2015; Baig *et al.* 2016; Ktenas *et al.* 2017; Barnes & Schneider 2019). To date, only one publication has focussed on the Phanerozoic exhumation history of the Wandel Sea Basin (Japsen *et al.* 2020a).

The study area of this report is the southern margin of the Eurasian Basin that opened along the Gakkel Ridge at ~56 Ma, leaving the Lomonosov Ridge as a sliver of continental crust north of Greenland that rifted from the Barents and Kara shelves (Brozena *et al.* 2003; Døssing et al. 2013; Jokat *et al.* 2016; Knudsen *et al.* 2017). The complex development

along the De Geer Line that formed the plate boundary between North Greenland and Svalbard during Cenozoic strike-slip movement, led to the formation of the Morris Jesup Rise and the Yermak Plateau, which today are located north of Greenland and Svalbard, respectively (Faleide *et al.* 2008; Jokat *et al.* 2016; Kristoffersen *et al.* 2020).

Here we present apatite fission-track analysis (AFTA®) data from the Wandel Sea Basin and Svalbard which shed light on the thermal and tectonic history of the region, both prior to and after the compressional tectonics of the Eurekan Orogeny. For the Wandel Sea Basin, we combine thermal history interpretations from new AFTA data in 16 outcrop samples and new VR data in 3 samples with previously published AFTA data in 46 outcrop samples and VR data (Japsen *et al.* 2020a). For Svalbard, we combine (1) new AFTA data in 10 outcrop samples from the north coast, (2) unpublished AFTA data in 11 outcrop samples from the Isfjorden region and from Bjørnøya, (3) new AFTA and VR in 10 samples from the Reindalspasset and Radderdalen boreholes and (4) new AFTA data in 3 samples and existing VR data from the Sysselmannbreen borehole.

The AFTA data provide definition of the timing and magnitude of key palaeo-thermal episodes (i.e. times at which rocks cooled from higher temperatures compared to present-day values) while the VR data provide independent determination of maximum post-depositional palaeotemperatures. We then relate the thermal history solutions from AFTA and VR data to former depths of burial and corresponding amounts of exhumation and produce a synthesis of the key late Palaeozoic to Cenozoic thermo-tectonic events that have affected the region. We integrate these results with observations from the geological record. Finally, we compare the results of this study with those of a similar studies of North-East Greenland (Japsen *et al.* 2020b), Arctic Canada (Arne *et al.* 1998, 2002), the Lomonosov Ridge (Knudsen *et al.* 2018) and southern Scandinavia (Japsen 2007, 2016, 2018) and set the results in a regional context.

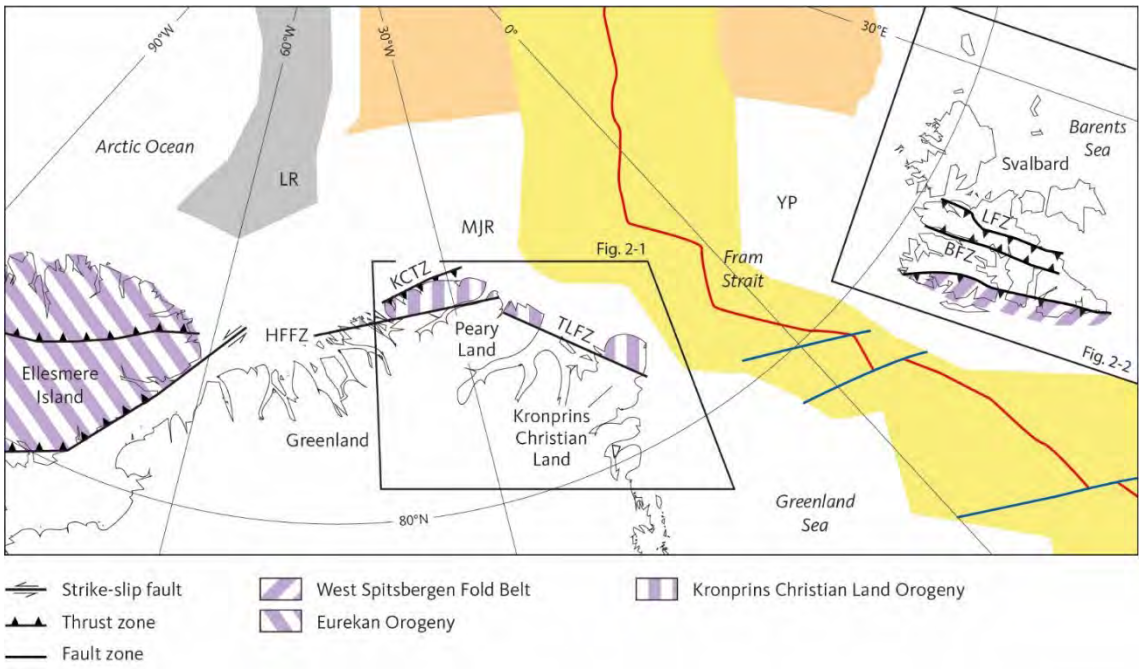

Figure 1-1. Present-day outline of the High Arctic around northern Greenland. Based on Japsen *et al.* (2020a) with modifications from von Gosen & Piepjohn (2003), Oakey & Chalmers (2012) and Piepjohn *et al.* (2015). Outline of the Kronprins Christian Land Orogeny after Håkansson & Pedersen (2001) and Japsen *et al.* (2020a). Orange: Oceanic crust, 55–35 Ma. Yellow: Oceanic crust, younger than 35 Ma. **BFZ:** Billefjorden Fault Zone. **HFFZ**: Harder Fjord Fault Zone. **KCTZ**: Kap Cannon Thrust Zone. **LFZ**: Lomfjorden Fault Zone. **LR**: Lomonosov Ridge. **MJR**: Morris Jesup Rise. **TLFZ**: Trolle Land Fault Zone. **YP**: Yermak Plateau.

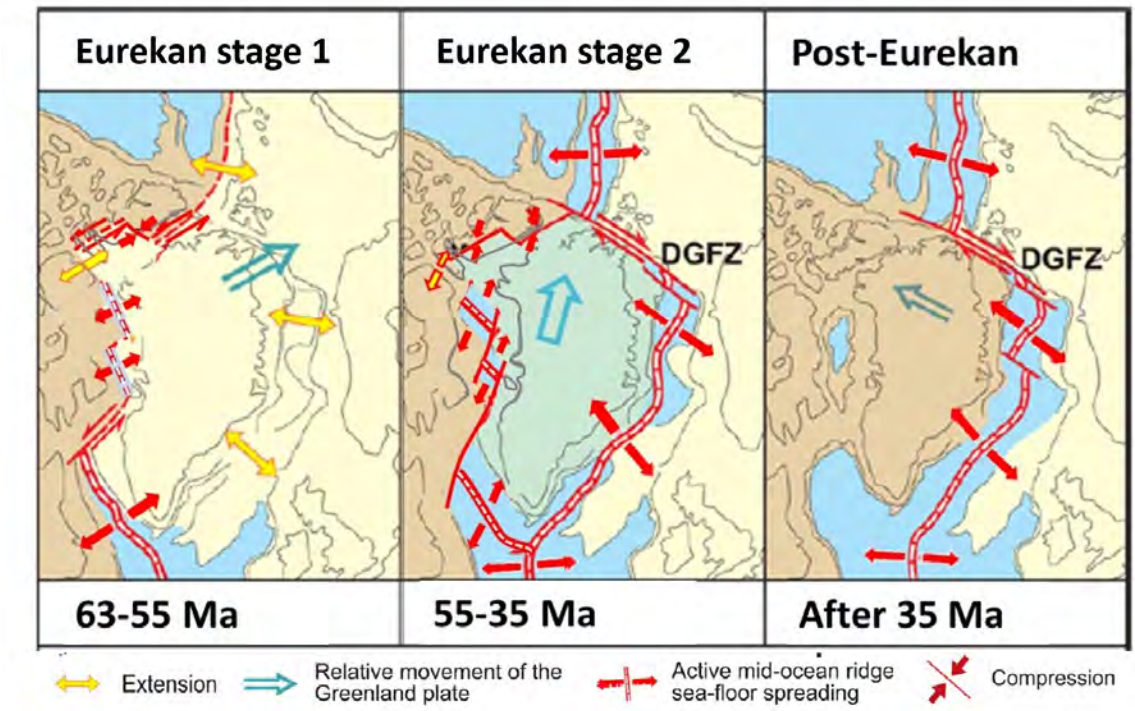

Figure 1-2. Eurekan deformation NE and NW of Greenland following the model for the Paleogene motion of Greenland relative to North America of Oakey & Chalmers (2012). Eurekan stage 1 caused by sea-floor spreading west of Greenland that started in the mid-Paleocene as Greenland and Eurasia moved together until the latest Paleocene. Eurekan stage 2 caused by the combined sea-floor spreading west and east of Greenland as Greenland moved north relative to the Arctic Islands. Spreading between Greenland and North America ceased at the end of the Eocene when Greenland became attached to North America and the Eurekan Orogeny ended. Maps after Piepjohn *et al.* (2016) modified by Japsen *et al.* (2020c). DGFZ: De Geer Fracture Zone.

2. Regional setting

The excellent exposures of the Carboniferous–Palaeogene strata on Svalbard have been studied intensely (Harland 1997; Dallmann *et al.* 2015), whereas it has been difficult to assess the Mesozoic development of the Wandel Sea Basin due to problems in correlating scattered outcrops and due to tectonic overprinting (Håkansson & Pedersen 2001, 2015) (Figs 2-1 to 2-3). However, the basins in Greenland and on Svalbard have a long common history which is particularly well documented based on studies of the Carboniferous–Permian strata (Håkansson & Stemmerik 1989; Stemmerik 2000; Stemmerik & Worsley 2005). Recent studies of the Wandel Sea Basin have improved the possibilities for correlating the Mesozoic strata there with those on Svalbard (Hovikoski *et al.* 2018, Bjerager *et al.* 2019).

East Greenland and Svalbard were affected by the Caledonian Orogeny (Early Ordovician to Early Devonian) which culminated between 420 and 410 Ma (Early Devonian). During the Late Devonian and early Carboniferous, the Ellesmerian Orogeny affected a belt from Ellesmere Island to northern Greenland and Svalbard (where it is called the Svalbardian Event; 370–355 Ma; Dallmann *et al.* 2015).

The Carboniferous–Paleogene Sverdrup Basin of Arctic Canada shares many aspects in common with the basins of North Greenland and Svalbard (Ricketts 1994; Håkansson & Pedersen 2015; Embry *et al.* 2018). The Late Cretaceous to Palaeogene development of the eastern portion of the Sverdrup Basin is particularly important for understanding the Eurekan deformation of the Wandel Sea Basin and the Central Tertiary Basin (CTB) of Svalbard (Ricketts 1994; Piepjohn *et al.* 2016; Embry *et al.* 2018; Embry & Beauchamp 2019).

2.1 The stratigraphic record of the Wandel Sea Basin

Three major fault zones define the structure of the Wandel Sea Basin and are therefore important for understanding the distribution of the sedimentary strata (Fig. 2-1; von Gosen & Piepjohn 2003; Håkansson & Pedersen 2015):

- The SW-NE trending Kap Cannon Thrust Zone (KCTZ) which is exposed over ~75 km in northernmost Peary Land. Ductile thrusting along the KCTZ is dated at between 49 and 47 Ma, based on Ar-Ar dating of volcanic rocks of the Campanian to earliest Paleocene Kap Washington Group (Tegner *et al.* 2011; Thorarinsson *et al*. (2011); Håkansson & Pedersen 2015).
- The E-W trending Harder Fjord Fault Zone (HFFZ), which is more than 300 km long and traverses Peary Land within the metasediments of the Palaeozoic Franklinian Basin. Sediments as young as Late Cretaceous occur within the fault zone.
- The NW-SE trending Trolle Land Fault Zone (TLFZ) which is more than 300 km long and 100 km wide. It traverses from eastern Peary Land to Kronprins Christian Land and consists of a number of linear faults that cut through sediments as young as Late Cretaceous.

Below we summarize key observations regarding the main lithostratigraphic units of the Wandel Sea Based (Fig. 2-3), primarily based on the review presented by Japsen *et al.* (2020a).

2.1.1 Palaeozoic strata

The fluvial deposits of the lower Carboniferous **Sortebakker Formation** (> 1 km) represent the oldest unit of the Wandel Sea Basin. They rest on crystalline basement affected by the Caledonian Orogeny on Holm Land (Stemmerik *et al.* 1998). The upper Carboniferous **Kap Jungersen** and **Foldedal Formations** vary from laterally widespread mixed siliciclastic-limestone cycles to dolomitised limestone. Above a lower Permian hiatus, follows the middle to upper Permian limestones and shales of the **Kim Fjelde** and the **Midnatfjeld Formations**. The upper Permian, fluvial to lacustrine deposits with syndepositional volcanics of the **Kap Kraka Formation** (>1.5 km) are located in the central part of Hyde Fjord, bounded by the faults of the HFFZ and strongly compressed (Håkansson & Pedersen 2015). Unnamed Permian carbonates and deep-marine shales (>2 km) are exposed on Ingeborg Halvø, where they appear as thrust sheets bounded by two of the main faults of the TLFZ (Håkansson & Pedersen 2015).

2.1.2 Mesozoic strata

Bjerager *et al.* (2019) presented a coherent Triassic lithostratigraphy of the Wandel Sea Basin in a biostratigraphic framework that represents a near-complete Triassic succession (~700 m) from the Induan to the Norian. They also presented palaeogeographic maps for the Induan to Carnian of the Wandel Sea Basin and the western Barents Sea including Svalbard, highlighting that the Triassic succession of the Wandel Sea Basin represents a well-constrained shallow shelf to deep shelf / basin floor transect. The basal part of the Early Triassic is fluvial, and the remaining Triassic is marine, with a sand-dominated basin marginal succession to the west and a marine basinal mudstone succession to the east. The succession includes the Lower Triassic **Parish Bjerg Formation** that rests unconformably on upper Permian sediments on Peary Land. The mainly Middle Triassic **Israng Formation** consists of mudstones accumulated in a slope and basin floor setting in the eastern and deeper part of the Wandel Sea Basin at the same time as shallow-marine mudstones of the **Dunken Formation** further west (Alsen *et al.* 2017). A marked erosional unconformity occurs at the base of the Carnian in Herluf Trolle Land with associated marine channel deposits of massive sandstones and conglomerates up to about 50 m thick, which belong to the lower part of the Upper Triassic **Storekløft Formation** (Bjerager *et al.* 2018). The interval is time-equivalent to deltaic mudstones and sandstones with abundant channelised sandy units in the lower part of the De Geerdalen Formation on Svalbard (the Kapp Toscana Group; see below).

A minor outcrop of Middle Jurassic (Bajocian) muddy sandstone occurs within a few square kilometres on central Herluf Trolle Land within a dense fault complex (Håkansson & Pedersen 2015). The Upper Jurassic – Lower Cretaceous mainly marine clastics of the **Ladegårdsåen Formation** (~250 m), with the upper part being non-marine, rest uncon-

formably on Palaeozoic rocks within fault-bounded occurrences across most of the TLFZ on Herluf Trolle Land (Håkansson & Pedersen 2015). The Turonian to Coniacian, fluvial to marginally marine sand-shale series of the **Herlufsholm Strand Formation** (~500 m) crops out on northern Herluf Trolle Land, where they are bounded by the northernmost fault of the TLFZ and rest unconformably on Palaeozoic sediments (Håkansson & Pedersen 2015).

The thickest and stratigraphically most complete Jurassic–Cretaceous sedimentary succession in North Greenland is present in Kilen, Kronprins Christian Land (Hovikoski *et al.* 2018). The Jurassic succession (>500 m) consist of lagoonal and shallow-marine sediments, divided into four formations. The Lower Cretaceous interval (>1500 m) consist of deep shelf to fluvial and shoreface sediments, divided into three formations. The late Cenomanian to Santonian **Sølverbæk Formation** (~650 m) is dominated by marine mudstones and sandstone-mudstones. Intense compressive deformation affected the Mesozoic deposits in Kilen (Pedersen & Håkansson 2001, 2015; Svennevig *et al.* 2016, 2017). The poorly dated, Upper Cretaceous marine sandstone of the **Nakkehoved Formation** (>600 m) crops out on the north coast of Kronprins Christian Land, near the northern margin of the TLFZ (Håkansson & Pedersen 2015). The sandstone is gently folded, but intensely cut by a swarm of mono-mineralic quartz veins in the modestly deformed sandstone.

Unnamed, deep-marine, siliciclastic sediments (>400 m) of Santonian age occur in the Frigg Fjord area, bounded by the HFFZ. Their near-vertical orientation indicates substantial shortening (Håkansson & Pedersen 2015). The sediments are intruded by doleritic dikes and sills of similar composition to the basalts of the Campanian to lowermost Palaeogene **Kap Washington Group**. These intrusions are affected by the deformation along the HFFZ (Paech & Estrada 2018). Further east along the HFFZ, about 500 m of Upper Cretaceous mainly fluvial sandstone occur in the Depotbugt area (Håkansson & Pedersen 2015). Their similarity with the Herlufsholm Strand Formation has been used to infer the age of these sediments.

Volcanic and volcanoclastic rocks interbedded with fluvial and lacustrine deposits of the **Kap Washington Group** (>5 km) occur on the north coast of Peary Land (Håkansson & Pedersen 2015). Most of the volcanics were emplaced at 71–68 Ma but activity continued into the Paleocene (Tegner *et al.* 2011). The deposits, which overlie Palaeozoic strata, are bounded on all sides by the thrusts of the KCTZ, interpreted as reactivated normal faults (Håkansson & Pedersen 2015).

2.1.3 Palaeogene strata

The fine-grained sandstones, siltstones and coal of the **Thyra Ø Formation** that crop out on Prinsesse Thyra Ø, Prinsesse Dagmar Ø, Prinsesse Margrethe Ø and on Prinsesse Ingeborg Halvø are dated as late Paleocene to possibly earliest Eocene age, with an estimated composite thickness of 50 m (Lyck & Stemmerik 2000). Håkansson *et al.* (1991) interpreted the depositional environment as dominantly fluvial, but Lyck & Stemmerik (2000) documented that deposition took place in a marine influenced environment. In contrast to the folded and thrusted Upper Cretaceous and older deposits within the HFFZ and

TLFZ (e.g. in Kilen), the deposits of the Thyra Ø Formation are undeformed (Håkansson & Pedersen 1982, 2015; Boyd *et al.* 1994; Lyck & Stemmerik 2000). However, the base of the Paleocene part of the formation is not known (Lyck & Stemmerik 2000. On Prinsesse Ingeborg Halvø, the Palaeogene deposits are in contact with late Paleozoic sediments along a wide fault zone.

Minor outliers of Palaeogene carbonaceous, terrestrial shales occur in the Depotbugt area near the Upper Cretaceous outcrops (Håkansson & Pedersen 2015; Paech & Estrada 2018). Croxton *et al.* (1980) dated a sparse pollen flora from these deposits as Eocene in age, and Paech and Estrada (2018) noted they were flat-lying. Piasecki *et al.* (2018) identified the upper 5–10 m of the sedimentary section exposed at Kap Rigsdagen to be of early to middle Eocene age and to be part of the Thyra Ø Formation, separated by a 65 Myr hiatus from underlying sediments of Ladegårdsåen Formation. Abundant, reworked Cretaceous dinoflagellate cysts are common in the Thyra Ø Formation (Lyck & Stemmerik 2000; Piasecki *et al.* 2018). Extensive reworking shows that Cretaceous units were exposed and actively eroded during deposition of the Thyra Ø Formation (Piasecki *et al.* 2018).

2.2 The stratigraphic record of Svalbard

Here we summarize key observations regarding the main lithostratigraphic units on Svalbard based on Dallmann *et al.* (2015) – unless otherwise indicated (Figs 2-2, 2-3).

2.2.1 Palaeozoic strata

The Devonian **Andrée Land Group** (>3000 m) contains Old Red Sandstone strata eroded from the Caledonian mountains and were deposited in fault-bounded intra-montane molasse basins. Deposition of conglomerates towards the end of the Devonian records the onset of tectonic activity during the Svalbardian/Ellesmerian Event, which led to folding and thrusting. A pronounced unconformity at the Devonian–Carboniferous transition correlates with the Svalbardian Event. The overlying lower Carboniferous **Billefjorden Group** (<1000 m) contains a succession of conglomerates, sandstones and shales intercalated with coal seams, accumulated on a tectonically unstable shelf during a warm and humid climate. A shift towards semi-arid and arid conditions during the mid-Carboniferous led to the collapse of the ecosystem and a change in the depositional system recorded in the lower part of the lower Carboniferous to lower Permian **Gipsdalen Group** (<1800 m). At the same time, rifting began along pre-existing fault zones (e.g. the **Billefjorden and Lomfjorden Fault Zones**) and led to the formation of horsts and grabens. A significant hiatus (~330–325 Ma), reflecting major regional uplift (Worsley 2008), separates the deposits of the **Billefjorden** and **Gipsdalen Groups**. The Gipsdalen Group contains a succession of basal clastic red beds that pass upwards into evaporites and carbonates. During post-rift subsidence, the depositional environment changed from terrestrial to coastal, then to shallow-marine shelf, and finally, after a global sea-level fall in the early Permian, emergence and karstification of the platforms. A major hiatus (~285 Ma) separates the Gipsdalen Group from the middle to upper Permian **Tempelfjorden Group** (<460 m), consisting mainly of cherts, interbedded

with black shales, limestone successions and sandstone beds deposited in an epicontinental sea.

2.2.2 Mesozoic strata

The Lower to Middle Triassic **Sassendalen Group** (<700 m) contains marine clastics sourced from the west, deposited in a low-relief, fairly deep, boreal shelf embayment with coastal to deltaic sediments along western Spitsbergen. The Upper Triassic to Middle Jurassic **Kapp Toscana Group** (<475 m) records a drastic change in the sedimentation pattern, as the main source of sediments instead came from the newly formed Ural Mountains in the east. The erosional products from the Ural Mountains gradually filled the embayment with thick successions of sandstones and shales and were subsequently reworked under globally rising sea levels. During the latest Triassic to Middle Jurassic, reduced subsidence resulted in condensed deposits and erosive events with non-deposition; e.g. a Rhaetian hiatus within the Kapp Toscana Group on Spitsbergen (~210–200 Ma). The Lower–Middle Jurassic part of the Kap Toscana Group is a continuation of the Upper Triassic inner shelf facies. A Middle Jurassic hiatus (~170 Ma), reflecting uplift and erosion of Svalbard (coeval with uplift in NW Europe; Underhill & Parkington 1993; Japsen *et al.* 2016, 2018) marks the base of the Middle Jurassic to Lower Cretaceous **Adventdalen Group** (<1600 m) which accumulated in an epicontinental basin. Organic-rich mudstone dominates the lower part, whereas the upper part of the group contains a south-eastward prograding wedge of coarse-grained sediments derived from uplifted areas in the north. This wedge was later drowned by a shallow sea.

Igneous rocks of Early Cretaceous age occur in Svalbard and many places along the margins of the Arctic Ocean. Together, they record multiple pulses of igneous activity with peak activity in the Barremian and the Aptian–Albian. Based on their regional extent, it has been suggested that they belong to the High Arctic Large Igneous Province (HALIP) that developed during the opening and development of the Amerasian Basin (Maher 2001). Several hundreds of metres thick igneous sequences and extensive dyke swarms occur in Arctic Canada and Franz Josef Land, and this suggest that Svalbard was located in a more peripheral setting of the HALIP. In Svalbard, the igneous activity is evident through the presence of mafic intrusions and a high content of plagioclase and volcanic rock fragments in the Aptian–Albian Carolinefjellet Formation (attributed to erosion of volcanic terrain north and east of Svalbard), together with flood basalts in Kong Karls Land. Sedimentary strata of Carboniferous to Lower Cretaceous age as well as Precambrian rocks are cut by dolerite sills of Early Cretaceous age.

2.2.3 Cenozoic strata

A major hiatus (~105–62 Ma; Jones *et al.* 2017) separates the Albian deposits of the uppermost part of the Adventdalen Group and the Paleocene strata of the Firkanten Formation, which represents the basal part of the Paleocene–Eocene **Van Mijenfjorden Group** of the CTB (<1900 m). Whereas the Paleocene sequence (Firkanten, Basilika and Grumantbyen Formations) mainly comprises sediments eroded from eastern source areas,

the Eocene deposits (Frysjaodden, Hollendardalen; Battfjellet and Aspelintoppen Formations) are sourced from the west due to the emerging West Spitsbergen Fold Belt with the change in source area beginning approximately at the lower boundary of the Eocene (Fig. 2-4; Sætre 2011; Dallmann *et al.* 2015; Elling *et al.* 2016; Petersen *et al.* 2016). The change is marked by the presence of coarser deposits within the shaly Frysjaodden Formation. Based on Ar-Ar dating, Schneider *et al.* (2018) suggested that Ellesmerian structures on Prins Karls Forland (west of Spitsbergen, part of the West Spitsbergen Fold Belt) were reactivated during the early Eocene (55–44 Ma), progressing under warm, yet brittle, conditions. The steep western flank of the CTB was involved in early Eocene folding and thrusting, and the entire basin was detached by thrust faults situated in the underlying Mesozoic strata.

The age of the formation boundaries in Palaeogene sediments are not well defined; in particular, the age of the youngest deposits of the mid-late Eocene Aspelintoppen Formation which forms the uppermost unit of the Van Mijenfjorden Group (Helland-Hansen & Grundvåg 2020). As pointed out by Dörr *et al.* (2018), the stratigraphic age of the Aspelintoppen Formation is interesting because it provides the maximum time constraint for the onset of the exhumation of the CTB. The age of the basal part of the Firkanten Formation has also been disputed, but recently, Jones *et al.* (2017) used U-Pb zircon dates from tephra layers close to the base-Paleocene unconformity to estimate that sedimentation in the CTB began in mid-Paleocene times at ~61.8 Ma (near the Danian–Selandian boundary). They concluded that the sustained and increasingly rapid subsidence that began at this time happened in response to compression between Greenland and Svalbard.

The Forlandsundet Graben is a prominent part of the Palaeogene basins on Svalbard. It is an elongated graben structure, part of the Hornsund Fault Complex along the western margin of Spitsbergen, which is filled with more than 3 km of folded and poorly dated late Eocene – early Oligocene clastics of the **Buchananisen Group**.

Remnants of a once coherent cover of the late Miocene basalts of the **Seidfjellet Formation** occur on northern Spitsbergen (Andrée Land, Ny-Friesland). The lavas are dated to 8.7–11.5 Ma, and they erupted onto an erosion surface (now at ~1 km asl), that truncates Devonian Old Red Sandstones and Precambrian basement (Dörr *et al.* 2019). The total thickness of 15 lava flows amounts to ~400 m.

The Quaternary **Bockfjorden Volcanic Complex** consists of 3 eruptive centres within a distance of 25 km, located adjacent to the remnants of the Miocene volcanics on northern Svalbard. Geothermo-barometry calculations on xenoliths from the eruptive centres define a high geotherm consistent with their location near the Yermak hotspot.

Quaternary sediments are mainly derived from the later stages of the last (Weichselian) glaciation and younger, Holocene, glacial, glacifluvial and marine depositional processes.

2.3 Tectonic framework

A sequence of Late Cretaceous – Cenozoic tectonic events define the present-day layout of the Carboniferous–Palaeogene basins in the Arctic. We briefly outline these events and some other relevant aspects in the following.

2.3.1 The late Maastrichtian unconformity

Ricketts (1994) noted that uplift of Sverdrup Basin, probably in the latter part of the Maastrichtian, and development of a sub-Paleocene unconformity is a signal event in the eastern Arctic:

- In northern Yukon and the Mackenzie Delta a regional unconformity separates late Maastrichtian and younger rocks from mid-Cretaceous and older depositional sequences as a consequence of widespread Late Cretaceous to Palaeogene tectonism (Dixon 1986).
- A major sub-Paleocene unconformity (the 'Bylot unconformity') extends from the Labrador Shelf to north Baffin Island (McWhae 1981).
- On Bylot Island this unconformity occurs below the Mount Lawson Formation (Miall 1986), and on southeast Baffin Island, below the Cape Searle Formation (Burden & Langille 1990).
- On Spitsbergen, the Palaeogene succession overlies with profound unconformity Lower Cretaceous strata; the product of Late Cretaceous uplift (Atkinson 1963; Nøttvedt 1985).

Ricketts *et al.* (1994) concluded that the latest Cretaceous event was widespread across the North American Arctic and Barents Shelf region, prior to opening of the North Atlantic.

The late Maastrichtian unconformity is also an important marker in Greenland. In West Greenland, Upper Cretaceous deltaic sediments are unconformably overlain by latest Maastrichtian and Danian sediments and are in turn overlain by mid-Paleocene picritic and basaltic hyaloclastites and lavas (Dam *et al*. 2009; see also figures 37–39 of Green *et al.* 2013). In North-East Greenland, a latest Cretaceous unconformity is bracketed by Campanian and Danian sediments, and a large amount of reworked Cretaceous marine palynomorphs including a late Maastrichtian flora documents uplift of Cretaceous marine sediments and major erosion during the early Palaeogene (Nøhr-Hansen *et al.* 2011). In North Greenland, a significant hiatus separates the youngest, well-dated Upper Cretaceous sediments of Santonian age from late Paleocene deposits (Fig. 2-3; the Sølverbæk and Thyra Ø Formations, respectively; Lyck & Stemmerik 2000; Hovikoski *et al.* 2018).

2.3.2 The Eurekan Orogeny

We use the term Eurekan Orogeny to mean deformation caused by the Palaeogene convergence between Greenland, the Canadian Arctic and Svalbard (Fig. 1-2):

- Seafloor spreading in the Labrador Sea and Baffin Bay started in the mid-Paleocene (chron C27; ~62 Ma), and this movement of Greenland relative to the Canadian Arctic and Svalbard caused **the first stage of the Eurekan Orogeny**

(phase 1 of Gion *et al.* 2017 and phase 2 of Oakey & Chalmers 2012).

- Greenland and Eurasia moved together until the latest Paleocene (before chron C24, ~55 Ma; Gaina et al 2017), when seafloor spreading started between Greenland and Europe after which Greenland moved north relative to the Arctic Islands caused **the second stage of the Eurekan Orogeny** (phase 2 of Gion *et al.* 2017 and phase 3 of Oakey & Chalmers 2012).

- Spreading between Greenland and North America ceased at the end of the Eocene (C13; ~35 Ma), when Greenland became attached to North America and the Eurekan Orogeny ended.

Oakey & Chalmers' phases 1 and 4 consist of the purely continental extensional movements between Greenland and North America prior to the mid-Paleocene and of the continued movement of the new Greenland/North America plate relative to Eurasia after the Eocene. There were no Eurekan orogenic movements during either of these phases.

Movement during the Paleocene led to the formation of a foreland basin related to compressional loading driven by the seafloor spreading west of Greenland, and that basin may have extended from the eastern Sverdrup Basin to the Central Tertiary Basin of Svalbard during the first Eurekan stage (Ricketts 1994; Oakey & Chalmers 2012; Bruhn & Steel 2003; Jones *et al.* 2017; Embry & Beauchamp 2019). The change of direction of Greenland relative to North America during the Eocene caused compression on Ellesmere Island and transpression on Svalbard during the second Eurekan stage (Steel et *al.* 1985; Faleide et *al.* 2008). The Svalbard margin evolved through strike-slip movements along the plate boundary, the De Geer Line, when Greenland slid past Svalbard (Steel et *al.* 1985; Faleide et *al.* 2008). The Eurekan Orogeny came to an end when movement ceased between Greenland and North America at the end of the Eocene (Oakey & Chalmers 2012; Piepjohn et *al.* 2016).

2.3.3 The Kronprins Christian Land Orogeny and the fault zones of the Wandel Sea Basin

Håkansson & Stemmerik (1989) suggested that the Upper Jurassic to Cretaceous sediments of the Wandel Sea Basin accumulated in increasingly smaller sub-basins formed by strike-slip tectonics and transtension in the 'Wandel Hav Strike-Slip Mobile Belt'. According to Håkansson & Pedersen (1982, 2001, 2015), the 'Wandel Hav Strike-Slip Mobile Belt' is a NW–SE-striking wrench-fault deformation zone that was instrumental in all basin-forming events from the late Permian onwards and includes three major fault systems (Fig. 2-1).

Håkansson & Pedersen (2015) noted that there is a 45° offset in the plate boundary between North Greenland and Svalbard relative to the main trend of rifting and spreading in the north-east Atlantic. As a result, this segment of the plate boundary experienced episodes of combined transtension and transpression, in part controlled by the movement of a temporarily independent Greenland Plate. They concluded that the late Permian – Mesozoic deposits of the Wandel Sea Basin record the plate-boundary history along this offset, in a

series of disturbed, pull-apart basins, most of which they assigned to four major, tectonic episodes that were finally overprinted by the compressional Kronprins Christian Land Orogeny. According to these authors, the timing of this orogeny is bracketed by the age of the deformed strata (Upper Cretaceous) and the age of the undeformed cover successions (the Palaeogene Thyra Ø Formation) and thus happened during a comparatively brief period around the Cretaceous–Palaeogene boundary.

von Gosen & Piepjohn (2003), however, argued that the Eurekan transpressive deformation of the Wandel Sea Basin is younger than the Thyra Ø Formation and thus of post-Paleocene age, i.e. Eocene. They interpreted that a dextral displacement of the Thyra Ø Formation relative to upper Palaeozoic strata within a wide NW-SE fault zone on Prinsesse Ingeborg Halvø occurred in the early Eocene, during the deformation of the HFFZ and KCTZ. In contrast, Pedersen & Håkansson (2001) explained the displacement of the Thyra Ø Formation along the fault in terms of post-Paleocene down-faulting after cessation of compression. Therefore, Håkansson & Pedersen (2001, 2015) suggested that the compressive tectonics had come to an end before the deposition of the Thyra Ø Formation.

Svennevig *et al.* (2016, 2017) described the Mesozoic Wandel Sea Basin as a rift basin, dominated by post-Coniacian extensional faults followed by N-S compression, possibly during the Paleocene–Eocene. Svennevig *et al.* (2016) considered the age of the compressional event on Kilen to be post-Coniacian since the youngest Cretaceous outcrops are Coniacian in age. They presented a range of arguments in favour of a late Paleocene – early Eocene age for the N-S compression on Kilen.

Japsen *et al.* (2020a), in a precursor to this study, used AFTA and VR data to define a phase of mid-Paleocene exhumation that affected the major fault zones of the Wandel Sea Basin. They suggested that this event defined the timing of the compressional event responsible for folding and thrusting of Upper Cretaceous and older sediments along these fault zones. They further inferred that the mid-Paleocene inversion of the fault zones represents the onset of the Eurekan Orogeny.

2.3.4 West Spitsbergen Fold Belt

The West Spitsbergen Fold Belt developed along the western part of Spitsbergen by east-northeast directed folding and thrusting along an intra-plate structure as part of the Eurekan Orogeny during the early Eocene between chron C24 and C21 (Dallmann *et al.* 2015). The West Spitsbergen Fold Belt formed as a product of the transpression that also affected the CTB of Svalbard (Steel *et al.* 1985). A continental transform fault, the Hornsund Fault Complex (or the De Geer Fault Complex) between northern Greenland and Svalbard developed by reactivation of a pre-existing zone of crustal weakness with the onset of seafloor spreading in the North-East Atlantic and the Eurasian Basin (Eurekan stage 2; Fig. 1-2). The West Spitsbergen Fold Belt is about 300 km long and less than 50 km wide and consists of a thick-skinned thrust zone in the west, where metamorphic basement rocks are involved in thrusting, and a thin-skinned or foreland-thrust-belt-like zone in the east within the post-Caledonian sedimentary succession. The thin-skinned thrust deformation contin-

ues within Mesozoic strata underneath the Palaeogene succession, forming a detachment zone.

From anomaly C21 onwards, the relative motion between Greenland and the Barents Shelf and Svalbard changed into a transform plate movement with initially sinistral, but later long-lasting dextral strike-slip. The main transform fault system was the Hornsund Fault Complex, while the sub-parallel fault zones (the Billefjorden and Lomfjorden Fault Zones) experienced similar slip on lesser scales. Finally, transform movement ceased, when Svalbard had passed the North Atlantic spreading zone, and a passive continental margin developed with the opening of the Fram Strait that most likely began at ~20 Ma (Jokat *et al.* 2008; Dumais *et al.* 2020).

2.3.5 Aspects of the development of the Eurasia Basin

The Lomonosov Ridge divides the Arctic Ocean into the Eurasia Basin and the Amerasian Basin. It is a sliver of continental crust that rifted from the Barents and Kara shelves during the early Cenozoic (~56 Ma) opening of the Eurasia Basin (Brozena *et al.* 2003; Jokat *et al.* 2016). Brozena *et al.* (2003) reconstructed a magnetic anomaly orthogonal to the spreading centre of the Eurasia Basin at times prior to chron C13. They suggested that this anomaly marks the locus of shortening and possibly subduction as Greenland collided with the nascent Eurasia Basin and impinged upon the southern Gakkel Ridge. This collision may have contributed to volcanism on the Morris Jesup Rise. By chron C13 Greenland had ended its northward motion and had become fixed to North America, and the plateau north of Greenland had rifted apart to become the submarine Morris Jesup Rise and the Yermak Plateau, north of Greenland and Svalbard, respectively (Fig. 1-1; Brozena *et al.* 2003; Kristoffersen *et al.* 2020).

Jokat *et al.* (2016) found that strong positive magnetic anomalies characterize the Morris Jesup Rise, and that the anomalies across the plateau indicated the presence of distinct volcanic centres. They argued that the massive magmatism had occurred latest in conjunction with the Oligocene initial stages of plate divergence between Svalbard and North Greenland that led to the development of Fram Strait. Further, they interpreted both plateaus, the Morris Jesup Rise and the Yermak Plateau, to be of continental origin and, in the initial rift stage of the Eurasia Basin, to have been contiguous with the Lomonosov Ridge. Kristoffersen *et al.* (2020) presented plate reconstructions at 56, 47 and 34 Ma illustrating the development of the Eurasia Basin and the movement of Svalbard relative to North Greenland along the De Geer Line (Fig. 2-5). According to these reconstructions, the Morris Jesup Rise and the Yermak Plateau are located north-east of Peary Land by the end of the Eocene. Kristoffersen *et al.* (2020) found that the Yermak Plateau became part of the European plate prior to chron C13 as the Gakkel Ridge propagated into the margin of North Greenland.

A distinct plateau across the Lomonosov Ridge is characterized by a smooth bathymetry (~400 m depth) in a 350 km wide zone north of Greenland. Døssing *et al.* (2010) suggested that Eurekan crustal shortening contributed to the formation of this plateau against an important fault zone north of Greenland.

2.4 The Campanian–Eocene Eureka Sound Group of the eastern Canadian Arctic

Ricketts (1994) investigated the Eureka Sound Group of the eastern archipelago of the Canadian Arctic (Axel Heiberg and Ellesmere Islands) that records a 40-45 Myr stratigraphic history, including the final events of the long-lived late Carboniferous to middle Eocene Sverdrup Basin. The definitive ages for the >4 km succession range from middle Campanian to middle Eocene but may extend into the late Eocene. The Eureka Sound Group strata preserve the transition from thermally-dominated subsidence that characterized much of Sverdrup Basin's earlier history, to foredeep subsidence beginning in the Paleocene. Clastic sediment deposited during the middle Campanian and Maastrichtian resulted in a continuation of the stratigraphic style which characterized much of Sverdrup Basin. Regional uplift at the end of the Cretaceous and development of a basin-wide sub-Paleocene unconformity, signalled the end of this era and subsequent formation of a foredeep-like basin which survived until the middle Eocene. Crustal shortening, beginning in the early Eocene and culminating in middle Eocene time (the Eurekan Orogeny) destroyed the contiguous Sverdrup Basin, and in its place produced several small intermontane, synorogenic basins. Ricketts (1994) found no onshore stratigraphic evidence that the Eurekan deformation continued into the late Eocene.

Ricketts extracted five third-order depositional sequences from the lithostratigraphic and lithofacies framework (Fig. 2-6). Middle Campanian to Maastrichtian deltas in Sequence 1 reflect a continuation of typical Sverdrup Basin sedimentation and subsidence. Throughout eastern Sverdrup Basin, upper Maastrichtian, and in some places all Maastrichtian deposits, were eroded, marking the base of Sequence 2. Uplift and subaerial erosion during late Maastrichtian time was followed by early Paleocene transgression. The mid-Paleocene transgression initiating Sequence 3 appears to have extended over much of the Arctic. In addition to the foredeep succession, Sequence 4 (the main phase of Eurekan deformation) also contains synorogenic deposits in small, fault-bounded half grabens signalling the earliest effects of crustal failure within the foredeep. Sequence 5 (middle Eocene), is entirely synorogenic and signifies the complete destruction of Sverdrup Basin with very high sedimentation rates in intermontane basins.

2.5 Comparison between the Palaeogene development in the eastern Canadian Arctic and Svalbard

There are remarkable similarities between the geological development in Svalbard and in the eastern Canadian Arctic prior to and during the Eurekan orogeny (Figs 1-1, 2-6, 2-7). In particular, Paleocene sand occurs above a marked unconformity which is dated as late Maastrichtian in the Sverdrup Basin and at 68 Ma in the Beaufort-Mackenzie Basin (Ricketts 1994; Embry *et al.* 2018). On Svalbard, the unconformity has wide limits (Albian – mid-Paleocene; Jones *et al.* 2017).

As discussed above, Ricketts (1994) suggested that the late Maastrichtian unconformity reflects a phase of uplift and erosion that was widespread across the North American Arctic and Barents Shelf region, prior to opening of the North Atlantic. He also noted that the sub-

Paleocene unconformity signals the transition to greater sedimentation rates in the rapidly subsiding Sverdrup foredeep, and that the mid-Paleocene transgression appears to have extended over much of the Arctic (cf. Harrison *et al.* 1999). The eastern portion of the Sverdrup Basin thus underwent rapid subsidence related to compressional loading driven by the opening of the Labrador Sea and Baffin Bay and the consequent Palaeogene impingement of Greenland on the Canadian Arctic Islands area during the Eurekan Orogeny (Embry & Beauchamp 2019). Other parts of the basin, however, underwent uplift. These authors summarized the succession in the foreland basins as a basal transgressive sandstone unit (upper Expedition Fm) followed by regressive, marine shale, and siltstone (Strand Bay Fm) and thick, sand-dominated, coastal to fluvial deposits with abundant coal (Iceberg Bay Fm) (Fig. 2-7). In the Beaufort-Mackenzie Basin, a mid-Paleocene unconformity has been dated at 62 Ma (Embry *et al.* 2018).

On Svalbard, rapid subsidence of the CTB began in the Paleocene, at the Danian-Selandian boundary, 61.8 Ma (Jones *et al.* 2017). Therefore, the base-Paleocene unconformity must reflect a phase of earlier uplift and erosion, that may well correspond to the late Maastrichtian phase as suggested by Ricketts (1994). According to Jones *et al.* (2017) this subsidence happened in response to compression between Greenland and Svalbard induced by the onset of seafloor spreading in the Labrador Sea. However, Steel *et al.* (1985) found that the initial formation of the CTB during the Paleocene happened during extension (possibly transtension), in particular, because these authors found no evidence for compression in the west at this time. However, subsidence in the initial phase of formation of the CTB was increasingly asymmetrical and greatest towards the De Geer Line (~56 Ma; Fig. 2-8-I). This indicates that the relative movement between Greenland and Svalbard provided the overall control, and thus that the initial basin formation there had much in common with the foredeep-like basin that developed in the eastern Sverdrup Basin related to compressional loading driven by the onset of sea-floor spreading west of Greenland (Ricketts 1994; Bruhn & Steel 2003; Embry & Beauchamp 2019).

Reversal of drainage direction and an influx of metamorphic rock fragments from the west, characterized the late Paleocene–Eocene development of the CTB as the West Spitsbergen Fold Belt evolved during transpression. The region along and east of the De Geer Line was uplifted and became the main sediment source for the CTB (~45 Ma; Fig. 2-8-II). Some uncertainty surrounds the timing of these events as Steel *et al.* (1985) dated the Firkanten Formation as Danian, whereas the age is Selandian according to Jones *et al.* (2017). The youngest Palaeogene sedimentation on Svalbard is represented by the mid-late Eocene Aspelintoppen Formation that accumulated during transpression and collapse of the central fold belt (~35 Ma; Fig. 2-8-III). Post-Eurekan, Palaeogene sediments are thus not found on Svalbard.

In the Sverdrup Basin, deformation and uplift progressed through the Paleocene and Eocene, and syn-tectonic conglomerates (Buchanan Lake Fm) up to 1000 m thick were deposited in front of the advancing thrust sheets in mid-Eocene (Embry & Beauchamp 2019). According to Ricketts (1994), Eurekan tectonism climaxed in the early Eocene and ended in the middle Eocene, whereas Embry & Beauchamp argued that the Eurekan deformation climaxed in late Eocene, when the entire basin was uplifted, bringing to a close a 300-million-year history of deposition in the Sverdrup Basin. However, as we argued in Section

2.3.2, the Eurekan Orogeny came to an end when movement ceased between Greenland and North America at the end of the Eocene (as Greenland became attached to North America), and the late Eocene uplift phase identified by Embry & Beauchamp, thus most likely reflect post-Eurekan tectonics (Fig. 1-2).

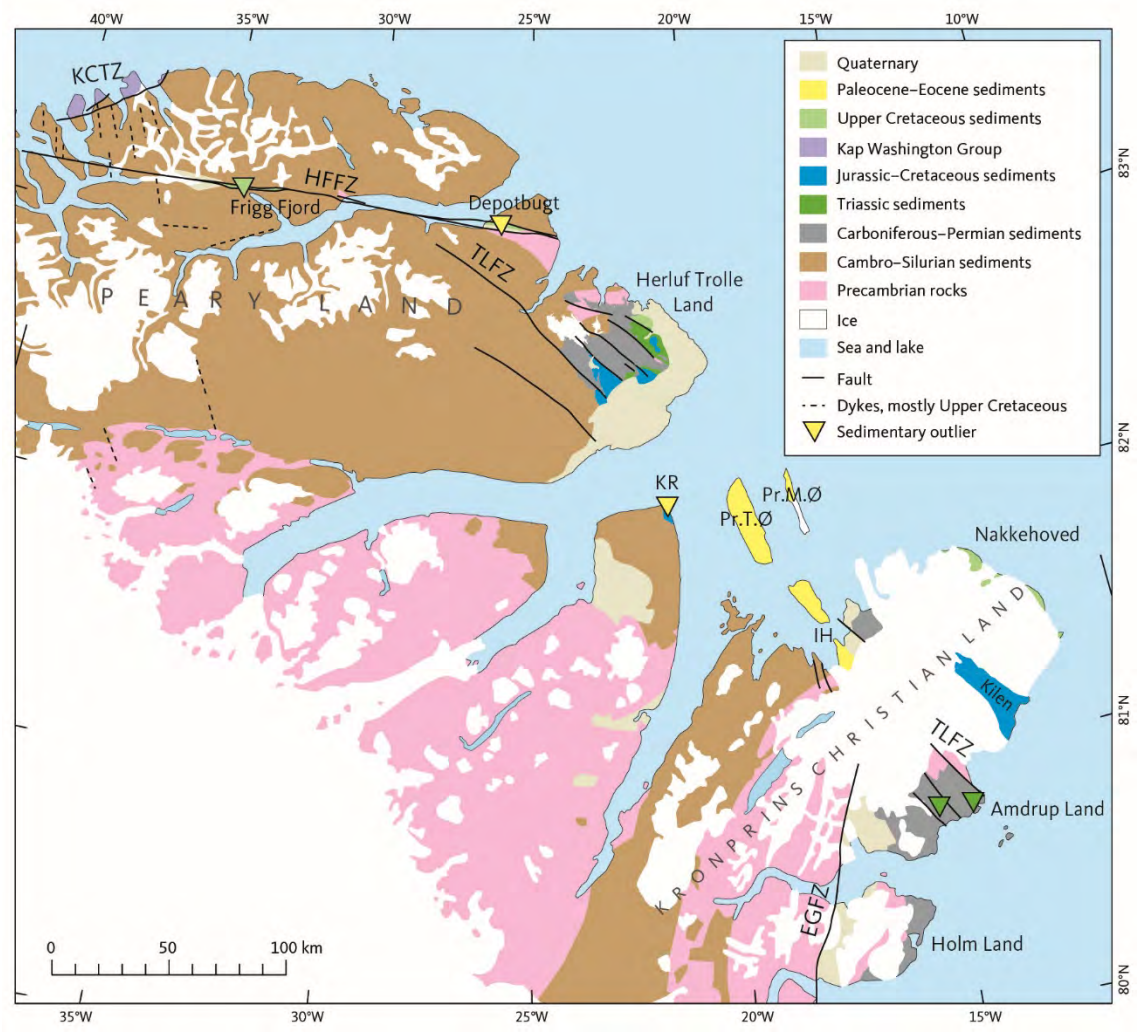

Figure 2-1. Geology of eastern North Greenland (stratigraphic column in Fig. 2-3). From Japsen *et al.* (2020a) based on Escher & Pulvertaft 1995 with modifications after Croxton et *al.* 1980; Hovikoski et *al.* 2018; Piasecki et *al.* 2018. **EGFZ**: East Greenland Fracture Zone. **HFFZ**: Harder Fjord Fault Zone. **KCTZ**: Kap Canon Thrust Zone. **KR**: Kap Rigsdagen. **Pr. M. Ø**: Prinsesse Margrethe Ø. **Pr. T. Ø**: Prinsesse Thyra Ø. **TLFZ**: Trolle Land Fault Zone.

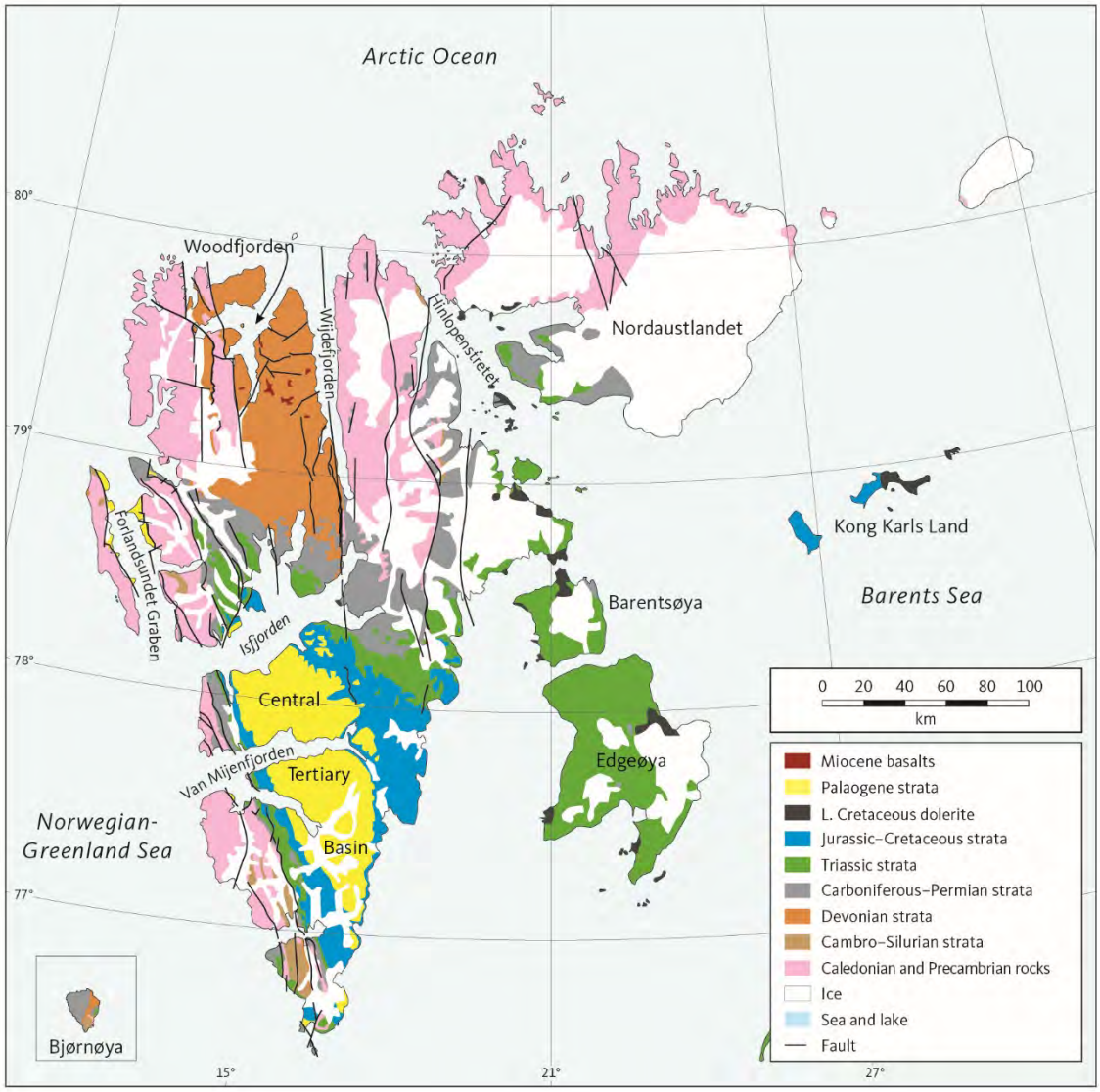

Figure 2-2. Geological map of Svalbard (stratigraphic column in Fig. 2-3). From Dörr *et al.* (2018) based on Dallmann *et al.* (2002).

Figure 2-3**.** Stratigraphic columns for the Wandel Sea Basin and Svalbard with selected formation names. The Palaeogene sediments to the left in the Svalbard column represent the Buchananisen Group in Forlandsundet. Simplified representation of the mixed volcanic, volcano-clastic and lacustrine deposits of the Kap Washington Group (K.W.). Wandel Sea Basin stratigraphy from Japsen *et al.* (2020a) based on Bjerager *et al.* 2019; Gautier *et al.* 2011; Håkansson & Pedersen 2015; Hopper *et al.* 2014; Hovikoski *et al.* 2018; Piasecki *et al.* 2018; Stemmerik *et al.* 1998; Svennevig *et al.* 2018; Tegner *et al.* 2011. Svalbard stratigraphy based on information from the Norlex website (http://www.nhm2.uio.no/norges/litho/Barents_Chart.html) and Abay (2017) with modifications after Dallmann *et al.* (2015) and Jones *et al.* (2017). K.C. Land: Kronprins Christian Land. P.B.: Parish Bjerg.
(Next page)

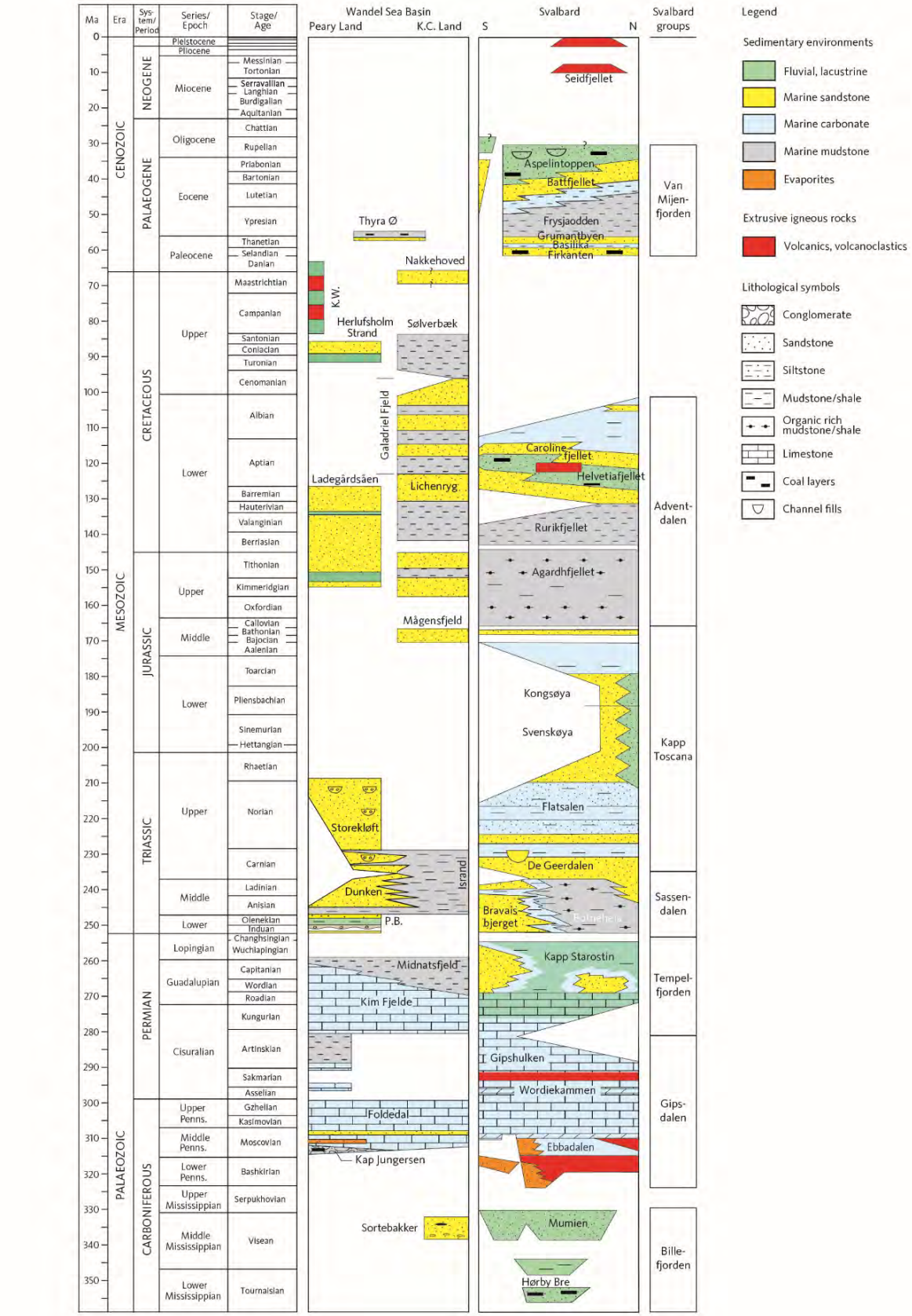
Ma
Era
System/ Period
Series/ Epoch
Stage/ Age
CENOZOIC
MESOZOIC
PALAEOZOIC
NEOGENE
PALAEOGENE
CRETACEOUS
JURASSIC
TRIASSIC
PERMIAN
CARBONIFEROUS
Pleistocene
Pliocene
Miocene
Messinian
Tortonian
Serravallian
Langhian
Burdigalian
Aquitanian
Oligocene
Chattian
Rupelian
Eocene
Priabonian
Bartonian
Lutetian
Ypresian
Paleocene
Thanetian
Selandian
Danian
Upper
Maastrichtian
Campanian
Santonian
Coniacian
Turonian
Cenomanian
Lower
Albian
Aptian
Barremian
Hauterivian
Valanginian
Berriasian
Upper
Tithonian
Kimmeridgian
Oxfordian
Middle
Callovian
Bathonian
Bajocian
Aalenian
Lower
Toarcian
Pliensbachian
Sinemurian
Hettangian
Upper
Rhaetian
Norian
Carnian
Middle
Ladinian
Anisian
Lower
Olenekian
Induan
Lopingian
Changhsingian
Wuchiapingian
Guadalupian
Capitanian
Wordian
Roadian
Cisuralian
Kungurian
Artinskian
Sakmarian
Asselian
Upper Penns.
Gzhelian
Kasimovian
Middle Penns.
Moscovian
Lower Penns.
Bashkirian
Upper Mississippian
Serpukhovian
Middle Mississippian
Visean
Lower Mississippian
Tournaisian
Wandel Sea Basin
Peary Land
K.C. Land
Thyra Ø
K.W.
Nakkehoved
Herlufsholm Strand
Sølverbæk
Galadriel Fjeld
Ladegårdsåen
Lichenryg
Mågensfjeld
Storekløft
Dunken
Israndi
P.B.
Midnatsfjeld
Kim Fjelde
Foldedal
Kap Jungersen
Sortebakker
Svalbard
S
N
Seidfjellet
Aspelintoppen
Battfjellet
Frysjaodden
Grumantbyen
Basilika
Firkanten
Caroline-fjellet
Helvetiafjellet
Rurikfjellet
Agardhfjellet
Kongsøya
Svenskøya
Flatsalen
De Geerdalen
Bravais-bjerget
Kapp Starostin
I. Gipshuken
Wordiekammen
Ebbadalen
Mumien
Hørby Bre
Svalbard groups
Van Mijen-fjorden
Advent-dalen
Kapp Toscana
Sassen-dalen
Tempel-fjorden
Gips-dalen
Bille-fjorden
Legend
Sedimentary environments
Fluvial, lacustrine
Marine sandstone
Marine carbonate
Marine mudstone
Evaporites
Extrusive igneous rocks
Volcanics, volcanoclastics
Lithological symbols
Conglomerate
Sandstone
Siltstone
Mudstone/shale
Organic rich mudstone/shale
Limestone
Coal layers
Channel fills

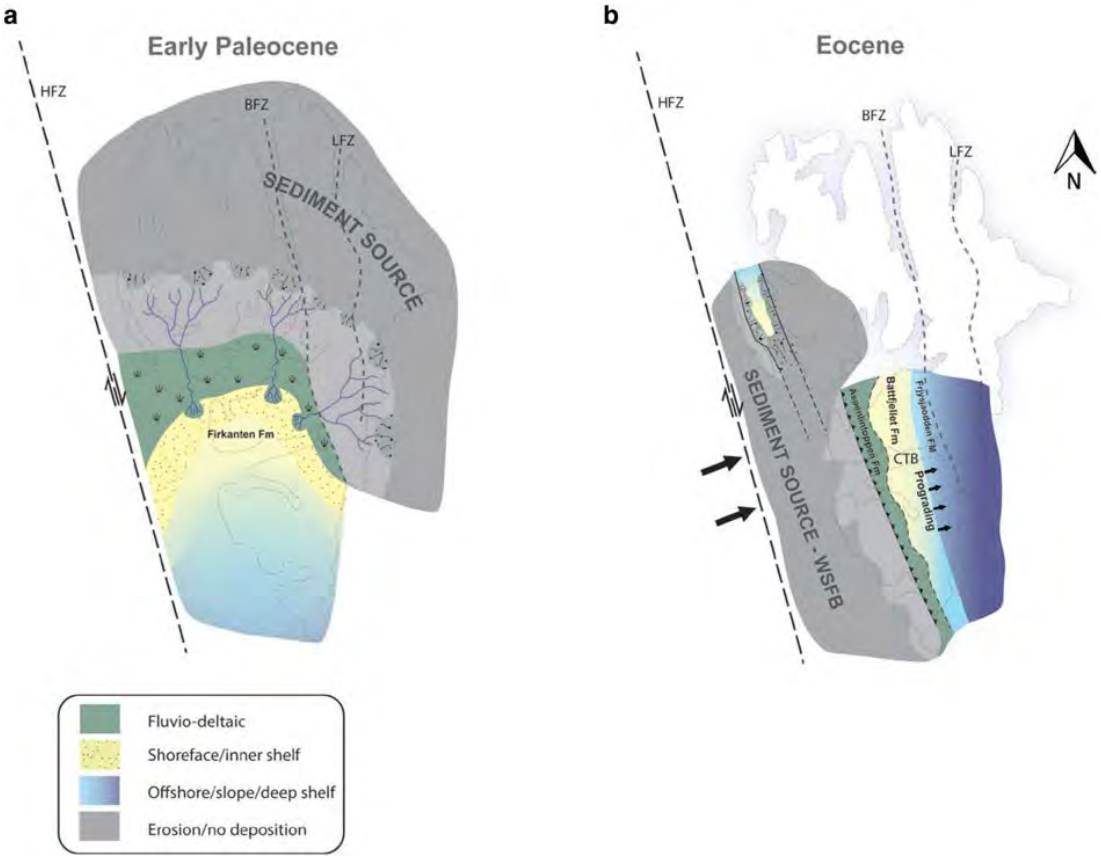

Figure 2-4. Distribution of source and sink areas onshore Svalbard. (a) Source area during the early Paleocene, where sediment source area is present east and NE of the Central Tertiary Basin. (b) Map of the middle Eocene source and sink distribution showing erosion of the West Spitsbergen Fold Belt (WSFB). BFZ, Billefjorden Fault zone; LFZ, Lomfjorden Fault Zone; HFZ, Hornsund Fault Zone; CTB, Central Tertiary Basin. From Petersen *et al.* (2016).

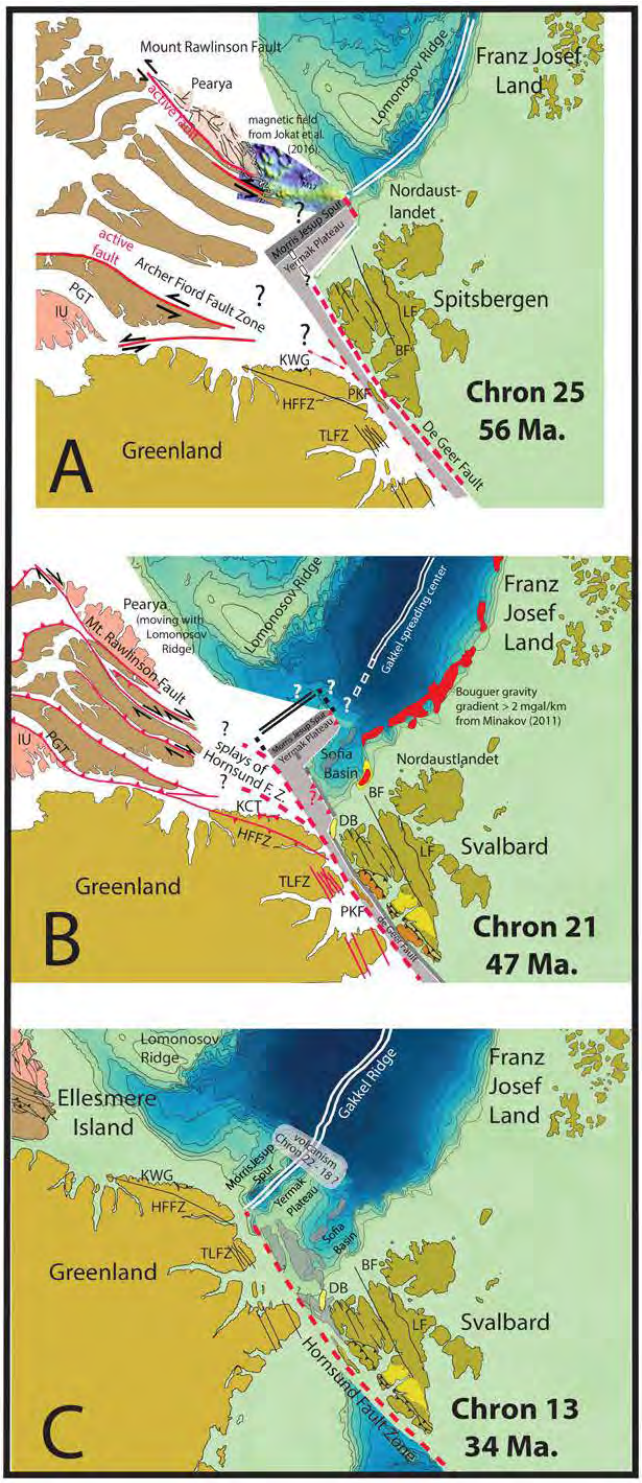

Figure 2-5. Plate reconstructions at 56, 47 and 34 Ma illustrating the development of the Eurasian Basin and the movement of Svalbard relative to North Greenland along the De Geer Line (Kristoffersen *et al.* 2020). Note that the Morris Jesup Rise and the Yermak Plateau are located north-east of Peary Land by the end of the Eocene. In **A**, 56 Ma corresponds to chron C24.

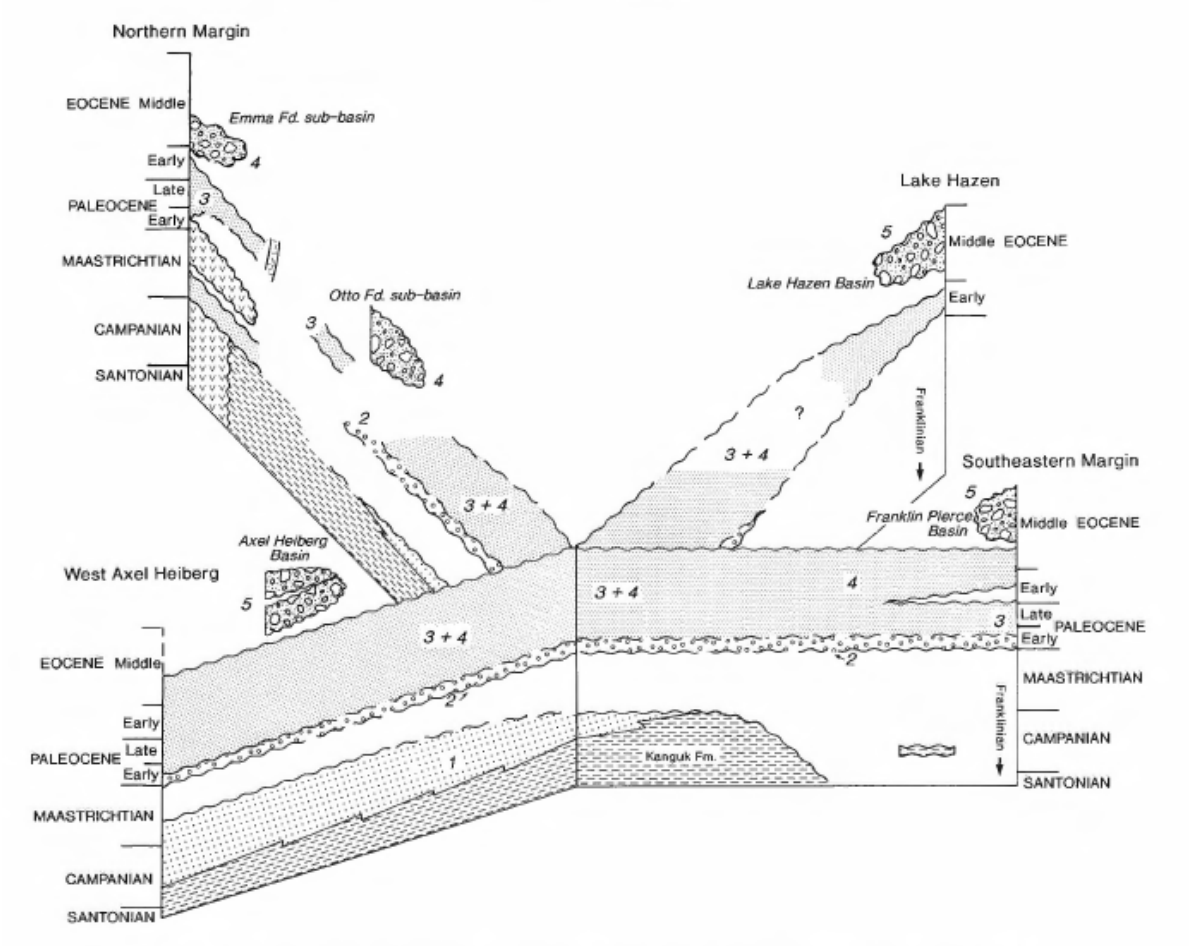

Figure 2-6. Third-order sequence stratigraphy of the Eureka Sound Group in the Sverdrup and intermontane basins. Lake Hazen is near the Nares Strait and the south-eastern margin is located near northern Baffin Bay. Numbers refer to depositional sequences 1 to 5 (Ricketts 1994).

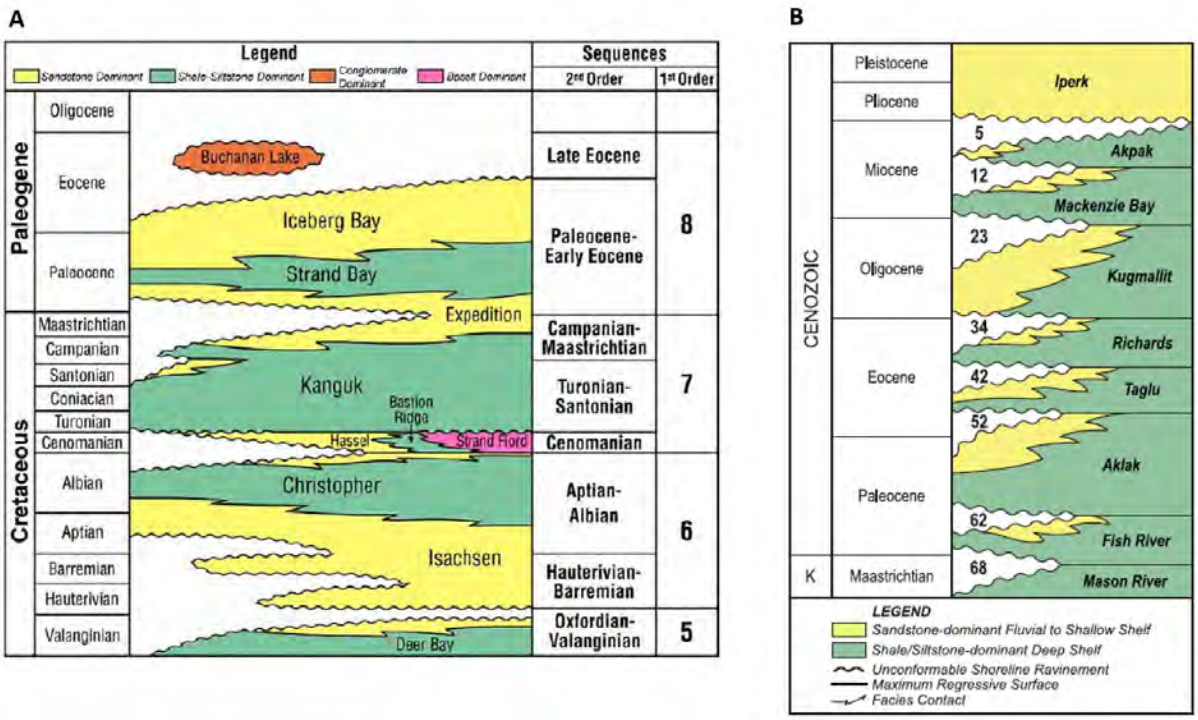

Figure 2-7. **A**. Cretaceous-Paleogene stratigraphic chart for the Sverdrup Basin with first-order sequences corresponding with the tectonic phases of the basin (Embry & Beauchamp 2019). **B**. Cenozoic stratigraphic chart for Beaufort-Mackenzie Basin where the best record of the Cenozoic succession in the Canadian High Arctic occurs (Embry *et al.* 2018).

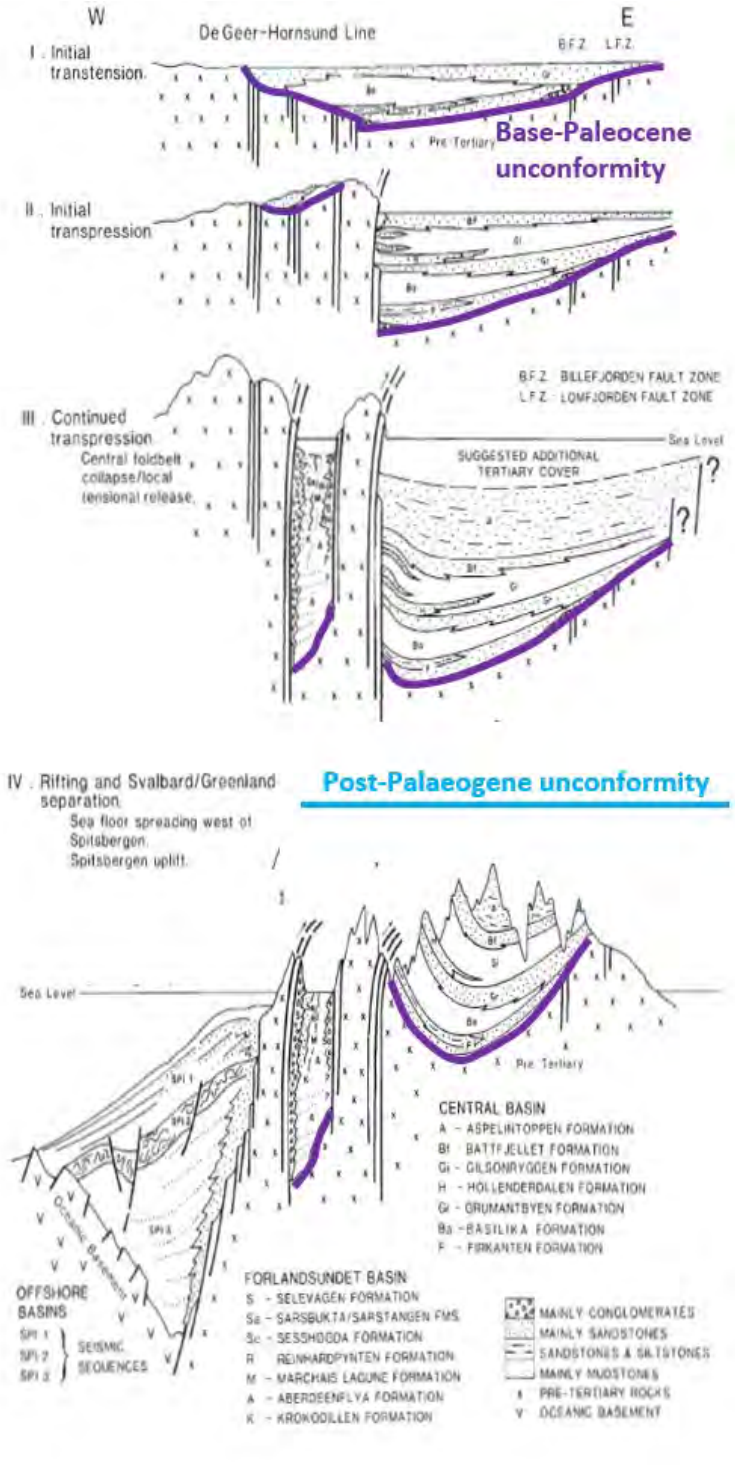

Figure 2-8. Schematic summary of the development of the Central Tertiary Basin in relation to tectonic evolution of the Svalbard margin (after Steel *et al.* 1985). **I**. End-Paleocene (56 Ma) after deposition of the Grumantbyen Formation (Gr). **II**. Mid-Eocene (45 Ma) after deposition of the Battfjellet Formation (Bf). **III**. End-Eocene (35 Ma) after deposition of the Aspelintoppen Formation (A) and prior to exhumation. **IV**. Present-day. Timing after Dallmann *et al.* (2015). **Purple line**: Base-Paleocene unconformity due to Maastrichtian exhumation. **Cyan line**: Post-Palaeogene unconformity due to end-Eocene exhumation.

3. Thermal history reconstruction based on AFTA and VR

3.1 Introduction

The thermal history reconstruction study of North Greenland and Svalbard was carried out by Geotrack, building on a previous Geotrack study of North Greenland provided to GEUS (Figs 3-1, 3-2; Geotrack reports GC1231, GC1113, respectively). For this study, those results were supplemented by new apatite fission-track analysis (AFTA®) and vitrinite reflectance (VR) data in samples from outcrops in both North Greenland, and Svalbard, and from three boreholes on Svalbard. Additional AFTA and VR data from outcrops on Svalbard, from Geotrack's non-exclusive regional study of the Barents Sea (Geotrack Report GC642), were also integrated into the study, together with legacy VR data in two of the Svalbard boreholes, provided by Equinor.

3.2 AFTA and VR data in samples from outcrops

AFTA data were obtained in 59 outcrop samples from North Greenland, including units varying in age from Paleocene sandstones to Precambrian crystalline basement. Data in 47 of these samples were presented and discussed by Japsen *et al.* (2020a) while data in a further 12 samples were generated for this study. Basic AFTA parameters in all samples, including sample details and locations, are listed in Table T.1 (Tables T.1 to T.5 in digital format accompany this report). Sampling was designed to provide regional coverage over a range of stratigraphic ages, but given the scale of the region, the study is very much of a reconnaissance nature. A number of samples were also collected for VR determinations, where suitable lithologies were encountered, with sample details and results summarised in Table T.2. Again, most of these data were presented and discussed by Japsen *et al.* (2020a), with three new samples analysed for this study. All sample locations in North Greenland are shown in Figure 3-1, which also shows the division of the region into 5 separate areas to aid in defining regional cooling episodes (see Section 3.5.1). All samples were provided by GEUS from existing collections.

Outcrop or shallow borehole samples supplied by Equinor from twelve locations on Svalbard were processed for AFTA. Ten of these samples were of Precambrian crystalline basement, nine of which are from locations along the North coast plus one in the southwest of the island. Two samples of Jurassic sandstones from Kong Karls Land were also analysed. One of these sandstone samples did not yield apatite, while the other samples provided varying yields of apatite suitable for analysis. Data in these samples has been integrated with existing data in nine outcrop samples from locations mostly along the south coast of Isfjorden in the centre of the island and taken from Geotrack's regional study of the Barents Sea (Geotrack Report GC642). These samples are sandstones with depositional ages varying from Carboniferous to Paleocene. Sample details and AFTA data in all outcrop samples from Svalbard are listed in Table T.1. Sample locations on Svalbard are shown in Figure 3-2. Data in two samples from outcrops on Bjørnøya (specific locations

unknown) were also included (also taken from Geotrack Report GC642). Results from these samples have previously been presented by Arne *et al.* (1998). One new outcrop sample from Svalbard for VR determination was provided by Equinor. In addition, VR data in 7 samples for VR from locations along Isfjorden are included in this study, again taken from Geotrack Report GC642. VR sample locations are also shown in Figure 3-2, while details of these samples are included in Table T.2.

The quality of AFTA and VR data in the samples discussed above is generally high, with the usual "target numbers" of measurement of fission-track ages in 20 apatite grains and 100 track lengths per AFTA sample, and 25 reflectance measurements per VR sample, achieved in many of the samples (details in Table T.1). The resulting thermal history interpretations are regarded as highly reliable within stated uncertainties (95% confidence limits).

Apatite fission-track ages in outcrop samples across North Greenland and Svalbard are shown in Figure 3-3. Results from samples analysed by Dörr *et al.* (2012, 2019) along the northern coast of Svalbard are also shown in Figure 3-3B. In Figure 3-4, mean confined track lengths are plotted against apatite fission-track age in samples from North Greenland and Svalbard, respectively. These Figures illustrate that all but one of the measured apatite fission-track ages are less than 300 Ma and are mainly less than 200 Ma. In areas dominated by Precambrian rocks this emphasises that thermal histories across both areas are dominated by the post-Paleozoic development of each region. In North Greenland (Fig. 3-3A), youngest ages are focussed along the north and northeast coasts, with older ages confined mainly to the interior. This suggests that the younger ages may reflect processes related to the development of the plate boundary. In contrast, youngest ages in Svalbard (Fig. 3-3B) are focussed along Isfjorden in the centre of the island, mainly within the CTB.

The relationship between mean confined track length and apatite fission-track age in samples from North Greenland in Figure 3-4A shows that the longest mean lengths are associated with the youngest (Cenozoic) ages, while shorter mean lengths occur in samples with older ages. The data broadly define a "boomerang trend" (Green 1986; Green *et al.* 2013) suggesting progressive resetting of older ages by Cenozoic heating, although considerable scatter is evident, suggesting some complexity in the regional thermal history framework. In contrast, data from Svalbard in Figure 3-4B define an inverse boomerang trend with longest mean track lengths associated with mid-range ages around 100 to 150 Ma, with shorter mean track lengths in samples with younger and older ages. Data from Dörr *et al.* (2012, 2019) are consistent with the data from this study albeit with some scatter towards shorter lengths. Similar to the interpretation of data from southern Sweden by Japsen *et al.* (2016, their figure 3c), the trend of data from Svalbard can be understood as the combination of opposite ends of two separate resetting (i.e. boomerang) trends, suggesting that samples were heated to temperatures sufficient to reset fission-track ages to varying degrees prior to cooling at ~100–150 Ma and were then similarly modified in one or more later events. The absence of an upturn in the trend at youngest ages suggests that the final event was relatively recent (younger than the youngest ages).

VR values from outcrops across North Greenland presented and discussed by Japsen *et al.* (2020a), together with new values determined for this study, are shown in Figure 3-5A.

The new values are consistent with previous values, which define significant variation across the region. Japsen *et al.* (2020a) showed that with just a few exceptions the variation in VR values across the region can be divided into three categories: 1) values between 0.4 and 0.6% in samples of Paleocene to Jurassic depositional age in inland regions, 2) values between 1 and 3% in samples of Cretaceous to Jurassic depositional age mainly within fault zones of the Wandel Sea Basin, and 3) Extreme values up to 10% in samples of Upper Cretaceous age from Nakkehoved at the tip of Kronprins Christian Land. As discussed in Section 4, integration of thermal history constraints from AFTA and VR following Japsen *et al.* (2020a) shows that this regional variation in VR levels results from a range of different processes at different times across the region.

Figure 3-5B shows VR values measured in outcrop samples from Svalbard for this study, together with a review of published values. Significant variation is evident across the region, and as in North Greenland integration with AFTA data discussed in Section 4 shows that this reflects a variety of different palaeo-thermal episodes across the region.

3.3 AFTA and VR data in samples from boreholes

AFTA parameters (fission-track ages and mean track length) in samples analysed from the Sysselmannbreen, Reindalspasset and Radderdalen boreholes located on Svalbard, together with sample details such as depth, stratigraphic age and present-day temperature, are summarised in Table T.3. Borehole locations are shown in Figure 3-2. Fission-track age and mean track length are plotted as a function of depth and present temperature in Figure 3-6, where the fission-track age data are contrasted with the variation of stratigraphic age through the section intersected in each borehole. Note that data in two samples with lower apatite yields collected from adjacent depth ranges in the Radderdalen borehole have been pooled into a single combined sample resulting in higher quality data, since they are from similar depths. Also shown in Figure 3-6 are the variation of fission-track age and length vs depth predicted from the respective Default Thermal Histories (see Section 3.4), for selected apatite chlorine contents. These trends define the parameter values expected if the samples have never been hotter than their respective present-day temperatures at any time since deposition and provide the basis for interpretation of the data (Green & Duddy 2010, Green *et al.* 2013).

In all but one of the samples from the three boreholes, measured ages are significantly younger than expected from the Default Thermal History scenario, showing that the section intersected in each well has been heated beyond the present-day temperature and subsequently cooled at some time after deposition. The one exception to this is the shallowest sample from the Sysselmannbreen borehole, in which the fission-track age is consistent with the Default Thermal History prediction. In this sample, as with many other samples, the mean track length is much less that the value predicted from the Default Thermal History, and this can only be explained by the sample having been hotter at some time after deposition.

Mean VR values in samples analysed from the three boreholes, together with sample details, are summarised in Table T.4. Values in samples from each borehole are plotted as a

function of depth in Figure 3-7, where they are contrasted with the depth trend predicted from the default thermal history. In all three boreholes, measured VR values are much higher than expected from the Default Thermal History, confirming that the section intersected in each borehole has been heated beyond present-day temperatures and subsequently cooled after deposition. In the Sysselmannbreen and Reindalspasset boreholes, the VR data obtained in this study define consistent linear profiles, sub-parallel to the profiles defined from the default thermal history but offset to higher values. In contrast, additional data taken from borehole completion reports show rather more scatter. In the Radderdalen borehole, only a single new sample was available, and the VR data in this sample is consistent with some of the values at similar depths taken from the well completion reports, although data throughout the well generally show too much scatter to define a profile with confidence.

In summary, both AFTA and VR data from the three boreholes provide evidence of major post-depositional palaeo-thermal effects. The following section discusses the principles involved in extracting quantitative thermal history constraints from AFTA and VR data, after which constraints in samples from North Greenland and Svalbard are presented and discussed in detail.

3.4 Extracting quantitative thermal history constraints from AFTA and VR data

The techniques involved in extracting thermal history constraints from AFTA and VR data have been discussed in detail elsewhere (Green & Duddy 2012; Green et al. 2013). A key aspect of the approach is that because AFTA and VR data are dominated by maximum temperature, they preserve no evidence of the history prior to the onset of cooling. We therefore do not attempt to define the entire thermal history from the onset of track retention, because AFTA data do not contain sufficient information (Green & Duddy 2020). Instead, we focus on determining the key aspects of the thermal history that are recorded in the data - i.e. the magnitude of maximum or peak palaeotemperatures and the time at which cooling began, with appropriate uncertainty limits. VR values are controlled effectively by the maximum post-depositional temperature while AFTA can define maximum or peak palaeotemperatures of multiple episodes of cooling, of decreasing magnitude through time (typically up to three in a single sample).

Thermal history solutions are extracted from AFTA data in each sample by comparing measured data with values predicted from candidate thermal histories involving up to three episodes of heating and cooling (three being the maximum number of cooling episodes that can be obtained from AFTA data in most cases). By varying the magnitude of maximum palaeotemperature and the onset of cooling in each episode (using assumed heating and cooling rates of 1°C/Myr and 10°C/Myr, respectively), the range of values giving predictions that are consistent with the measured data within 95% confidence limits can be defined using likelihood theory, using principles similar to those outlined by Gallagher *et al.* (1995). Results are presented in terms of 95% confidence limits on the maximum/peak palaeotemperature and the time at which cooling from that palaeotemperature began in each event, as Illustrated in Figure 3-8.

3.5 Thermal history constraints from AFTA and VR data in this study

Thermal history constraints obtained from the AFTA data in each sample in up to three palaeo-thermal episodes (i.e. times when samples began to cool from elevated palaeotemperatures, as illustrated in Figure 3-8), are summarised in Table T.5. Note that some values have changed from those originally reported in Geotrack Report GC1231, as a result of a reassessment of data from all regions in this study. AFTA data in samples from earlier studies have been reinterpreted using the more modern methods described in Section 3.3 (including measurement of wt% Cl in each sample), as applied to samples collected for this study, so that all interpretations are consistent and directly comparable.

Timing constraints on cooling episodes in individual datasets are compared in Figure 3-8. Where appropriate (i.e. in samples that were not totally annealed after deposition), these constraints include both pre-depositional and post-depositional cooling episodes for sandstone samples. In discussing implications for regional tectonics here, we focus only on post-depositional episodes, although constraints on pre-depositional cooling of provenance terrains are used to define timing of regional episodes and to provide insight into tectonic events, where appropriate.

For outcrop samples, we can synthesise results from all samples to define the timing of the major cooling events that have affected each region, if we assume that (1) the results represent the effects of regional processes which involved synchronous cooling over wide areas, and (2) episodes in adjacent samples that cooled from similar palaeotemperatures represent common events. Similar reasoning can be applied to samples from a downhole section. The timing of the dominant cooling events in each region and in each borehole are summarised in Figure 3-9 and Table T.5. We emphasise that these intervals define the time at which cooling in each episode began (Fig. 3-7), but we do not suggest that cooling was restricted to within these intervals.

3.5.1 North Greenland

AFTA data in outcrop samples from North Greenland define seven discrete episodes of cooling from elevated palaeotemperatures, in the following intervals:

331–320 Ma	(Carboniferous)
234–229 Ma	(Late Triassic)
173–150 Ma	(Middle–Late Jurassic)
138–75 Ma	(Cretaceous)
60–57 Ma	(Paleocene)
~35 Ma	(end-Eocene)
15–9 Ma	(Miocene)

Evidence for an earlier episode of cooling is seen in the pre-depositional history of sample GC1231-35 (Table T.5), but as this is not seen in any other sample, this is not discussed further. Maps showing the regional variation of palaeotemperatures characterising the seven episodes listed above are shown in Figures 3-10A to 3-16A. In these maps, maximum palaeotemperatures derived from VR data have been attributed to one of the regional cool-

ing episodes by comparison with AFTA data in adjacent samples. The effects of most of these episodes are seen across much of the region, but Paleocene cooling is notable in being restricted to fault zones of the Wandel Sea Basin. Note that in these figures we show only samples in which the effects of these episodes affect their post-depositional history. In many cases these episodes are also recognised in the pre-depositional history of samples in sediment provenance regions

Effects of the **Carboniferous** palaeo-thermal episode are restricted to inland areas and coastal areas in the southeast of the study area (Fig. 3-10A). **Late Triassic** palaeotemperatures show an essentially similar distribution (Fig. 3-11A) but values >110°C for this episode in the southeast are closer to the coast than samples in which the Carboniferous episode is identified. **Middle–Late Jurassic** palaeotemperatures are recognised over a wider area (Fig. 3-12A) and show more variation in magnitude than earlier episodes. Because many samples have been affected by later events (discussed below), evidence for these earlier events is only preserved where the effects of the later events has not been sufficiently severe to overprint them. On the basis of experience in similar regions, we consider it likely that these Paleozoic and Mesozoic exhumation events affected much or all of the study region to a similar degree.

The **Cretaceous** episode is recognised only in one sample from the study area (Fig. 3-13A). This event may correlate with mid-Cretaceous cooling which began between 95 and 90 Ma, and is extensively recognised to the south, between Store Koldewey and Scoresby Sund (Japsen *et al.* 2020b). The extent of this episode within the main study area is not clear. **Paleocene** palaeotemperatures (Fig. 3-14A) are localised within a belt along the north and north-east coastlines running from Kap Washington through Herluf Trolle Land to Nakkehoved and Kilen, coinciding closely with heavily deformed regions mostly within the Wandel Sea Basin. Most of the samples defining Paleocene cooling only began to retain tracks in this episode and provide minimum limits, typically >110°C, to the Paleocene palaeotemperature. The effects of **end-Eocene** cooling are much more widespread than other episodes and are seen in almost all samples across the region (Fig. 3-15A). Paleotemperatures over much of the region, from which samples cooled in this episode are around 60 to 80°C but are higher in coastal regions. Samples from locations north of the Harder Fjord Fault Zone (HFFZ) cooled from palaeotemperatures >100°C at this time. Local cooling from similar palaeotemperatures is seen in samples from Kilen. Because these samples only began to retain tracks in this episode, it is therefore possible that they had previously also undergone major Paleocene cooling, the effects of which are masked or overprinted by the Eocene palaeotemperatures. **Miocene** cooling from palaeotemperatures generally less than 60°C is recognised across a region close to the northern coast (Fig. 3-16A).

From the above discussion, it is clear that the study region has undergone at least seven cooling episodes, some of which are localised while others are more regional. With this in mind it should be emphasised that thermal history solutions derived from AFTA data in individual samples typically allow resolution of only three separate cooling episodes and will be compromised to some extent by the failure to resolve overlapping events.

Definition of these seven episodes of regional cooling confirm and extend the results of our earlier study of North Greenland (Japsen *et al.* 2020a). The additional data have allowed

refinement of some of the timings of individual events. The **Carboniferous (326–320 Ma)** episode replaces early Permian (295–290 Ma) cooling while **Middle–Late Jurassic (173–150 Ma)** cooling replaces Late Jurassic (165–150 Ma) cooling. The revised **Carboniferous** timing is earlier than cooling defined in other areas of Greenland and Scandinavia, while the revised Jurassic timing is closer to events in those regions (Japsen *et al.* 2014, 2016, 2018). The timing of other episodes remain little changed.

Japsen *et al.* (2020a) compiled existing VR data from sedimentary rocks of the Wandel Sea Basin and discussed the regional variation in relation to the AFTA database then available. VR values define maximum post-depositional palaeotemperatures which are consistent with the AFTA data in different palaeo-thermal episodes and in some cases assist in resolving pre-depositional from post-depositional events in some samples. The combination of AFTA and VR data is central for resolving the effects of localised Paleocene palaeo-thermal cooling from >110°C and more regional end-Eocene cooling from ~60–70°C. The conclusions reached by Japsen *et al.* (2020a) are not significantly altered by the new results presented here.

The palaeotemperatures derived from AFTA data characterising different episodes in Figures 3-10A to 3-16A show very different patterns of regional variation which have implications for the processes responsible for the observed cooling (and prior heating). These are discussed in terms of the regional tectonic development of the region in Section 4.

Two apparent anomalies in the AFTA data from samples collected for this study may reflect contamination or possibly mis-labelling of samples or could result from a yet more complex history than already defined from the region. Samples GC1231-32 and -35, from locations around Nakkehoved (Fig. 3-1), gave fission-track ages which are much older than values in nearby samples (Fig. 3-3A), and the thermal histories defined from AFTA data in these sample suggest much lower maximum post-depositional temperatures compared to regional values up to ~300°C in this region. These apparent anomalies may represent sample mis-identification or contamination of samples at some stage of processing. A photograph of the parent sample from which GC1231-32 was taken shows that it was a rounded boulder, and it seems likely that this sample has been transported from a different location. But an alternative explanation is that that some parts of the area may have escaped the heating defined from AFTA and VR data, such that the apparently anomalous thermal histories defined in these samples may indeed represent the thermal history of these locations. Further sampling will be required before such questions can be answered. These samples are not illustrated in the Paleocene palaeotemperature map in Figure 3-14A.

3.5.2 Svalbard

Timing constraints on cooling events identified from AFTA in individual outcrop samples on Svalbard plus samples from the three boreholes on Svalbard from which samples were analysed are compared in Figure 3-9C (results from the boreholes are discussed in Section 3.5.3). Following the procedure discussed in Section 3.5.1 for samples from North Greenland, all constraints from the region can be explained in terms of seven key episodes of cooling which began in the following intervals:

326–269 Ma	(Carboniferous–Permian)
247–210 Ma	(Triassic)
195–143 Ma	(Jurassic)
118–95 Ma	(Aptian–Cenomanian)
72–65 Ma	(Maastrichtian)
46–37 Ma	(Eocene)
11–9 Ma	(Miocene)

The timing of most of these events is similar to cooling episodes defined in samples from North Greenland in Section 3.5.1, and we will return to this aspect in Section 4. As in North Greenland, a single sample defines cooling which began prior to 462 Ma, but this is not considered further.

Svalbard outcrops

Paleotemperatures from which individual outcrop samples cooled in each of the seven regional cooling episodes listed above, defined from AFTA and VR data, are shown in Figures 3-10B to 3-16B. Again, palaeotemperatures derived from VR values have been assigned to different palaeo-thermal episodes on the basis of AFTA data in adjacent samples.

Paleotemperatures characterising both the **Carboniferous–Permian** episode and the **Triassic** episode (Figs 3-10B, 3-11B) are located in a small area of the northern coast of Svalbard. It seems likely that these episodes affected a much greater area, but over much of the region their effects have been overprinted by later events.

Jurassic (Fig. 3-12B) and **Aptian–Cenomanian** (Fig. 3-13B) episodes are registered in samples along the north coast, where many samples cooled from >110°C in these episodes, which will have overprinted the effects of earlier events. Jurassic palaeotemperatures indicate an increase from east to west, with highest values above 110°C in the northwest decreasing to between 77 and 93°C in the northeast. The small number of samples prevents us from drawing any major conclusions in regard to the regional variation in these episodes.

In contrast, **Maastrichtian** palaeo-thermal effects dominate the data in samples along Isfjorden in Figure 3-14B, with palaeotemperatures from AFTA all >110°C. AFTA data in three samples along the north coast also define Maastrichtian palaeotemperatures but are of lower magnitude compared to those along Isfjorden. Maximum palaeotemperatures derived from VR data in samples of pre-Cenozoic depositional age around Isfjorden are generally consistent with Maastrichtian palaeotemperatures from the AFTA data, although one VR value assigned to this episode defines a lower maximum palaeotemperature of 83°C (Table T.2) which is much lower than other values. This is thought to reflect suppression of reflectance due to the nature of the organic matter.

Eocene palaeotemperature constraints (Fig. 3-15B) defined from AFTA are seen only in samples along Isfjorden, with values generally in the range 100–110°C or above, supported by one value of 120°C from VR in a sample of Paleocene depositional age (Table T.2). Another VR value in a sample of Paleocene age assigned to the Eocene episode defines a

maximum palaeotemperature of only 76°C (Table T.2) which is much lower than other values, and is interpreted as due to suppression of reflectance, resulting from the nature of the organic matter in this sample.

Whereas evidence for each of the events discussed so far is to some extent localised, Miocene cooling (Fig. 3-16B) is seen in all samples across the region. While palaeotemperature constraints for individual samples in this episode are quite broad, results shown in Figure 3-16B suggest a possible increase from north to south.

Maastrichtian and **Eocene** palaeotemperatures in many samples are around 100 to 110°C or above, so the previous history in such samples has been overprinted. For this reason, it is uncertain if the effects of the earlier episodes, defined in samples along the north coast where these episodes were less severe, extended to the central regions. **Maastrichtian** cooling from lower palaeotemperatures is identified in some samples from the northwest of the region which retain evidence of **Jurassic** and/or **Aptian–Cenomanian** cooling from higher palaeotemperatures. It therefore seems likely that the effects of at least the **Maastrichtian** episode affected a wider area. The possible extent of **Eocene** palaeo-thermal effects is less clear. Outside the main locus of **Maastrichtian** and **Eocene** palaeo-thermal effects, it is possible that palaeotemperatures were too low to be resolved from Miocene values.

AFTA data in two outcrop samples from Bjørnøya provide constraints which are consistent with the **Maastrichtian** and **Miocene** events defined from the full data set in Figure 3-9C. No new VR data from Bjørnøya were obtained for this study. Ritter *et al.* (1996) published VR values in outcrop samples from Bjørnøya varying in depositional age from Triassic to Devonian. Regardless of depositional age, VR values are quite uniform, varying between 1.0% and 1.5%, indicating maximum post-depositional palaeotemperatures between 143 and 170°C. AFTA data in the two samples define **Maastrichtian** palaeotemperatures >105°C, so it is not clear if this event is the post-depositional maximum, or if the VR data may represent an earlier event which was overprinted in the AFTA data by the **Maastrichtian** event.

Svalbard boreholes

As illustrated in Figure 3-17, AFTA data in samples from the three boreholes define constraints which are consistent with the three most recent episodes of cooling defined from the full dataset.

In the **Sysselmannbreen** borehole, the **Maastrichtian** episode is recorded in samples of latest Paleocene to early Eocene depositional ages. This episode is interpreted as representing pre-depositional cooling in sedimentary provenance terrains, while **Eocene** and **Miocene** cooling episodes are both clearly post-depositional. Paleotemperature constraints derived from AFTA and VR in samples from this borehole are plotted against depth (below kb) in Figure 3-17A. Maximum post-depositional palaeotemperatures derived from VR data are highly consistent with the **Eocene** palaeotemperatures derived from AFTA data at similar depths, and the combined dataset can be described by a linear profile, sub-parallel to the present-day temperature profile but offset to higher temperatures by ~80–90°C. **Miocene** palaeotemperatures defined by AFTA can also be described by a similar profile but

offset by ~50°C from the present-day temperature profile. These profiles suggest that heating and cooling can be explained largely by deeper burial and exhumation, respectively, with little or no significant change in basal heat flow through time. This is consistent with the lack of post-early Eocene rocks in this borehole.

In samples of Carboniferous to Early Cretaceous depositional ages, from the **Reindalspasset (7816/12-1) borehole,** the **Maastrichtian, Eocene** and **Miocene** cooling episodes (Fig. 3-17B) are all clearly post-depositional. Paleotemperature constraints derived from AFTA and VR data in samples from this borehole are plotted against depth in Figure 3-17B. The maximum post-depositional palaeotemperatures derived from VR data are highly consistent with the **Maastrichtian** palaeotemperatures derived from AFTA data at similar depths, and again the combined dataset can be described by a linear profile, subparallel to the present-day temperature profile but offset to higher temperatures by ~120°C. **Eocene** and **Miocene** palaeotemperatures defined by AFTA can also be described by similar profiles but offset by ~70°C and ~45°C, respectively, from the present-day temperature profile. These profiles suggest a similar explanation as that suggested for the Sysselmannbreen borehole, in terms of heating and cooling largely by deeper burial and exhumation, respectively. Such an interpretation is consistent with the presence of a major unconformity between Lower Cretaceous and Quaternary rocks in this borehole, representing the approximate interval 130 to 2.5 Ma.

AFTA data in two samples from the **Radderdalen borehole** with Paleozoic depositional ages (combined into one sample for interpretation due to low apatite yields in the two samples), define constraints which are consistent with the **Maastrichtian** and **Miocene** episodes (Fig. 3-9). Vitrinite reflectance data from this borehole are too scattered to allow a detailed reconstruction, but values at similar depth to the AFTA samples define maximum palaeotemperatures that are broadly consistent with the **Maastrichtian** palaeotemperature constraint defined from AFTA, suggesting that this event defines the post-depositional palaeo-thermal maximum in the section intersected in this borehole. These **Maastrichtian** palaeotemperatures have overprinted the effects of any earlier events during the time interval represented by the lower Permian to Quaternary unconformity in this borehole, representing the approximate interval 280 to 2.5 Ma.

3.6 Burial/uplift history reconstructions in Svalbard boreholes

Quantitative analysis of the palaeotemperature profiles defined from AFTA and VR data in the **Sysselmannbreen** and **Reindalspasset** boreholes, in terms of the range of palaeogeothermal gradients allowed by the palaeotemperature constraints in each episode within ±95% confidence limits, and the corresponding amounts of additional burial required to explain the palaeotemperatures, are summarised in Figure 3-18. In both boreholes the range of allowed palaeo-gradients in each episode encompasses the present-day thermal gradient (30°C/km for **Sysselmannbreen**, 28°C/km for **Reindalspasset**), suggesting that an interpretation involving heating due to deeper burial and subsequent cooling due to exhumation (together with a small component due to change in surface temperature) provides an acceptable explanation of the palaeotemperature constraints. However, Figure 3-18

emphasises that a range of scenarios can explain the results from each borehole. In particular, the present-day thermal gradient of 30°C/km in the **Sysselmannbreen** borehole lies at the extreme of the allowed range for the **Eocene** event, and it is possible that the palaeogeothermal gradient in this well when cooling began at ~35 Ma may have been slightly higher than the present-day value.

Reconstructed burial/uplift histories for the **Sysselmannbreen** and **Reindalspasset** boreholes, based on the constraints illustrated in Figure 3-18 are shown in Figure 3-19. To illustrate the limitations on such reconstructions where multiple episodes occur within intervals represented by a single unconformity (Fig. 3-20), the two reconstructions have been made using different approaches. In the **Syssellmannbreen** borehole (Fig. 3-19A), the reconstruction is based on a scenario in which no re-burial took place between the two cooling (exhumation) events. In such situations it is important to realise that the total amount of reburial between multiple episodes cannot be defined, and only the amount of additional section present at the onset of cooling in each event is determined by the AFTA and VR data. Even then, estimation of these amounts is subject to a range of assumptions, the most critical being the linearity of palaeotemperature profiles through the now removed section (see Green & Duddy 2012). Table 3-01 provides a summary of the estimated magnitudes of additional burial of the sections penetrated by the Sysselmannbreen and Reindalspasset boreholes during the palaeo-thermal peaks defined by AFTA and VR data.

In contrast, the reconstruction for the **Reindalspasset** reconstruction (Fig. 3-19B) involves some amount of re-burial between the three exhumation events. Since Paleogene sediments are present to the west of the borehole location some degree of burial seems likely following **Maastrichtian** exhumation and prior to the onset of **Eocene** exhumation. However, the total amount of section removed during **Maastrichtian** exhumation, and the amount of reburial prior to Eocene exhumation, cannot be determined.

To further illustrate the range of possible reconstructions that are compatible with the palaeotemperature constraints derived from the AFTA and VR data in these boreholes, the reconstruction for the **Syssellmannbreen** borehole in Figure 3-19A employs an elevated **Eocene** palaeogeothermal gradient, decreasing to a value equal to the present-day thermal gradient when Miocene cooling began, while the reconstruction for the **Reindalspasset** borehole in Figure 3-19B involves a constant geothermal gradient throughout the history. As emphasised previously, a wide range of possible reconstructions is allowed and independent constraints from geological evidence is required in order to restrict the range of realistic scenarios.

Table 3-01. Summary of the estimated magnitudes of additional burial of the sections penetrated by the Sysselmannbreen and Reindalspasset boreholes during the palaeo-thermal peaks defined by AFTA and VR data.

Additional burial (km)	**Maastrichtian**	**End-Eocene**	**Late Miocene**
Sysselmannbreen (km)		**2.1 (2.0-2.3)**	**1.5 (1.4-1.8)**
Gradient (C/km)		*35*	*30*
Reindalspasset (km)	**4.1 (3.8-4.6)**	**2.1 (1.9-2.3)**	**1.2 (0.9-1.4)**
Gradient (C/km)	*28*	*28*	*28*
Surface temperature (°C)	20	20	10

Parameters used in the reconstructions shown in Figure 3-19 (upper numbers).
Range of removed section from Figure 3-18 (lower numbers).

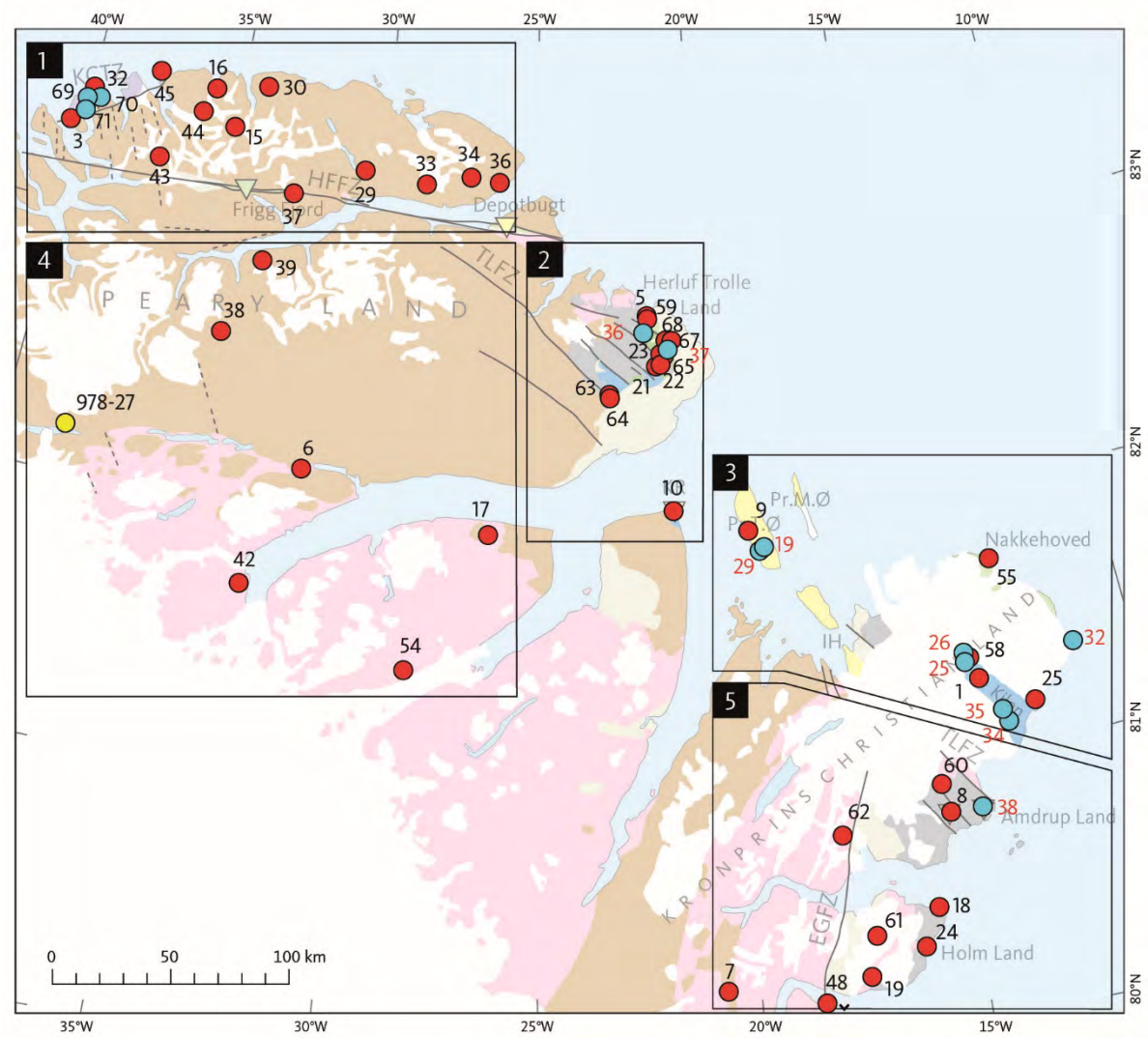

Figure 3-1. Locations of outcrop samples with AFTA data from North Greenland. VR Locations shown in Figure 3-5A. **Yellow circle**: GC978 sample. **Red circles**: GC1113 samples. **Cyan samples**: GC1231 samples.

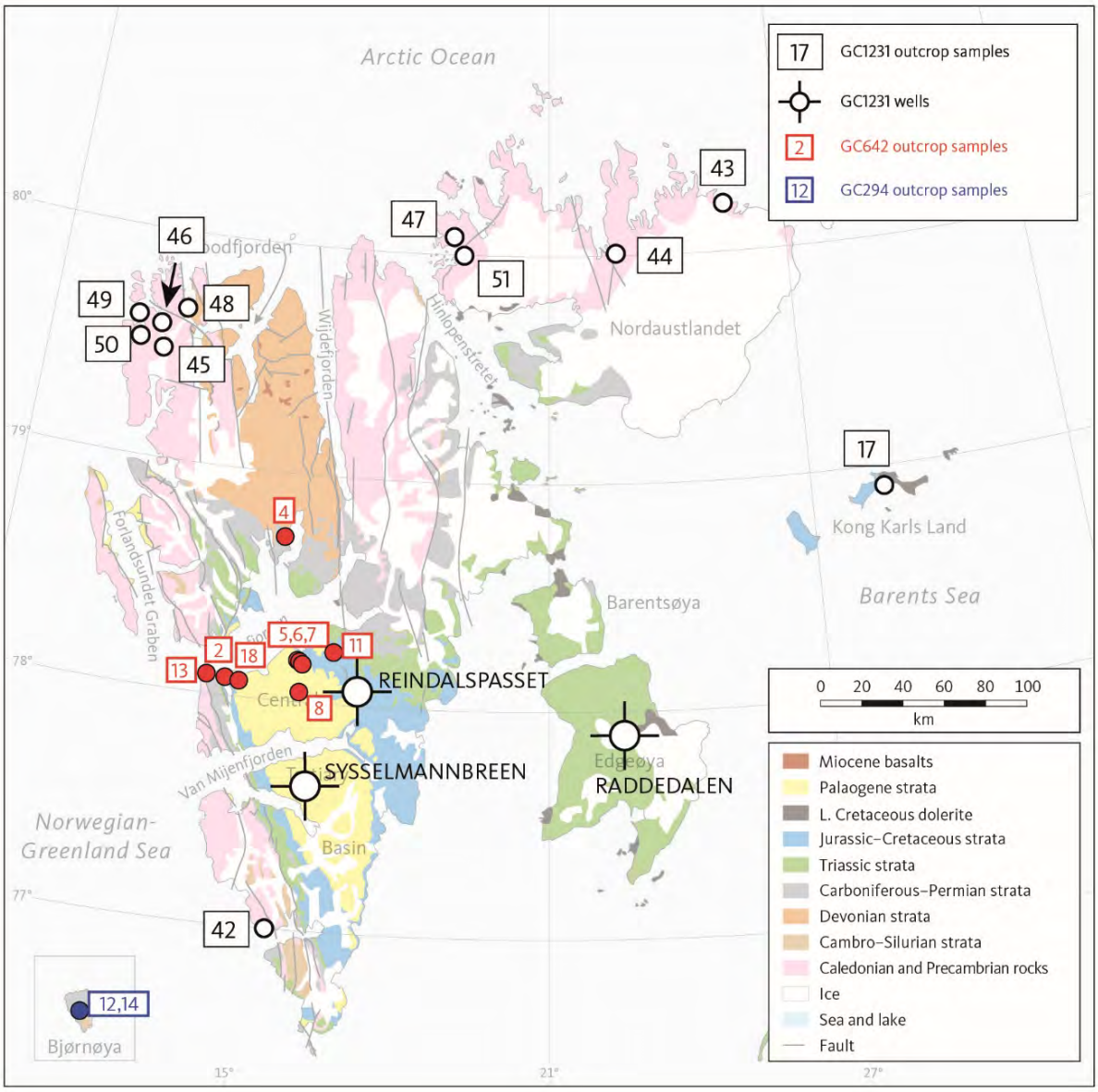

Figure 3-2. Locations of outcrop samples and wells with AFTA data from Svalbard. VR Locations shown in Figure 3-5B.

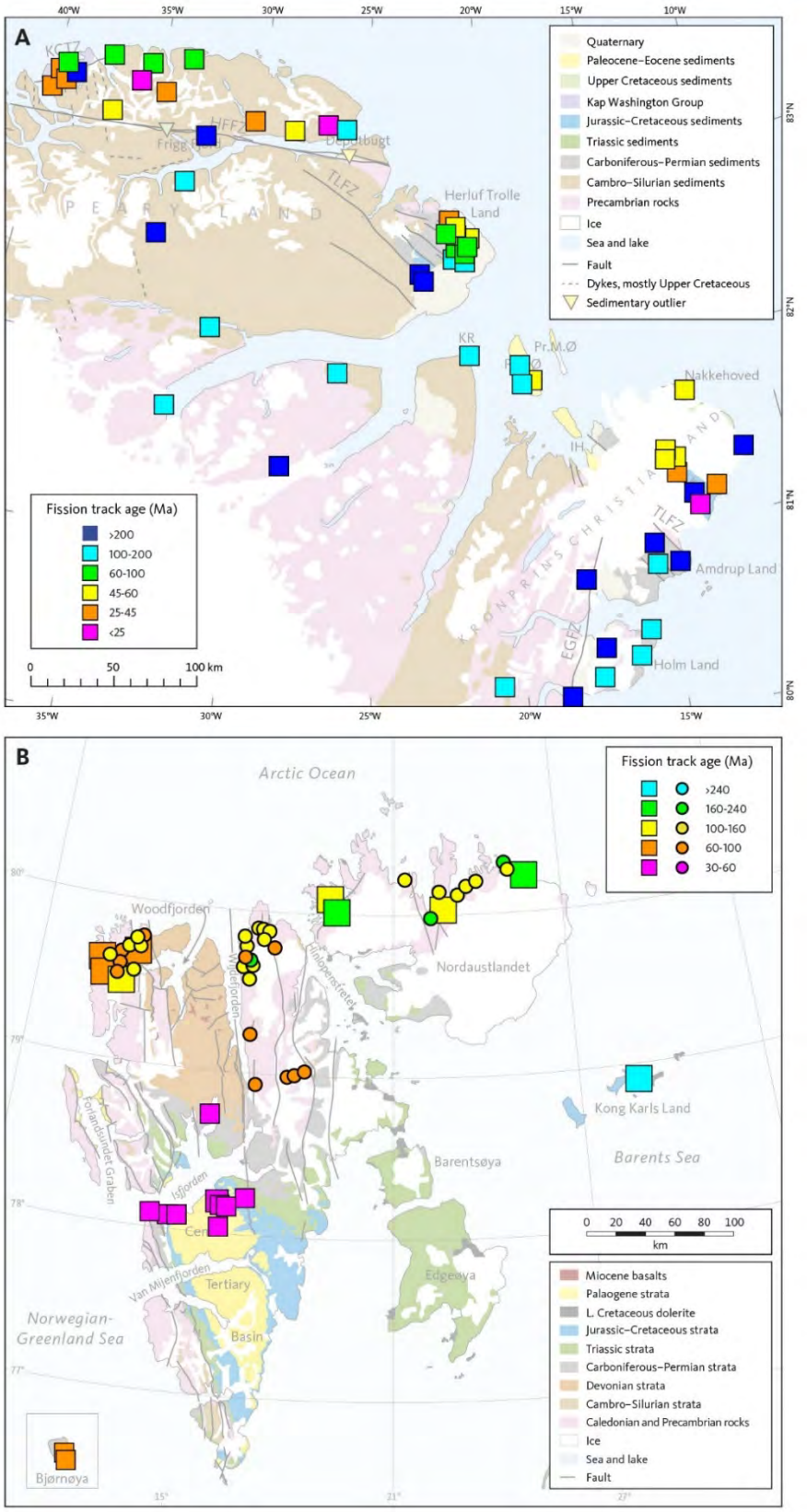

Figure 3-3. Apatite fission track ages measured in samples from outcrop locations in this study. **A** North Greenland, including samples reanalysed from GC1113 and new samples analysed for this report. **B**. Svalbard, together with published data from Dörr et al. (2012, 2019). **Squares**: this study. **Circles**: Dörr et al. (2012, 2019).

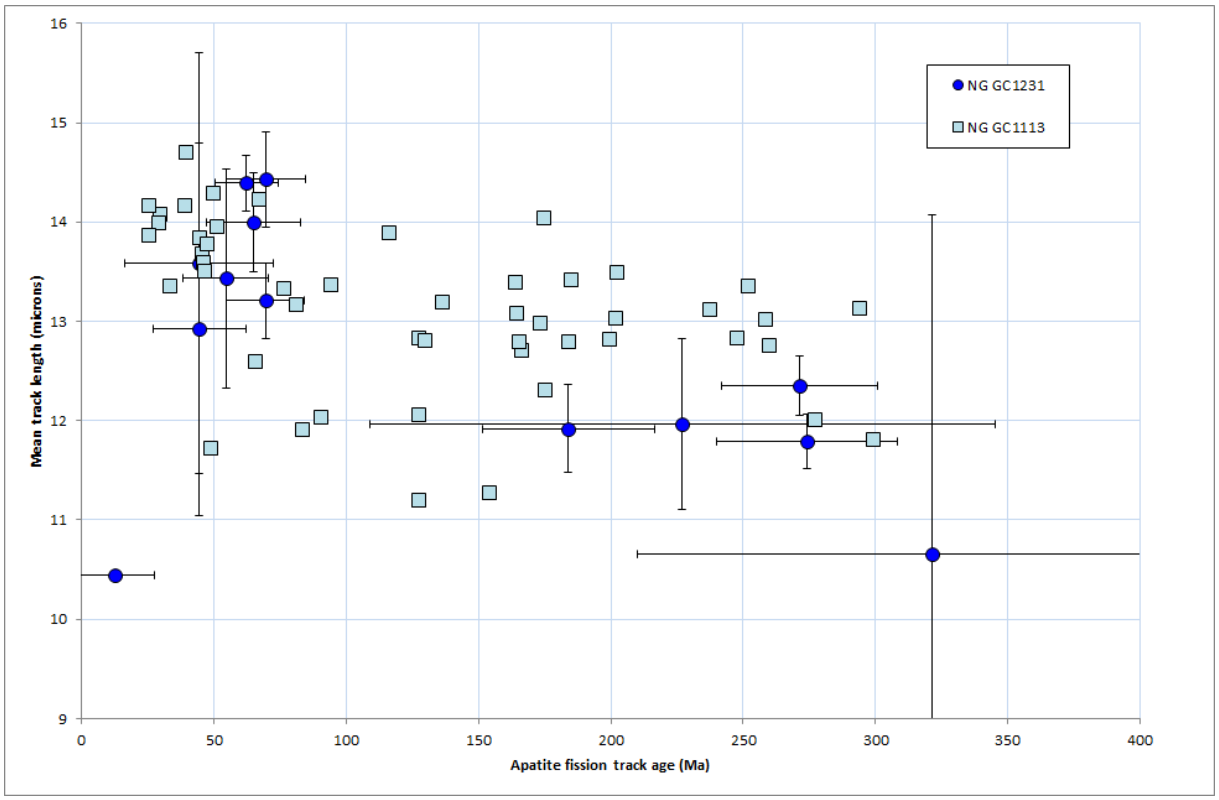

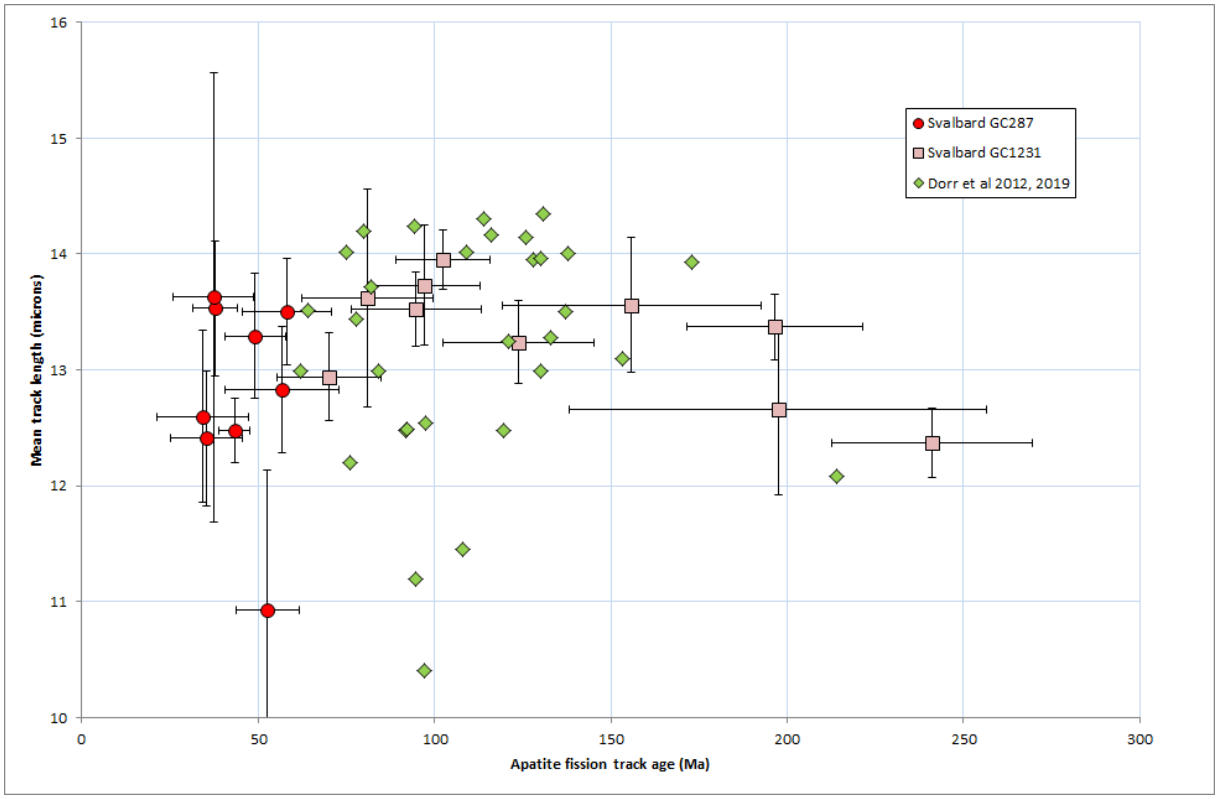

Figure 3-4. Relationship between mean track length and fission track age measured in samples from outcrops. **Upper panel**: North Greenland. **Lower panel**: Svalbard, together with data from Dörr et al. (2012, 2019).

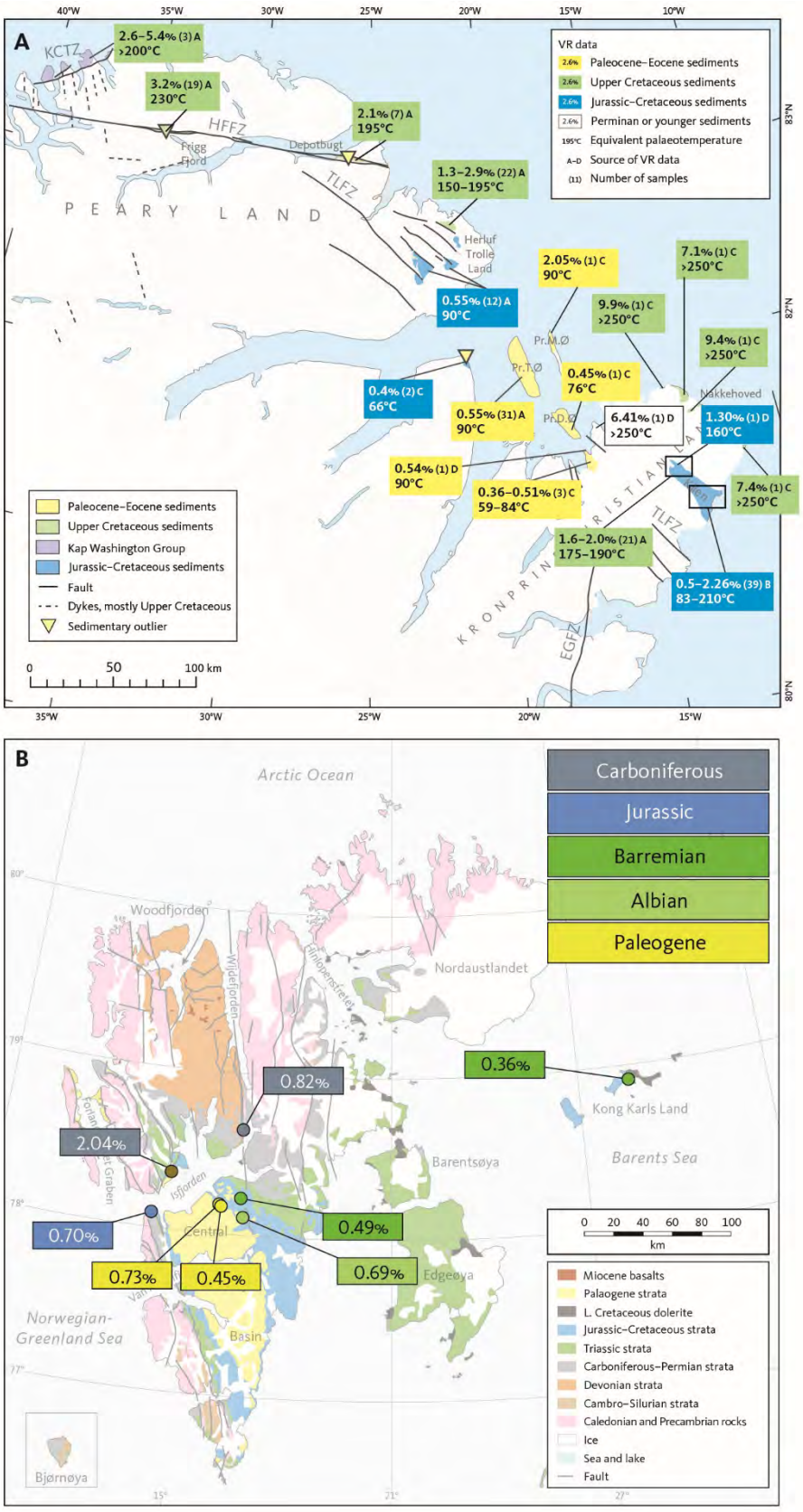

Figure 3-5. VR values in outcrops. **A**. North Greenland. Data from Japsen et al. 2020a. and new values from this report. **B**. Svalbard.

A

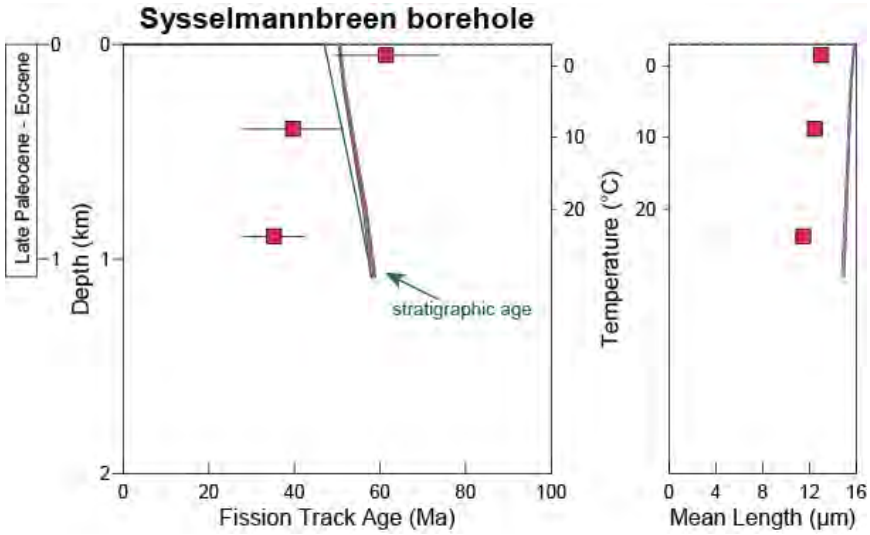

B

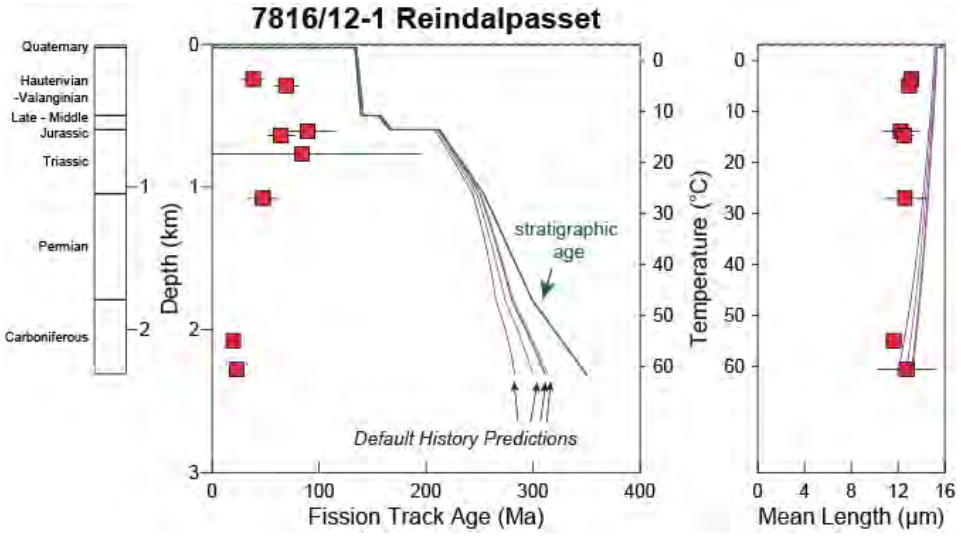

C

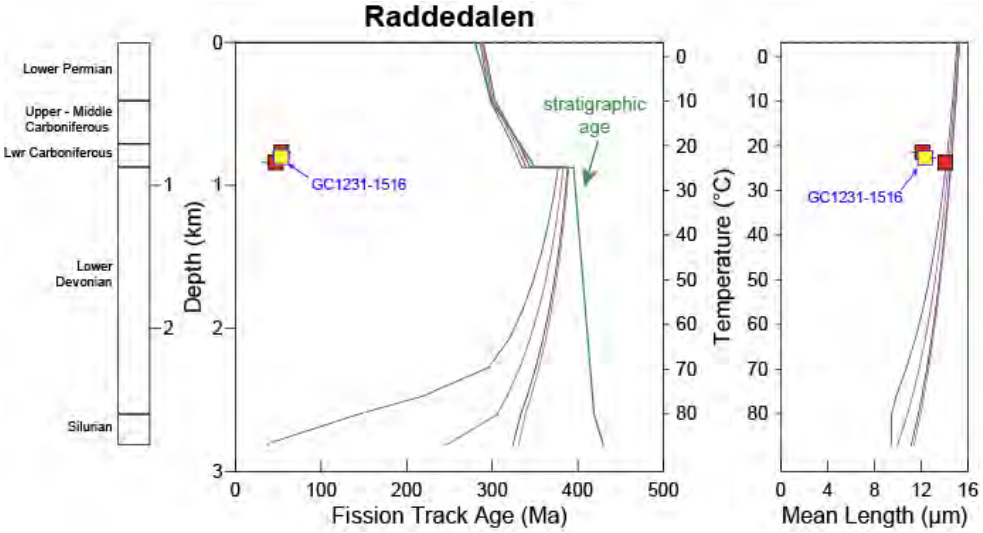

Figure 3-6. AFTA parameters for samples from boreholes plotted against sample depth and present-day temperatures. **A**: Sysselmannbreen. **B**: Reindalspasset. **C**: Radderdalen.

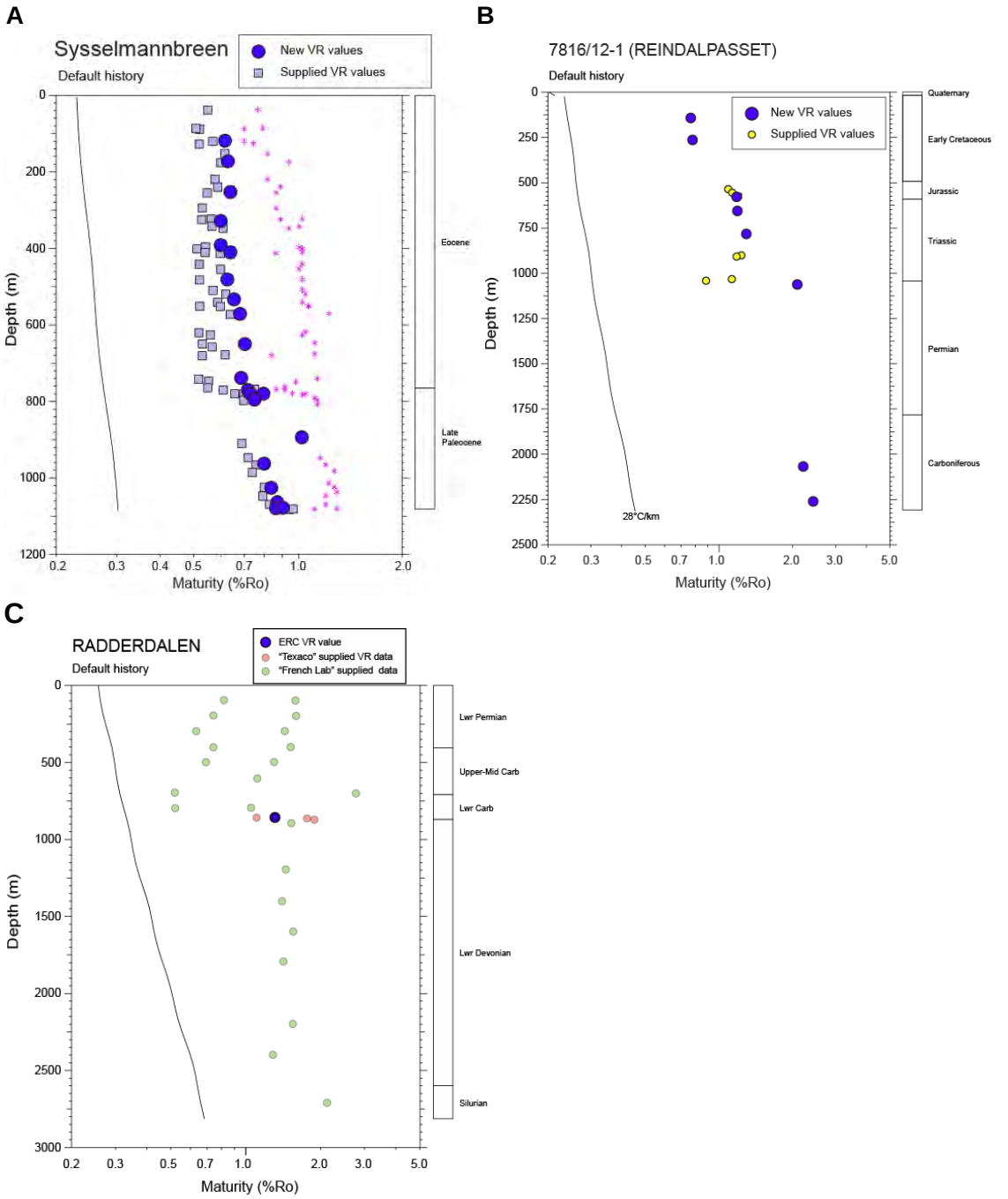

Figure 3-7. Mean VR values in boreholes. **A**: Sysselmannbreen. **B**: Reindalspasset. **C**: Radderdalen. ERC: New VR value supplied by ERC.

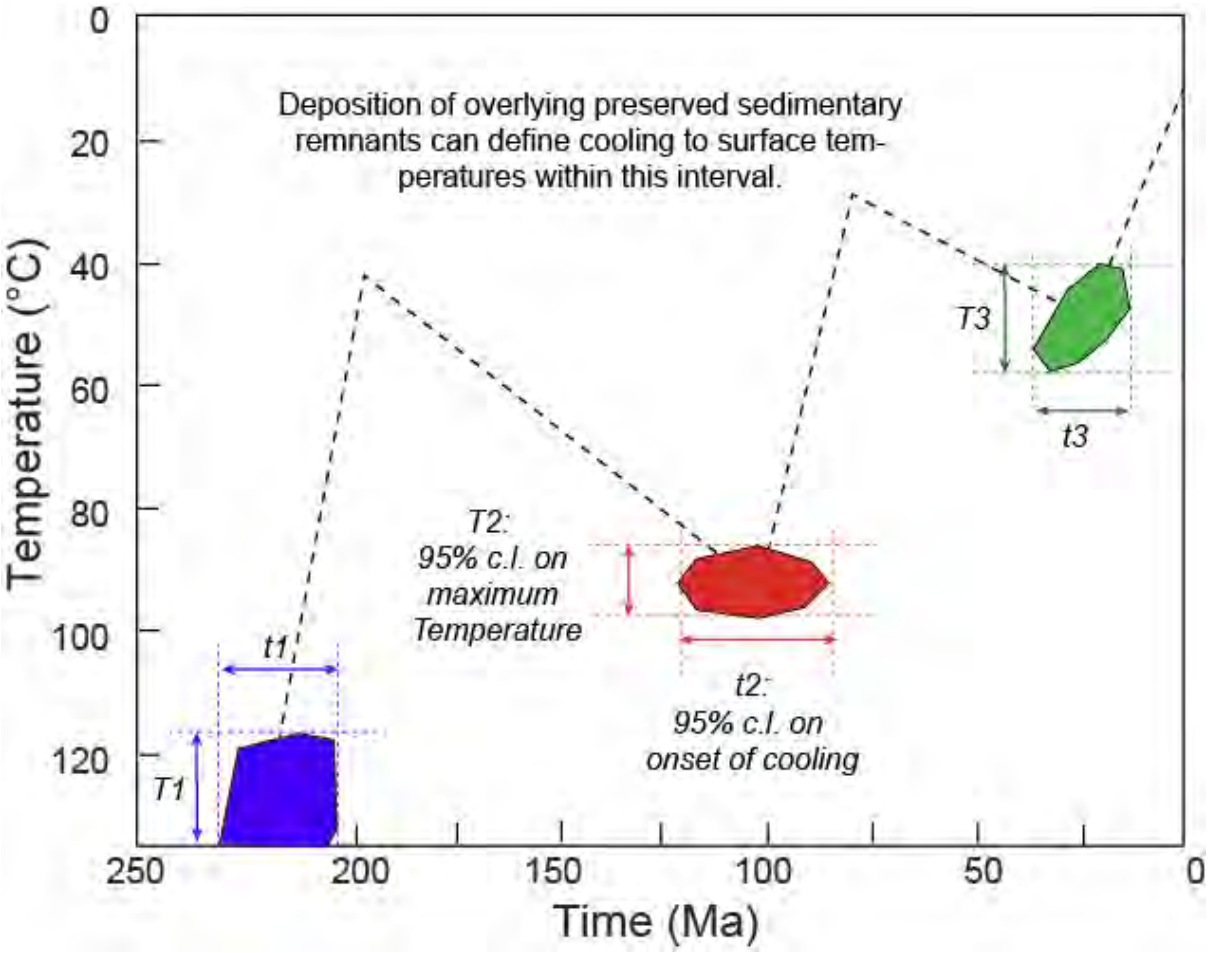

Figure 3-8. Illustration of thermal history solutions extracted from AFTA data. Results are presented in terms of up to three palaeo-thermal episodes, i.e. times when a rock sample was hotter than it is today. Note that the palaeotemperature constraint T1 is a minimum estimate because this is the event in which the apatites begin to retain tracks. In most situations, three events are the most that can be defined from AFTA, due to various factors including the natural spread in track lengths of a single population of tracks and the rapid decrease in the rate of annealing across the range from ~110°C to below 60°C.

A

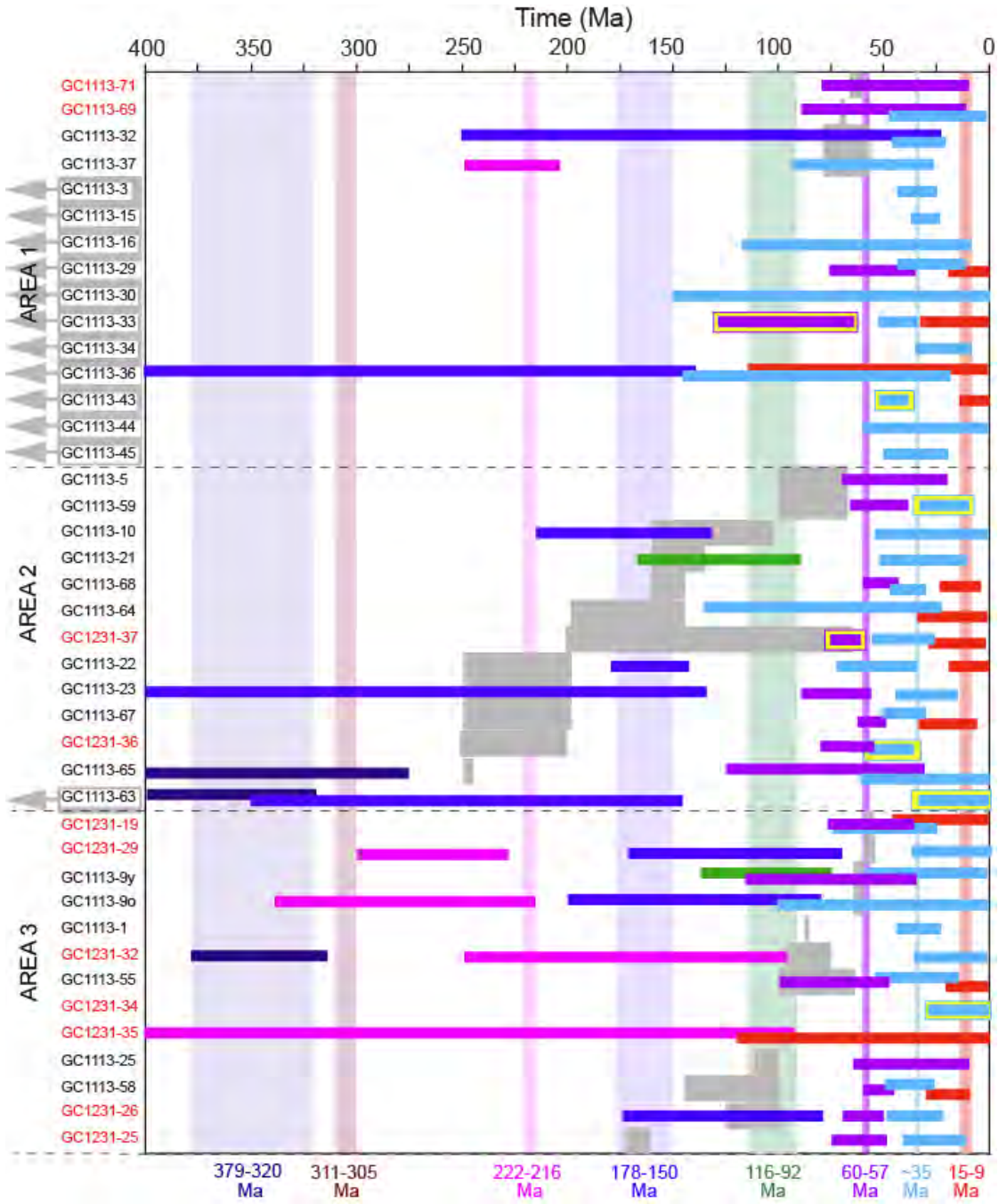

Figure 3-9. Timing constraints on the onset of cooling in multiple palaeo-thermal episodes, derived from AFTA data. **A**: North Greenland Areas 1–3. **B**: North Greenland Areas 4–5. **C**: Svalbard. **B'noya**: Bjørnøya. **Rad**: Radderdalen borehole. **Sysell**: Sysselmannbreen borehole.
(Subsequent pages).

B

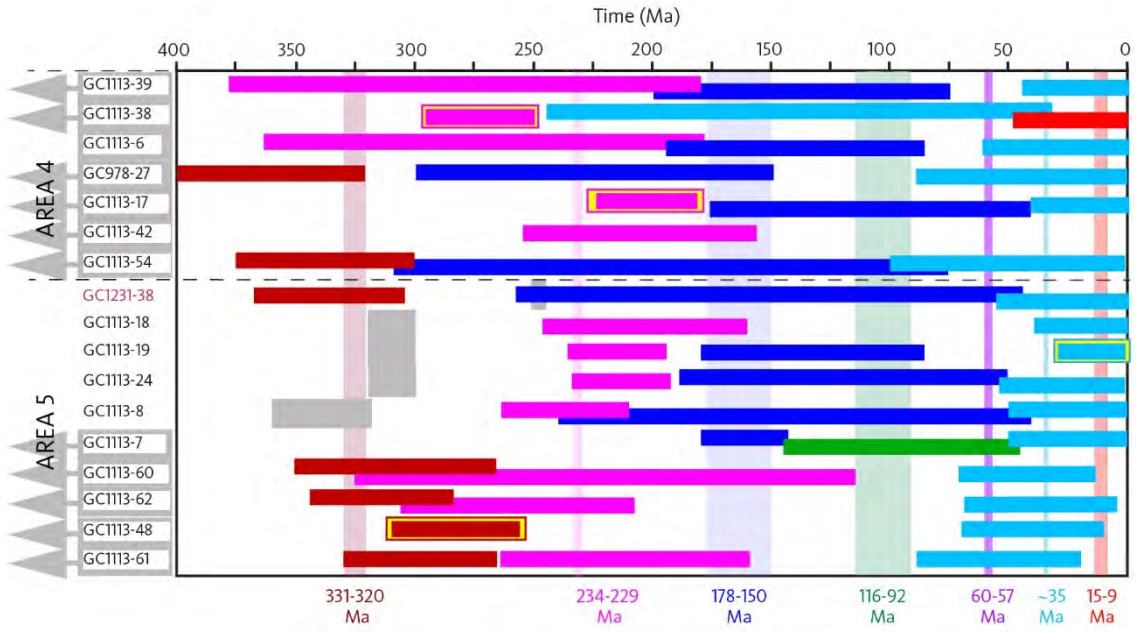
Time (Ma)
400
350
300
250
200
150
100
50
0
AREA 4
GC1113-39
GC1113-38
GC1113-6
GC978-27
GC1113-17
GC1113-42
GC1113-54
AREA 5
GC1231-38
GC1113-18
GC1113-19
GC1113-24
GC1113-8
GC1113-7
GC1113-60
GC1113-62
GC1113-48
GC1113-61
331-320 Ma
234-229 Ma
178-150 Ma
116-92 Ma
60-57 Ma
~35 Ma
15-9 Ma

C

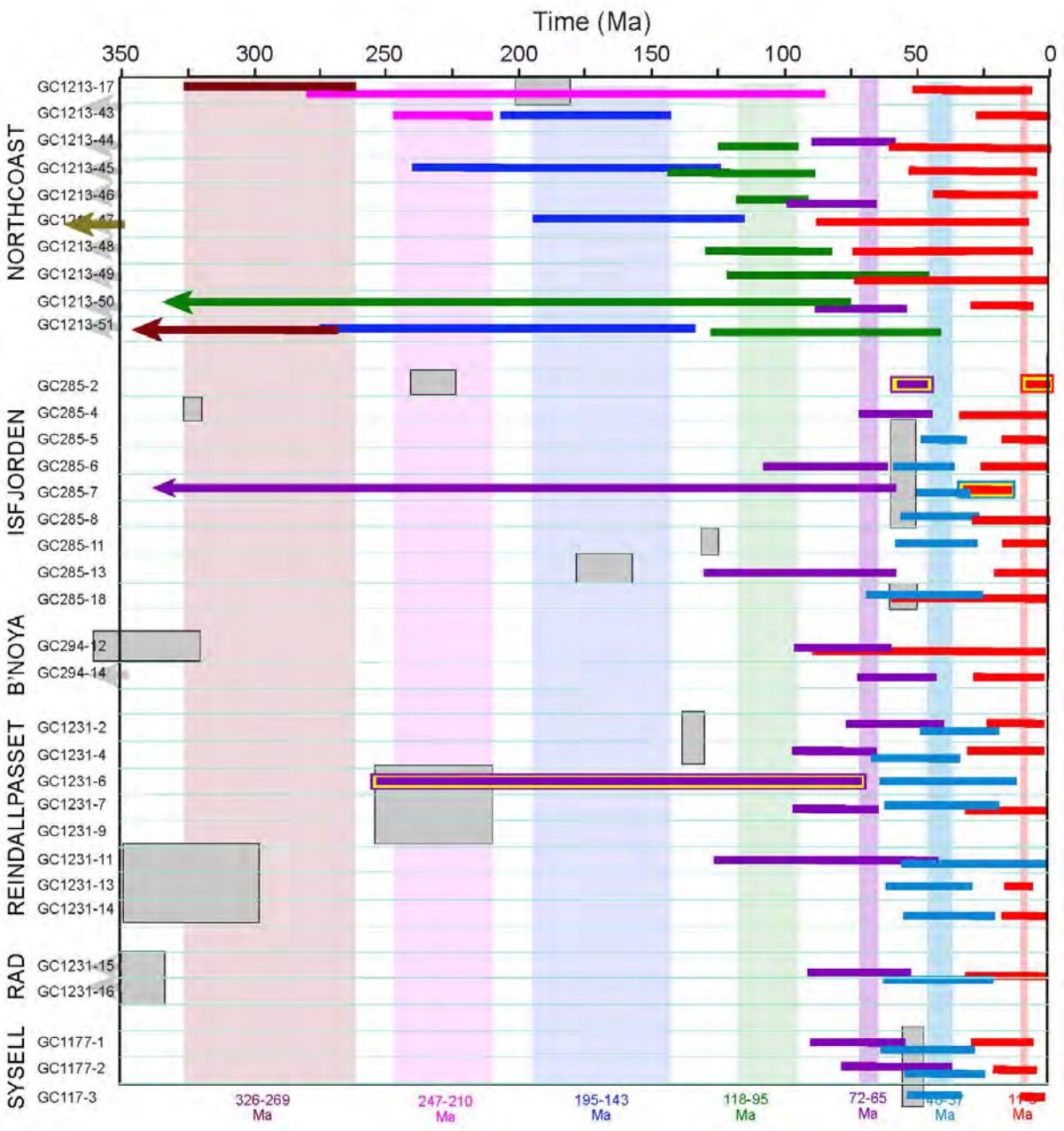
Time (Ma)
350
300
250
200
150
100
50
0
NORTHCOAST
GC1213-17
GC1213-43
GC1213-44
GC1213-45
GC1213-46
GC1213-48
GC1213-49
GC1213-50
GC1213-51
ISFJORDEN
GC285-2
GC285-4
GC285-5
GC285-6
GC285-7
GC285-8
GC285-11
GC285-13
GC285-18
B'NOYA
GC294-12
GC294-14
REINDALLPASSET
GC1231-2
GC1231-4
GC1231-6
GC1231-7
GC1231-9
GC1231-11
GC1231-13
GC1231-14
RAD
GC1231-15
GC1231-16
SYSELL
GC1177-1
GC1177-2
GC117-3
326-269 Ma
247-210 Ma
195-143 Ma
118-95 Ma
72-65 Ma

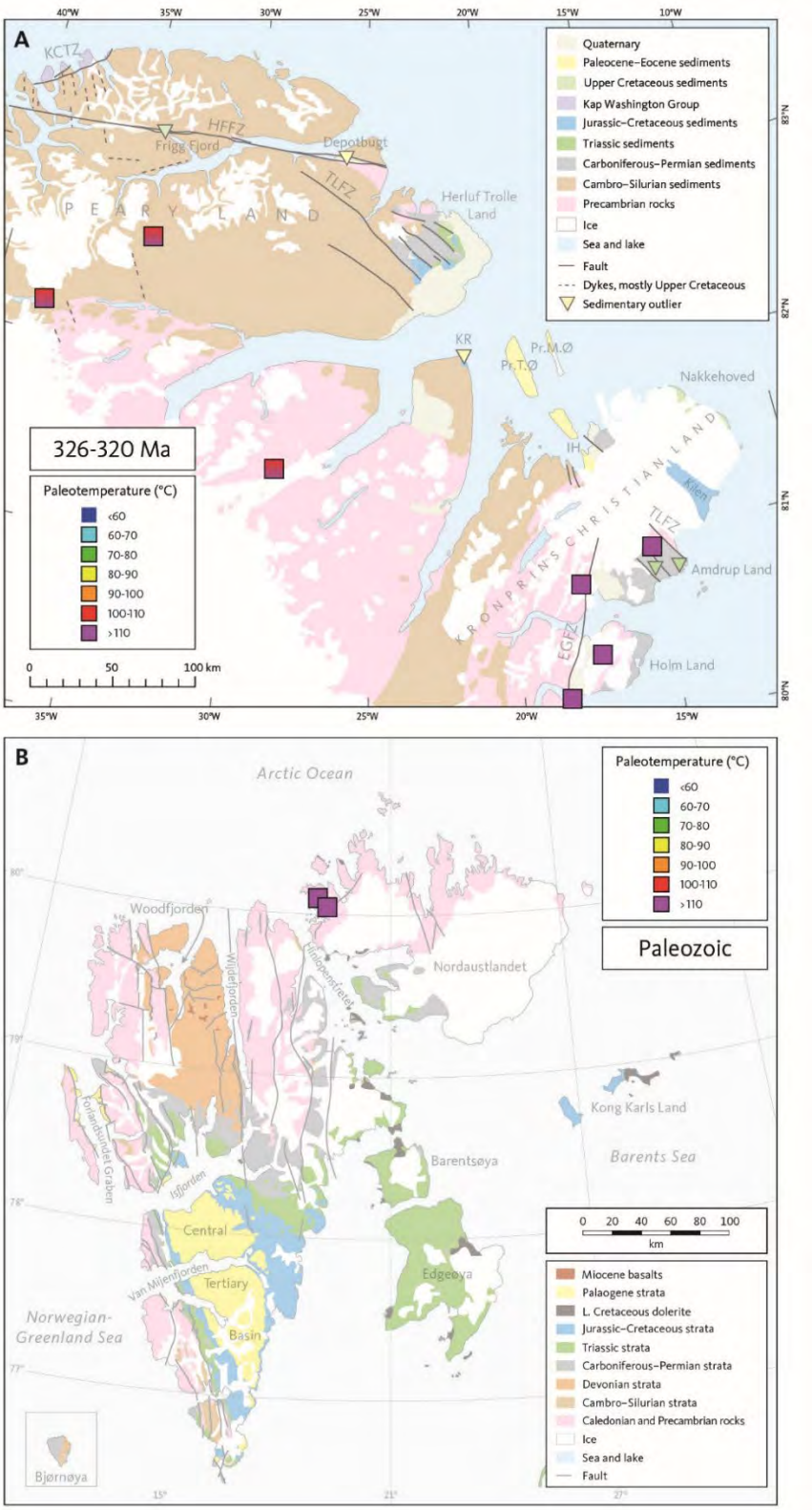

Figure 3-10. Paleotemperatures derived from AFTA data in outcrop samples. **A**. North Greenland, mid-Carboniferous (326–320 Ma). **B**. Svalbard, Carboniferous–Permian (326–269 Ma) and >426 Ma. The overlapping time intervals for the late Paleozoic events, indicate that mid-Carboniferous (326–320 Ma) cooling affected both parts of the study area. For sample numbers see Figs 3-1 and 3-2, respectively.

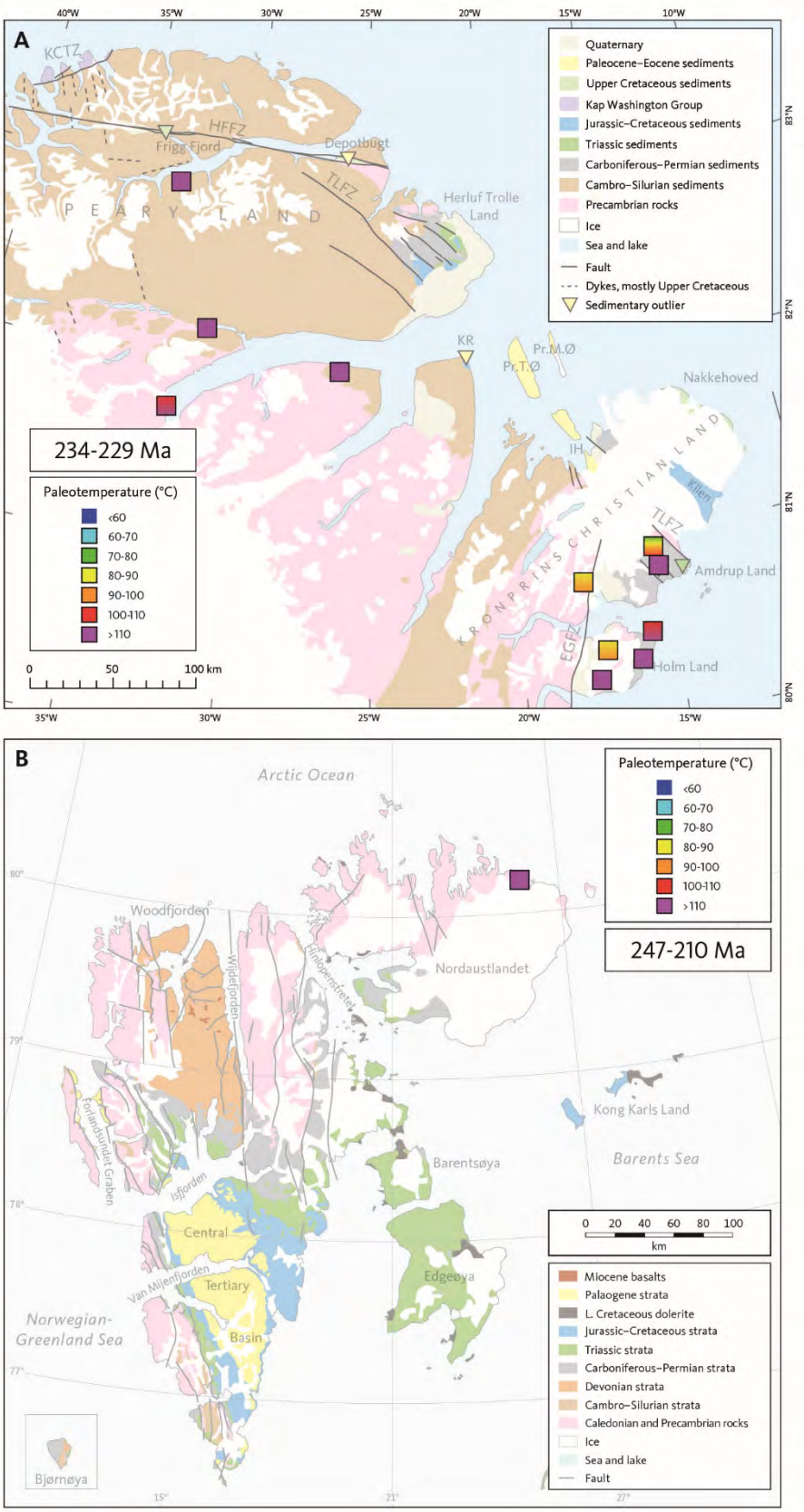

Figure 3-11. **Late Triassic (234–229 Ma)** palaeotemperatures derived from AFTA data in outcrop samples. **A**. North Greenland. **B**. Svalbard. For sample numbers see Figs 3-1 and 3-2, respectively.

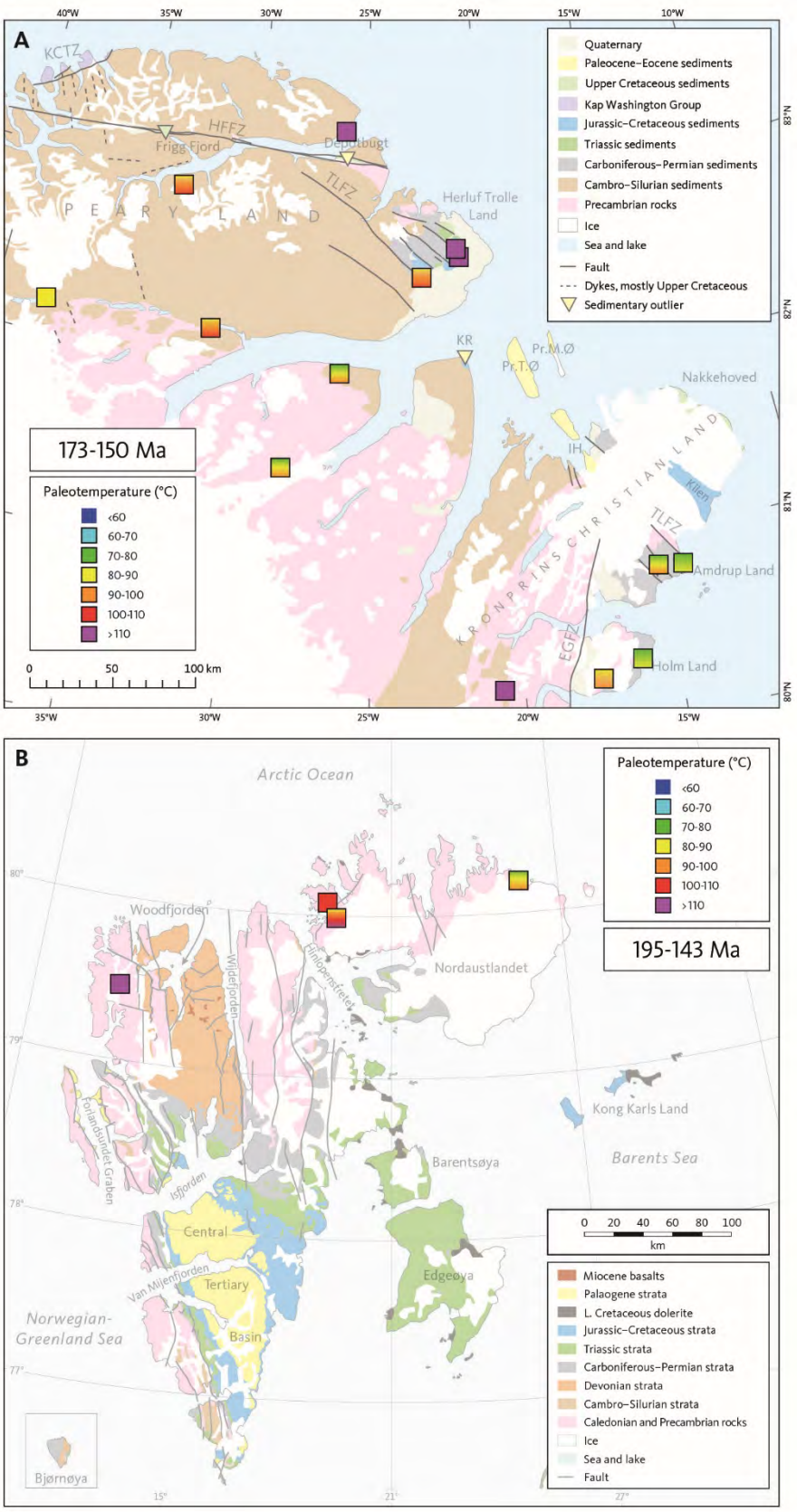

Figure 3-12. **Jurassic (173–150 Ma)** palaeotemperatures derived from AFTA data in outcrop samples. **A**. North Greenland. **B**. Svalbard. For sample numbers see Figs 3-1 and 3-2, respectively.

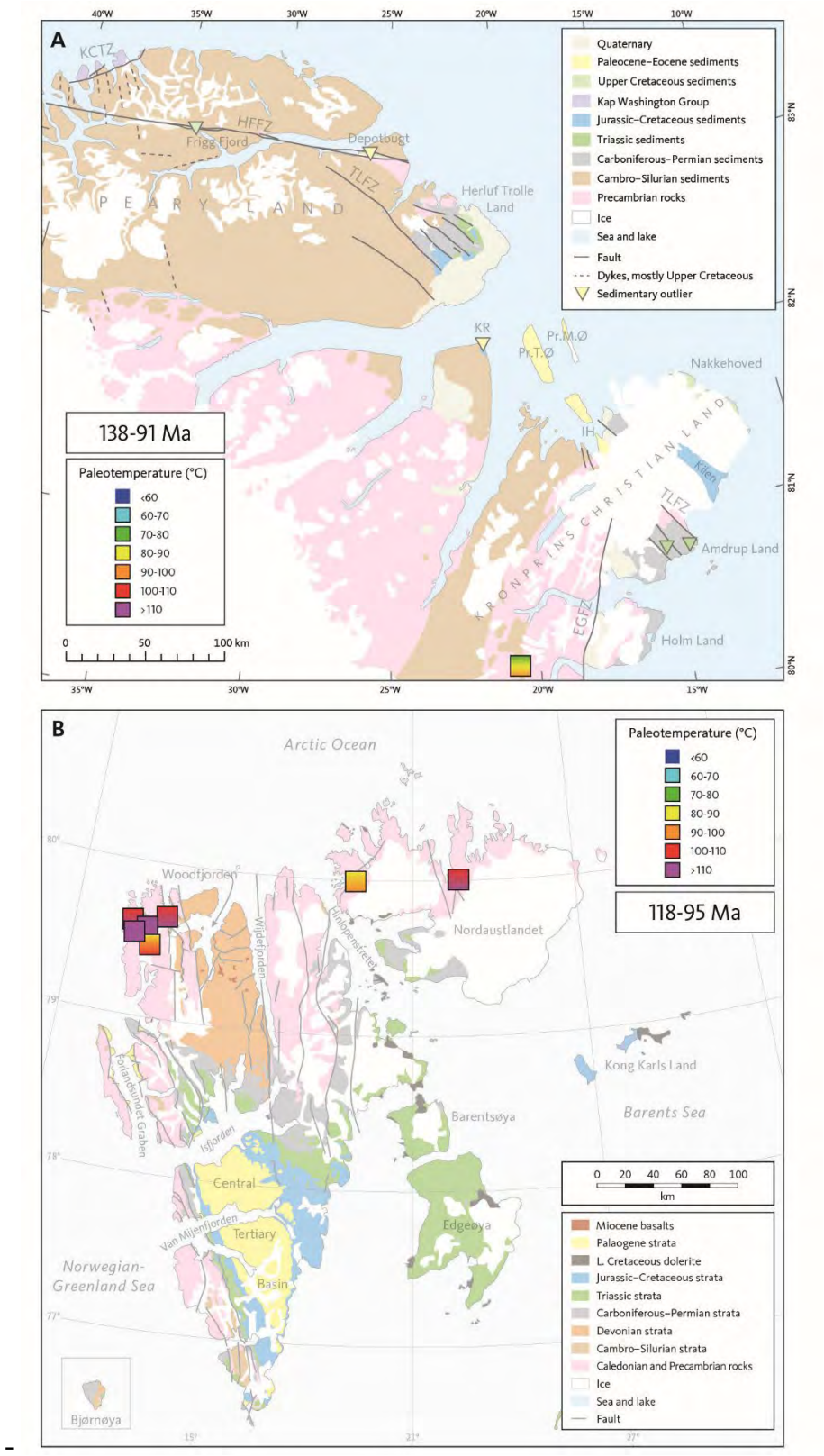

Figure 3-13. **Mid-Cretaceous (118–95 Ma)** palaeotemperatures derived from AFTA data in outcrop samples. **A**. North Greenland. **B**. Svalbard. For sample numbers see Figs 3-1 and 3-2, respectively.

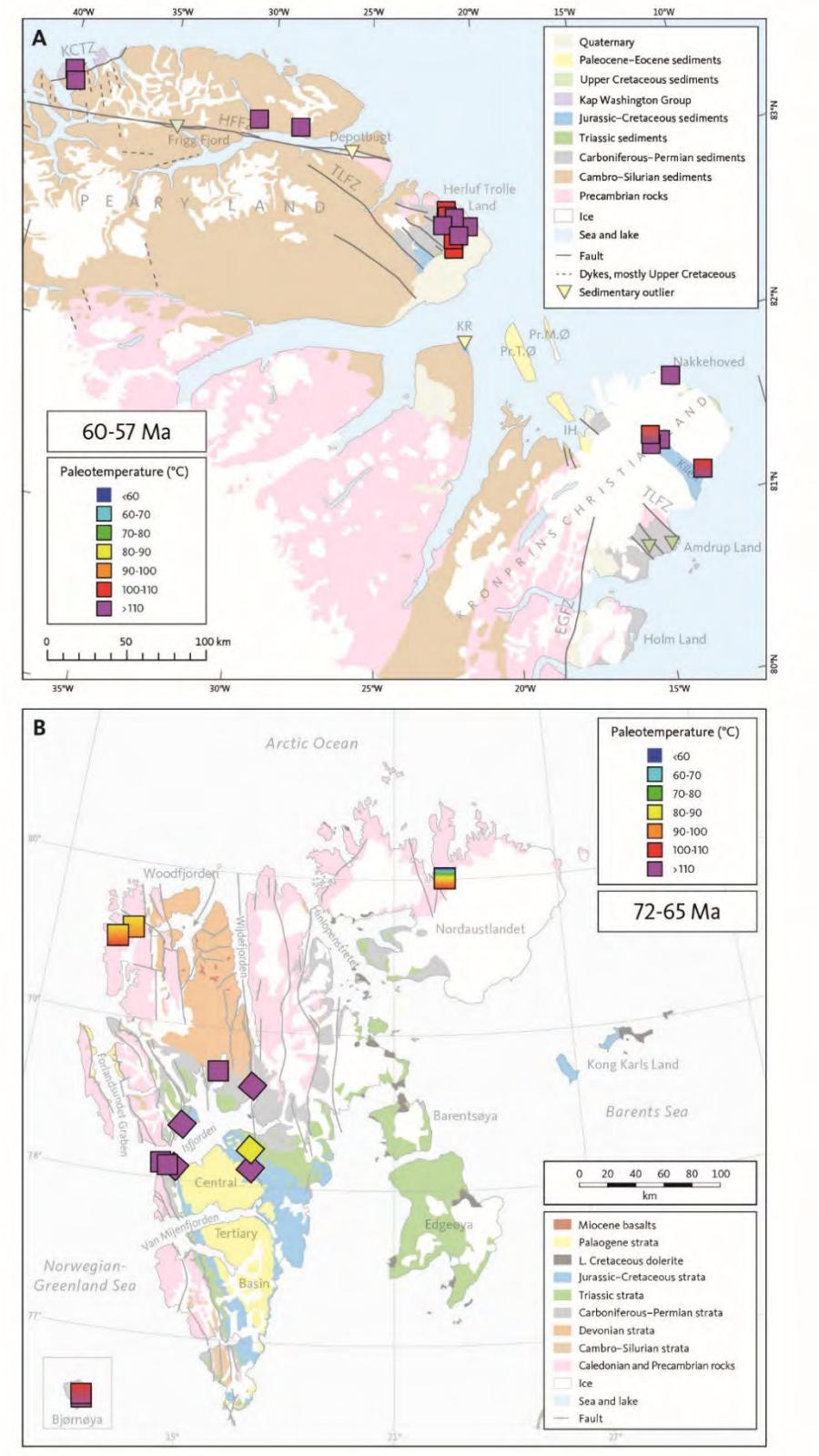

Figure 3-14. Paleotemperatures derived from AFTA data in outcrop samples. **A**. North Greenland, mid-Paleocene (60–57 Ma). **B**. Svalbard, Maastrichtian (72–65 Ma). Note that these time intervals do not overlap, thus indicating cooling during two different episodes. **Squares**: Values from AFTA. **Diamonds**: values from VR. For sample numbers see Figs 3-1 (North Greenland), 3-2 and 3-5B (Svalbard).

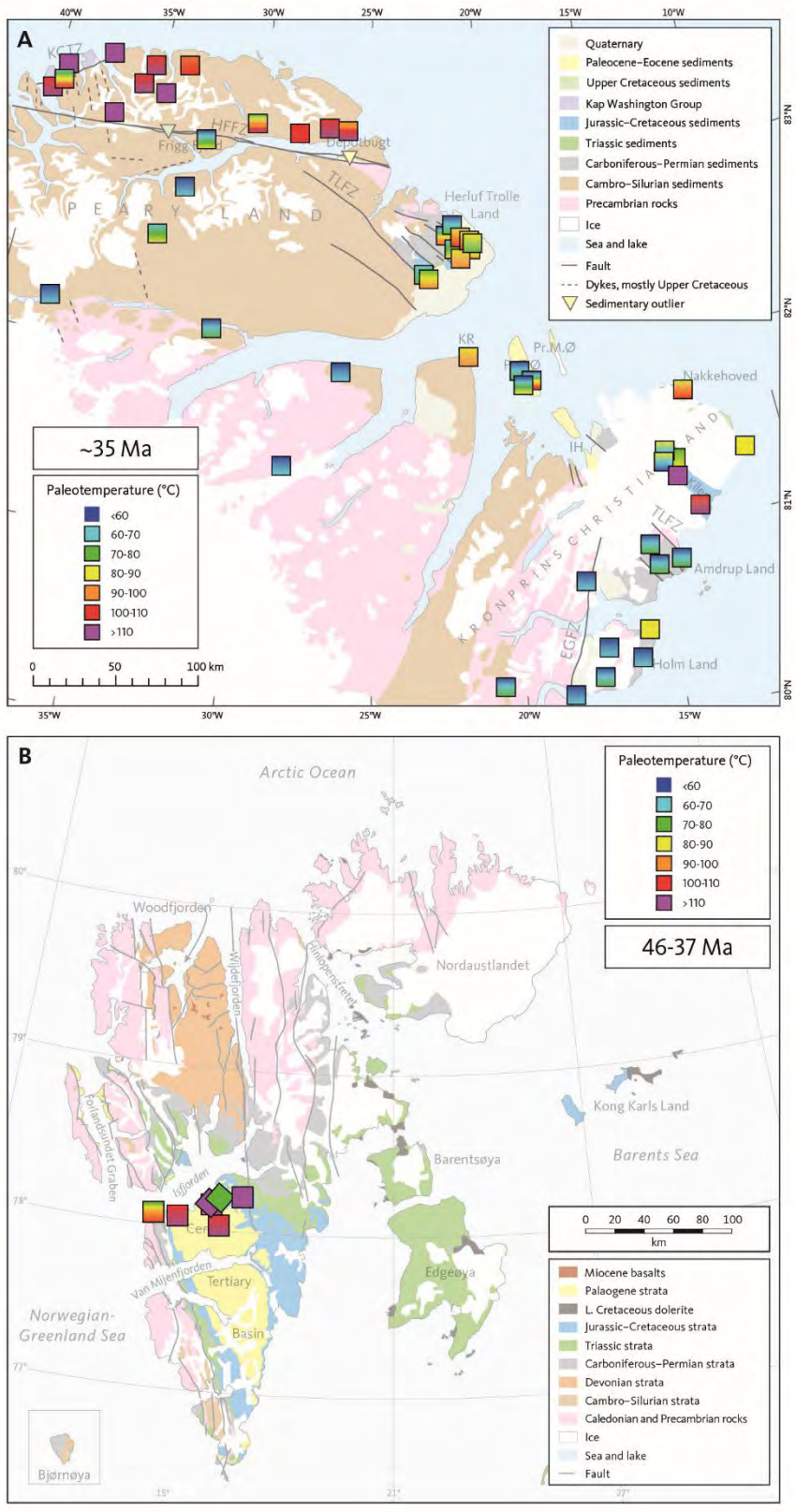

Figure 3-15. **End-Eocene (~35 Ma)** palaeotemperatures derived from AFTA data in outcrop samples. **A**. North Greenland. **B**. Svalbard. The timing constraint in one Svalbard sample regarded as a statistical outlier. **Squares**: Values from AFTA. **Diamonds**: Values from VR. For sample numbers see Figs 3-1 and 3-2, respectively.

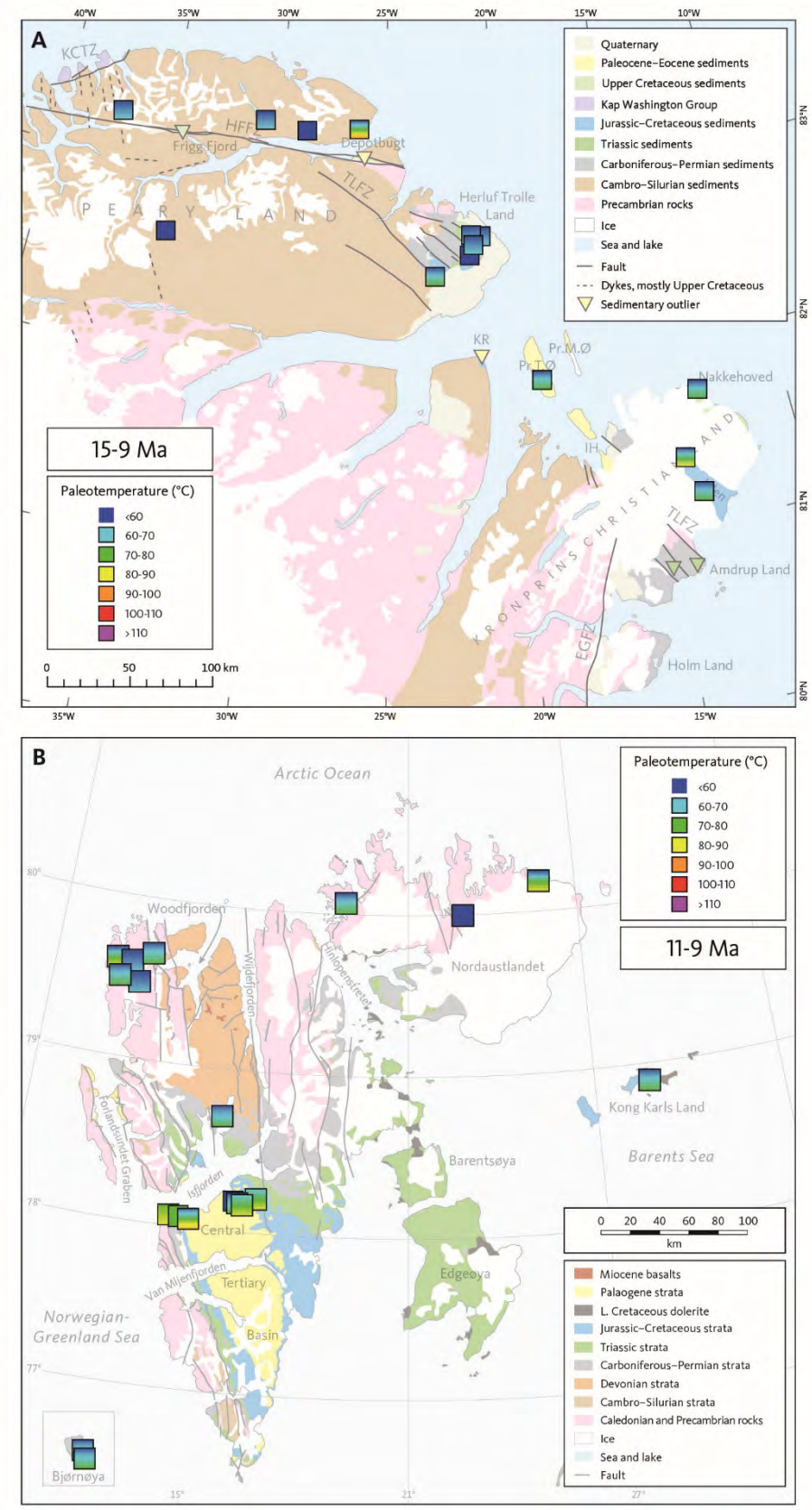

Figure 3-16. **Late Miocene (~10 Ma)** palaeotemperatures derived from AFTA data in outcrop samples. **A**. North Greenland. **B**. Svalbard. For sample numbers see Figs 3-1 and 3-2, respectively.

A

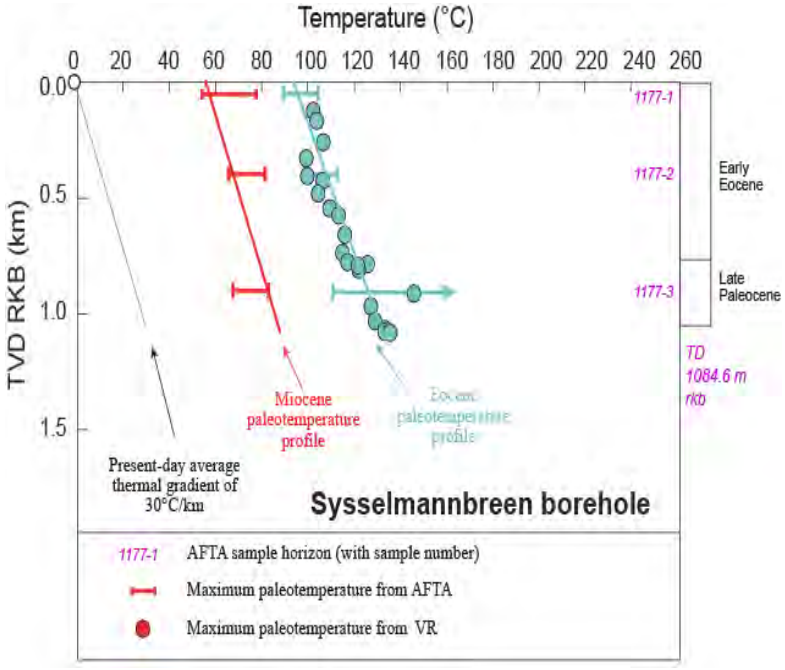

B

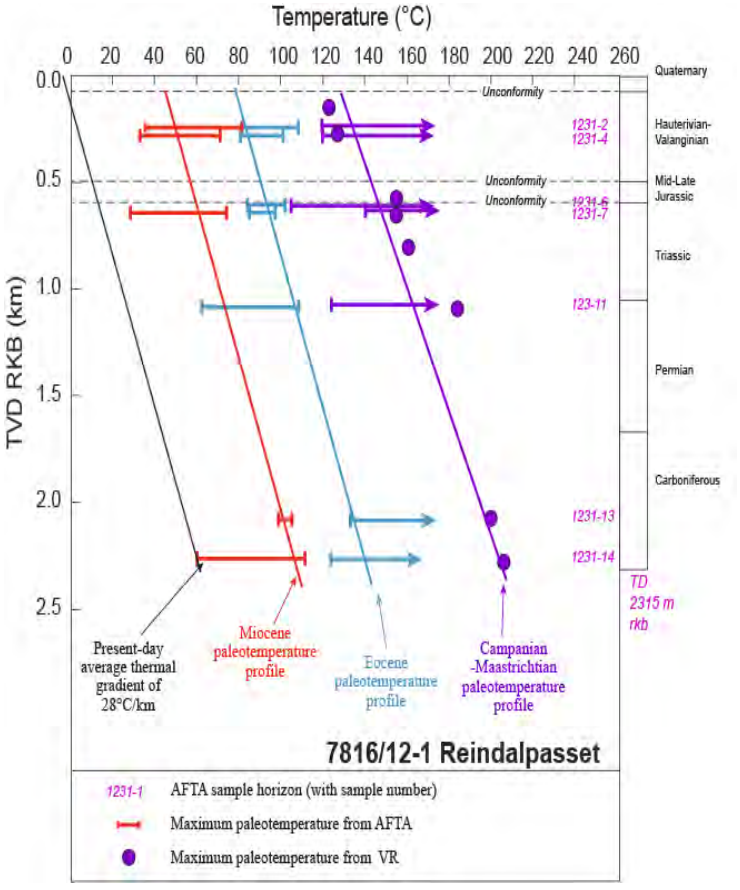

Figure 3-17. Paleotemperature constraints from AFTA and VR data in boreholes for the Campanian–Maastrichtian, end-Eocene and late Miocene palaeothermal episodes.
A: Sysselmannbreen. **B**: Reindalspasset.

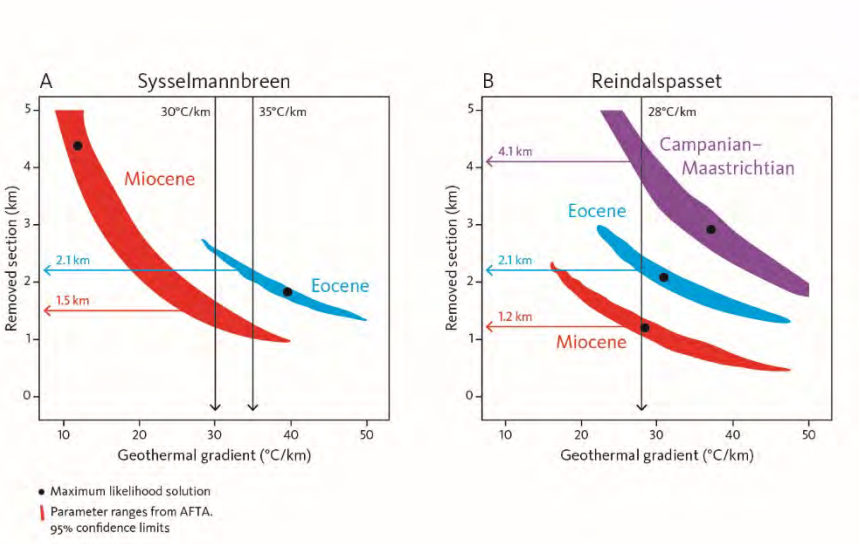

Figure 3-18. Allowed palaeo-gradients and removed section. **A**. Sysselmannbreen borehole. **B**. Reindalspasset borehole. Surface temperature: 20°C Campanian–Maastrichtian and Eocene, 10°C Miocene. Eocene: End-Eocene constraints. Miocene: Late Miocene constraints.

A

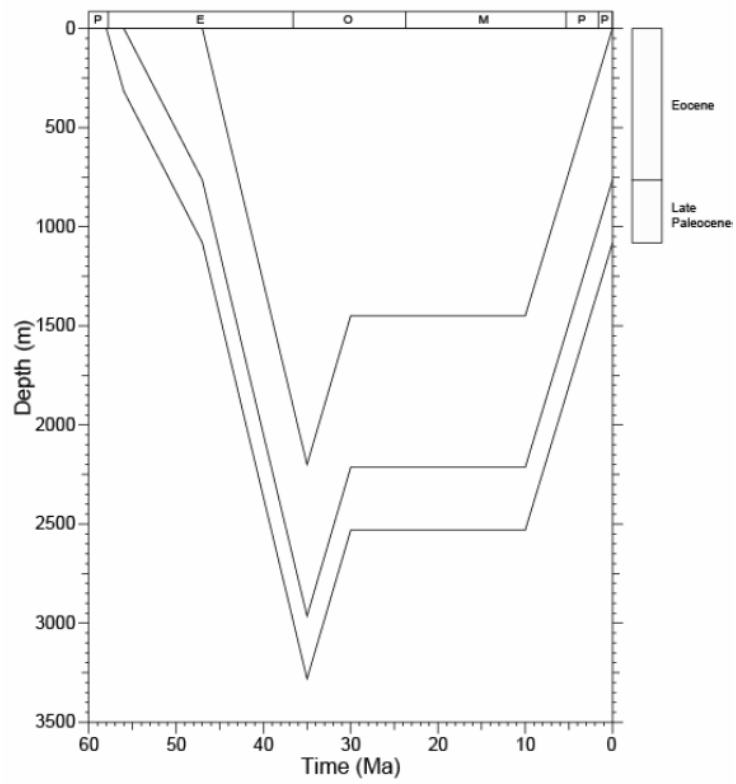

B

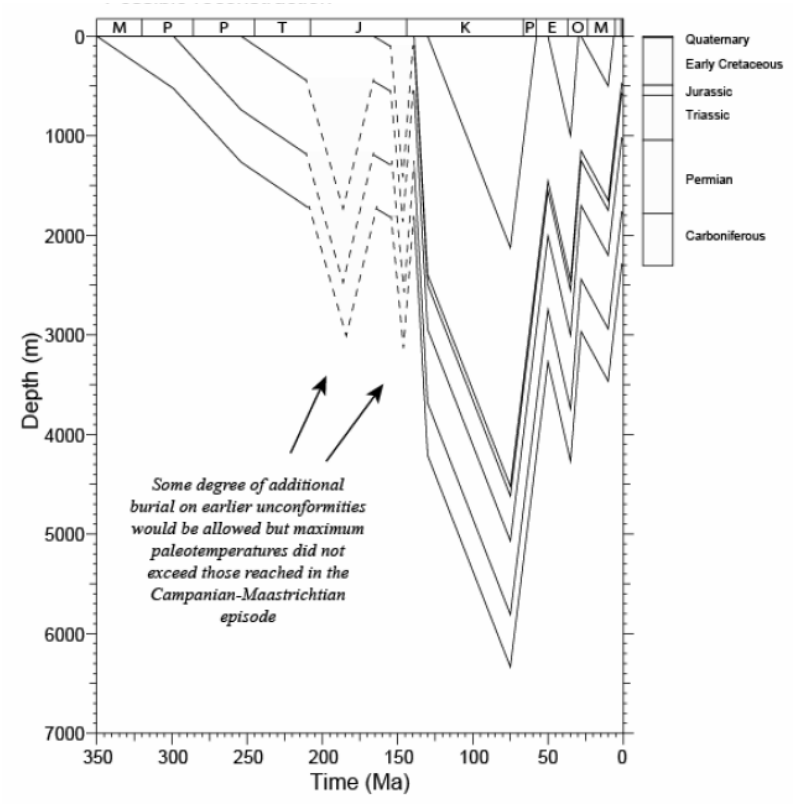

Figure 3-19. Reconstructed burial/uplift histories **A**: Syssellmannbreen. **B**: Reindalspasset

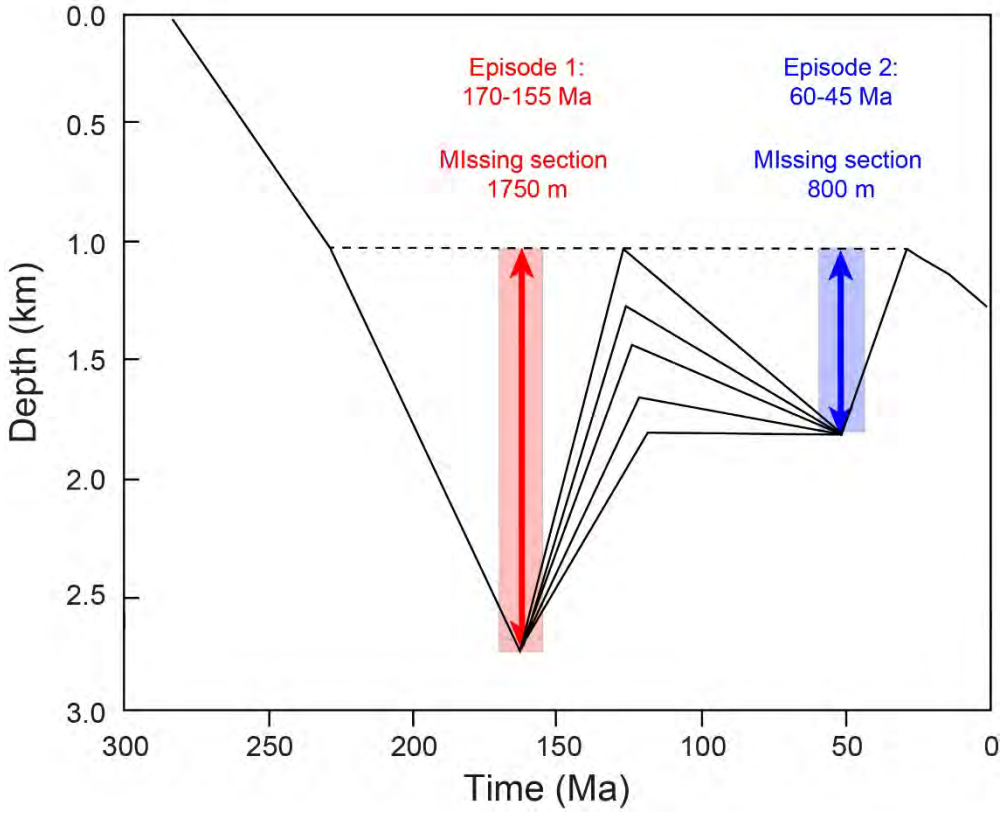

Figure 3-20. Limitations on estimating the amount of section removed in multiple events during a single unconformity. AFTA can determine the maximum or peak palaeotemperature from which a sample cooled in two (or three) discrete episodes, but cannot determine how much total cooling and re-heating (if any) took place between each episode. Thus, when palaeotemperatures are converted to depth of burial the same applies; the amount of additional section present when cooling began in each event can be estimated, but not the total amount of section removed in the earlier event(s).

4. Regional thermal history synthesis

4.1 Introduction

In this Section we discuss the results derived from AFTA and VR in samples from North Greenland and Svalbard presented in Geotrack Report GC1231 (with some revisions following a reassessment of the data, as discussed in Section 3), together with insights from Geotrack's non-exclusive study GC642, in the context of the regional tectonic framework. After a brief review of Paleozoic to mid-Cretaceous events, particular emphasis is placed on Late Cretaceous to Paleogene tectonism associated with continental breakup and sea floor spreading in the Labrador Sea and North Atlantic and its relevance to the Eurekan Orogeny, the West Spitsbergen Fold Belt and the Kronprins Christian Land Orogeny. This is not intended to provide a detailed regional synthesis but aims to place results from different areas in a regional context.

As we discuss in the following, six cooling episodes are identified in overlapping time intervals in North Greenland and Svalbard, while one episode was only identified in the Wandel Sea Basin and one episode only in Svalbard. In Fig. 4-1 we summarize these episodes and refer to them by the chronostratigraphic timing for the onset of cooling in the overlapping time intervals (Table 4-01). We also discuss published thermochronology data from Svalbard, the Canadian Arctic and the Barents Sea in relation to the results of this study. The implications of these results for hydrocarbon exploration in the Barents Sea are discussed in Chapter 9.

4.2 Paleozoic to mid-Cretaceous episodes

Comparison of timing constraints on the regional cooling episodes defined from AFTA data in samples from North Greenland and along the northern coast of Svalbard summarised in Table T.5 and Figure 3-9 shows that events in the two areas are at least broadly synchronous, viz. (in Ma):

North Greenland	Northern Svalbard	Overlap	Chronostratigraphy
331–320	326–269	326–320	Mid-Carboniferous
234–229	247–210	234–229	Late Triassic
173–150	195–143	173–150	Jurassic
138–75	118–95	118–95	Mid-Cretaceous

Samples from other areas of Svalbard are dominated by Late Cretaceous to Cenozoic palaeo-thermal effects (see Section 4.3) which will have overprinted any effects of these earli-

er events. Results from other areas discussed here, as well as previous experience (Green *et al.* 2013, 2018) suggest it is likely that the events defined above originally affected much wider areas before being overprinted by later palaeo-thermal episodes, but further sampling is required before this can be confirmed.

The good agreement between the timing of the dominant cooling episodes in the two areas suggests that cooling in each area was likely to be the consequence of the same controlling processes (see Chapter 5). AFTA studies in other regions around the North Atlantic, Labrador Sea and Arctic regions have defined cooling events in broadly correlative intervals as those defined above, as summarised below (in Ma):

Region	"Devo-nian"	"Carboni-ferous"	"Trias-sic"	Juras-sic"	"Jur.–Cret."	"Mid-Cret."
Lomonosov Ridge				219–143		110–81
West Greenland	370–355		230–220	160–150		
East Greenland	370–310		260–210	200–175		125–85
Northeast Greenland		320–300	~240	~180	145–140	95–90
North Greenland		331–320	234–229	173–150		138–75
Northern Svalbard		326–269	247–210	195–143		118–95
Southern Sweden	>380	314–307	245–240	171–142		107–92
Southern Norway	411–333		251–243	172–164		
Labrador–Newfound-land	395–387	303–299	247–244	161–157		
Scottish Highlands			245–225		140–130	110–90

Sources for the above information are as follows:

Lomonosov Ridge	Knudsen *et al.* (2018)
West Greenland	Japsen *et al.* (2006, 2007)
South-East Greenland	Japsen *et al.* (2014)
Northeast Greenland	Japsen *et al.* (2020a)
North Greenland	This study
Northern Svalbard	This study
Southern Sweden	Japsen *et al.* (2016)
Southern Norway	Japsen *et al.* (2018)
Labrador-Newfoundland	Japsen *et al.* (2017)
Scottish Highlands	Holford *et al.* (2010)

We do not imply that these whole regions underwent cooling at these times, but evidence for the cooling episodes shown have been reported in at least part of each region at the times stated.

Some differences do exist in the timing of events between various regions in the above Table. For example, constraints on the onset of Triassic cooling in North Greenland and West Greenland are somewhat younger than those in other areas, which are generally consistent with cooling at around 245 to 240 Ma. Some differences are also present in the onset of Jurassic cooling in different regions. Whether these differences are real or due to chance differences in the outcomes of interpretations in different areas is not clear. But despite these minor discrepancies, the broad synchronicity of cooling in these various episodes over a vast region clearly suggests that these events are controlled by processes acting on a continental scale.

These regional Paleozoic and Mesozoic cooling episodes belong to a group of phenomena recognised in many regions around the world, which are as yet not fully understood, but involve km-scale regional burial and subsequent exhumation affecting continental-scale regions, at broadly similar times in different regions. For example, Japsen *et al.* (2016, 2018) defined Late Carboniferous, Middle Triassic and mid-Jurassic exhumation episodes across the Baltic Shield and surrounding regions, which they interpreted as representing epeirogenic uplifts accompanying fragmentation of Pangaea, caused by accumulation of mantle heat beneath the supercontinent. Green *et al.* (2013, 2018) reviewed evidence regarding the nature of these episodes and concluded that they show a broad level of synchroneity across continents and oceans and correlate with plate boundary events and changes in plate motions.

4.3 Late Cretaceous to Cenozoic episodes

Results from both North Greenland and Svalbard define three major episodes of Late Cretaceous to Cenozoic cooling in each region (Table T.5, Fig. 3-9). Constraints on the three most recent cooling episodes defined from the various datasets analysed for this study are summarised below (in Ma):

Dataset	**First episode**	**Second episode**	**Third episode**
North Greenland outcrops	60–57	~35	15–9
Svalbard outcrops and boreholes	72–65	46–37	11–9

Comparison of timing estimates of the cooling episodes listed above in the different regions shows that all constraints on the most recent episode are consistent with cooling that began **between 11 and 9 Ma** (**late Miocene**). Estimates of the timing of the second cooling episode are almost all consistent with cooling that began **at ~35 Ma**, the single exception being a single outcrop sample from Svalbard (GC285-6), for which the youngest limit is **37 Ma**. If the timing constraint in this sample was to be regarded as a statistical outlier, the younger limit on the time of cooling on Svalbard would be 34 Ma, and results from Svalbard

would then be consistent with the timing constraints for the **Eocene** episode from North Greenland. On this basis, we regard the value of **~35 Ma** as the most likely value for the onset of the **end-Eocene** cooling episode.

Estimates of the timing of the earliest of the three cooling episodes are more variable, although all are broadly consistent with Late Cretaceous to Early Cenozoic cooling. A reassessment of the timing constraints in individual samples from Svalbard presented in Geotrack Report GC1231 shows that the younger limit of 71 Ma in sample GC1231-6 from the **Reindalspasset** borehole is based on a very broad timing constraint and on lesser quality data compared to other samples. In the synthesis illustrated in Figure 3-9 and Table T.5 we have treated this value as unreliable. On this basis, the constraint on the onset of cooling in this borehole becomes 84 to 65 Ma and for the combined Svalbard dataset the overall constraint becomes **72 to 65 Ma**.

This **Maastrichtian** timing of 72 to 65 Ma for the onset of cooling in Svalbard is earlier than the **Paleocene** constraint of 60 to 57 Ma defined for samples from North Greenland. Thus, it is possible that a real difference exists in the onset of cooling between the two areas. However, the onset of cooling of 60 to 57 Ma for North Greenland is based on samples which cooled below a certain limiting palaeotemperature at that time, corresponding to the onset of track retention, and cooling from the maximum palaeotemperature in this episode may have begun earlier. Of three samples from North Greenland which cooled from a finite range of palaeotemperatures in this episode, sample GC1231-26 provides the tightest constraint on the onset of cooling, between 69 and 51 Ma. Combining this value with other constraints from the region results, an alternative range for the onset of cooling in North Greenland of between 69 and 57 Ma is indicated. In this case, constraints on the onset of the earliest of the three most recent cooling episodes in both North Greenland and Svalbard would all be consistent with Maastrichtian cooling that began between 69 and 65 Ma**.**

Since this reasoning is not definitive, we regard both alternative interpretations as possible. Both these scenarios are considered further in discussing the nature of the various palaeothermal episodes identified in this study in Chapter 5, where integration with geological evidence leads us to prefer different timings in the two regions (Maastrichtian, 72–65 Ma in Svalbard and mid-Paleocene, ~60 Ma in North Greenland). Regardless of the precise timing of this episode in North Greenland, available data support an interpretation involving synchronous **Eocene (~35 Ma)** and **Miocene (11–9 Ma)** cooling in both North Greenland and Svalbard, and this is our preferred interpretation of the most recent history.

Cooling events at similar times to the three Late Cretaceous to Cenozoic episodes defined in North Greenland and Svalbard have been recognised over a much wider region from Alaska and Canada to West and East Greenland, the British Isles and the North Sea (e.g. Green & Duddy 2010; Green *et al.* 2013, 2018). As discussed by Green & Duddy (2010), these events also correlate closely with major unconformities defined along the Atlantic margin from the Porcupine region to Lofoten reported by Stoker *et al.* (2005) and Praeg *et al.* (2005). As with earlier episodes discussed above, we interpret each of these cooling episodes as due to km-scale exhumation in response to regional stresses related to plate motions. Again, we emphasise that none of these events affected this entire region, but

each of the events is recognised in various parts of the region, emphasising the overall importance of regional controls.

In detail there may be differences in timing across the region in each event, and it is possible that the situation is more complex, with multiple episodes of cooling occurring within a narrow interval around the specified timings. More data across a wider area is required before this becomes clear. AFTA data in dredge samples from the Lomonosov Ridge (Knudsen *et al.* 2017) define cooling which began in the interval 95–62 Ma, which could correlate with the Maastrichtian cooling episode identified on Svalbard. The AFTA data from the Lomonosov Ridge samples also define cooling which began between 26–4 Ma, which correlates with the late Miocene cooling identified in samples from North Greenland and Svalbard in this study and also more regionally in studies listed above. Note, however, that end-Eocene cooling was not detected in samples from the Lomonosov Ridge.

A final Pliocene phase of uplift and associated denudation is recognised or inferred in AFTA studies from several areas, including West Greenland (Japsen *et al.* 2005; Green *et al.* 2013), North-East Greenland (Japsen *et al.* in 2020a,b) and Denmark (Japsen *et al.* 2007). This Pliocene uplift phase is thought to be responsible for the final development of the modern day elevation of North Atlantic margins, in particular the elevation of southernmost Norway (Japsen *et al.* 2018), and probably affected the regions studied for this report, but the effects are not sufficiently large to be recorded in the AFTA data.

4.4 Comparison with published studies

No previous thermochronology studies have been carried out in North Greenland, but a number of studies have provided data from a variety of approaches in Svalbard and in Arctic Canada. These studies are reviewed in the following Sections in the context of our preferred interpretation of AFTA data from North Greenland and Svalbard.

4.4.1 Thermochronology studies in Svalbard

Blythe & Kleinspehn (1988) reported apatite fission-track data in 32 samples from Svalbard, five of basement and the remainder of Paleogene sandstone mainly from the CTB. They interpreted data from the Paleogene sandstones as showing a three-phase history:

1. initial cooling of apatites from 120°C or above between 70 and 50 Ma, representing exhumation of sediment provenance regions;
2. heating to ~100°C or more between ~60 and 35 Ma due to burial during basin filling prior to exhumation which began at ~35 Ma;
3. final cooling of ~70°C to surface temperatures within the last 5 Myr due to denudation enhanced by glaciation.

This history is remarkably consistent with that presented in this study for samples from Svalbard, except for our preference for a tectonic cause of Miocene cooling, instead of glacially enhanced denudation within the last 5 Myr.

Dörr *et al.* (2012) presented apatite fission-track data in 28 Devonian and older samples, mainly of crystalline basement, from locations along the northern coasts of Svalbard (see Chapter 3). They found that northern Svalbard underwent major Jurassic–Cretaceous denudation, while any Cenozoic effects in this region could not be resolved, although some reactivation of fault zones was suggested. This interpretation is again broadly consistent with our interpretation of AFTA data from the same region presented in Chapter 3, despite the differences in the approach to the interpretation (i.e. episodic heating and cooling vs continuous cooling).

Dörr *et al.* (2018) analysed samples from three boreholes in the CTB using apatite fission track and (U-Th-Sm)/He thermochronology, vitrinite reflectance and clay mineral crystallinity. They concluded that maximum heating and burial was attained at ~50±5 Ma, and involved a significantly elevated basal heat flow during the early Paleocene. Basin inversion at 45±5 Ma and rapid erosion until ~40 Ma was followed by slow, continuous erosion to the present day. This is at odds with our results and with those presented by Blythe & Kleinspehn (1988). We suspect that this may be due in part to the inclusion of apatite (U-Th-Sm)/He thermochronology by Dörr *et al.* (2018). Although this technique is widely applied, it is subject to a range of complicating factors, including poor reproducibility and uncertainty surrounding the thermal response. For this reason we regard interpretations based on this technique as unreliable (see Green & Duddy 2018). We also note that some of the thermal histories presented by Dörr *et al.* (2018) show cooling closer to 35 Ma than 50 Ma. Based on the results presented here in samples from both outcrops and boreholes, we believe that the main Paleogene phase of exhumation in the CTB began around 35 Ma.

Dörr *et al.* (2019) extended the study of northern Svalbard (Dörr *et al.* 2012) with apatite fission-track data in additional samples from the same area as well as new apatite (U-Th-Sm)/He data in several samples. They concluded that the expanded dataset, combined with regional geological constraints, defined a three-stage history involving Late Cretaceous/Paleocene exhumation and re-burial, renewed exhumation in the Oligocene and final uplift of the modern topography in the Miocene. This style of history is more consistent with the interpretation of Blythe and Kleinspehn (1988) and also with our own preferred interpretation. One difference is that Dörr *et al.* (2019) interpreted the Oligocene exhumation as due to formation of the passive margin following separation of Greenland and Svalbard, whereas we regard this phase of exhumation as reflection a response to regional tectonic stresses over a wide area, as discussed in Chapter 6.

Schneider *et al.* (2018) presented Ar-Ar ages in individual white mica grains from basement samples on Prins Karls Forland (within the West Spitsbergen Fold Belt) that are suggested to have been heated to >350°C. Results showed a notable dispersion between different samples, but the most consistent results were interpreted as defining reactivation of the region in the earliest Eocene (~55 Ma). They considered this to be the first documented Eurekan deformation ages from Svalbard. No palaeo-thermal effects at this time have been identified in this study.

Barnes & Schneider (2018) presented zircon (U-Th)/He data in a number of basement samples from four areas of Svalbard along the western margin with samples from each area giving very different results. Samples from Prins Karls Forland in the northwest gave

the youngest ages, consistently around 30 Ma, while samples from Oscar II Land, also in the northwest on the east flank of the Forlandsundet Graben, gave slightly older ages mainly around 50 Ma. Samples from two areas in the southwest gave a range of ages from ~50 Ma to over 300 Ma. Application of the zircon (U-Th)/He method is far from straightforward, because the He-retention systematics of zircon depend strongly on the amount of radiation damage within the crystal lattice. As radiation damage increases, the degree to which He is retained decreases, such that high uranium zircons that have retained radiation damage for 10s to 100s of Myr tend to have He-retention characteristics close to those of fission tracks in apatite. Thus, results need to be considered in relation to both the degree of radiation damage and the thermal history. Barnes & Schneider (2018) used the He-retention model of Guenthner *et al.* (2013) to quantitatively model the pattern of zircon He age vs equivalent uranium for various candidate thermal histories and interpreted their data as defining an increased Late Cretaceous geothermal gradient >40°C/km, with possible lower values in the south. They also claimed that their data support Eocene cooling (53–47 Ma due to compression and 47–34 Ma reflecting strike slip evolution of the West Spitsbergen Fold Belt). They suggested that Prins Karl Forland underwent post-Eocene exhumation during post-Eurekan compression. They estimated that over 4 km of basement and former cover was removed from Prins Karl Forland since 47 Ma, with lower amounts in other areas.

While the results presented by Barnes & Schneider (2018) provide a clear demonstration of Cenozoic cooling from elevated palaeotemperatures, more pronounced in the north than in the south, the detailed interpretation of their data is far from clear, due to the deficiencies of the Guenthner *et al.* (2013) model. In fact, data from Barnes & Schneider (2018) provide a prime demonstration that this model does not give an accurate representation of the thermal sensitivity of the zircon (U-Th)/He system. According to Barnes & Schneider (2018), their samples were subject to greenschist facies metamorphism or greater (250–450°C) during the Caledonian Orogeny (470–420 Ma). The Guenthner *et al.* (2013) model predicts that this would be expected to remove all radiation damage and reset the system, but Barnes & Schneider (2018) found that they could not explain their data on this basis and they needed to employ much longer times for damage retention in order to accumulate sufficient radiation damage levels to explain Cenozoic resetting of the system. They attempted to circumvent this problem by artificially allowing longer retention times in their models, but given this deficiency, any quantitative outcome from their modelling must be considered with caution.

In our view, the data reported by Barnes & Schneider (2018) are best interpreted as showing major cooling in Prins Karls Forland in the mid Cenozoic (~30 Ma) and slightly earlier (perhaps Late Cretaceous-early Cenozoic) cooling in Oscar II Land, and cooling from lower temperatures in the south (probably also Late Cretaceous – early Cenozoic). Viewed in this context, these results are consistent with our own results and those of Blythe & Kleinspehn (1998) and Dörr er al. (2019).

4.4.2 Published estimates of section removed during Palaeogene exhumation on Svalbard

Manum & Throndsen (1977) measured VR on coals and dispersed organic matter in the Palaeogene deposits on Spitsbergen. They established a maturation gradient based on data from a profile over an elevation range of 900 m at Nordenskiöldfjellet in the northeastern part of the CTB. They estimated that the total depth of burial for the base of the Palaeogene succession (the Firkanten Formation) at this location to be 2.7 km, implying that about 1.7 m of sediments have been eroded off the top. They also found the maximum depth of burial of the Firkanten Formation in the deepest part of the CTB to more than 3 km, possibly 3.5 km at the location of the Sysselmannbreen borehole, where we estimate that at least 3.2 km of Paleocene–Eocene have been present (Table 3-01). Our Paleocene samples from the eastern part of Isfjorden are located near Nordenskiöldfjellet. If we extrapolate our end-Eocene palaeotemperatures to the elevation of the summit of Nordenskiöldfjellet, we find that a cover of about 2.5 km has been removed by erosion, higher than the estimate of Manum & Throndsen (1977) but of the same order of magnitude.

Marshall *et al.* (2015) studied the maturity of coal of the basal Paleocene Firkanten Formation in the CTB and found a maximum burial temperature of 120°C in the basin centre and 100°C at the basin margins with an elevated thermal gradient of approximately 50°C/km. These parameters led Marshal *et al.* (2015) to estimate a maximum thickness of the overburden relative to the Firkanten Formation (Paleocene–Eocene succession) of 2 km of which 1 km has been removed by erosion. Their estimates of maximum palaeotemperatures for the basal part of the Paleocene are lower than our estimates (marginal location in the eastern part of Isfjorden ~110°C, central location based on results from the Sysselmannbreen borehole at least 130°C). But more importantly, their preferred palaeogeothermal gradient of 50°C/km is much higher compared to our estimated end-Eocene gradient of 28 and 35°C/km based on data for the Reindalspasset and Sysselmannbreen boreholes, respectively.

Dörr *et al.* (2018) estimated that nearly 4 km of early Eocene overburden was removed from the CTB (above the Aspelintoppen Formation) during exhumation which began at 45±5 Ma. Surprisingly, they found their estimate to be in agreement with the much lower estimate of Manum & Throndsen (1977). They estimated that samples of the Aspelintoppen Formation had experienced temperatures >85°C and that the Aspelintoppen Formation, the Battfjellet Formation, and the Frysjaodden Formation experienced post-depositional heating between 85 and 120°C. If we apply our estimate of the end-Eocene palaeotemperature of 90°C for the Aspelintoppen Formation at outcrop at the location of Sysselmannbreen borehole, the presence of a former cover of 4 km would result in a palaeothermal gradient of only 18°C/km. In contrast, we estimate that a cover of ~2.1 km has been removed above the outcrop of Aspelintoppen Formation at the borehole location and that that the end-Eocene gradient was 35°C/km (Table 3-01).

4.4.3 Thermochronology studies of Arctic Canada

Arne *et al.* (1998, 2002) reported apatite fission-track (AFT) and vitrinite reflectance data from various outcrop locations and exploration wells in the Sverdrup Basin. Their results

showed clear evidence of Palaeocene cooling due to both regional exhumation and as differential offsets across thrusts. In detail, the samples that provided well-defined thermal histories all cooled from elevated palaeotemperatures sufficient to totally anneal all tracks, and the histories defined by Arne *et al.* (2002) showed regional cooling to temperatures at which tracks could be retained began at 66±3 Ma, somewhat earlier than a timing of 61±3 Ma for differential exhumation on the Vesle Fjord Fault from Arne *et al.* (1998). Following the conclusions of Arne *et al.* (2002), these results suggest a distinction between Maastrichtian regional exhumation and later, mid-Paleocene localized exhumation related to thrusting and inversion associated with the early stage of the Eurekan Orogeny.

Vamvaka *et al.* (2019) reported AFT and apatite (U-Th-Sm)/He data (AHe data) in a suite of samples from the northernmost part of the Sverdrup Basin (the Pearya terrain in northern Ellesmere Island). They reported AFT ages between ~50 and 40 Ma over an elevation range of ~1600 m, while He-ages in individual grains showed a much wider range, from which they selected certain values that they used to derive thermal history constraints. The logic behind their selection of ages to include is not clear, as none of the measured ages show any consistent relationship with either equivalent uranium content or grain size, as required by the models that are used to interpret these data; see Green & Duddy (2018) for details. Vamvaka *et al.* (2019) also reported evidence of rapid Late Cretaceous–Paleocene cooling in provenance regions from detrital ages in samples of Eureka Sound Group sandstones of Paleocene depositional age.

From the combination of AFT and AHe data in their basement samples, Vamvaka *et al.* (2019) presented a preferred scenario involving three periods of cooling, ~55–48 Ma, 44–38 Ma, and 34–26 Ma, showing close correspondence to the three phases of the Eurekan Orogeny defined on independent grounds by Piepjohn *et al.* (2016). However, we note from the supplementary information presented by Vamvaka *et al.* (2019) that their solutions were artificially constrained to begin cooling from temperatures between 140 and 160°C between 60 and 50 Ma. This cooling episode is broadly consistent with the Paleocene cooling episode defined from AFTA in the Wandel Sea Basin (though later than Maastrichtian cooling in Svalbard). It seems highly likely that this major Paleocene cooling which is required in order to explain the Canadian results was of a common origin to that detected in this study in North Greenland, in terms of regional tectonics, although Paleocene cooling is considered to have a non-tectonic origin by Vamvaka *et al.* (2019).

We consider it highly unlikely that the data presented by Vamvaka *et al.* (2019) could independently define three cooling episodes between 55 and 26 Ma, particularly since their selection of He-ages to include in the modelling was highly selective. Instead we believe that a more reasonable interpretation would be in terms of two major cooling episodes beginning at ~60 and ~35 Ma, as in North Greenland. This would suggest a similar tectonic evolution in both North Greenland and in Ellesmere Island. Figure 4-2 shows that apatite fission-track data from Svalbard, North Greenland and Arctic Canada define similar trends, suggesting a common style of underlying thermal history. Late Cretaceous-Paleocene cooling defined from detrital ages in Paleocene sandstones (Vamvaka *et al.* 2019) is consistent with Maastrichtian cooling defined in Svalbard in this study.

Taken together, these results suggest that Arctic Canada shares a similar regional thermal history to North Greenland and Svalbard, involving regional Maastrichtian and end-Eocene exhumation, together with inversion and thrusting related to localised compression which affected the Sverdrup Basin in the mid-Paleocene during the onset of the Eurekan Orogeny.

4.4.4 Thermochronology studies of the Barents Sea

Green & Duddy (2010) presented AFTA and VR data from Hammerfest Basin well 7120/9-2, taken from Geotrack's non-exclusive Barents Sea study (Geotrack Report GC642). These results were interpreted as defining two episodes of cooling from higher temperatures in the intervals 40-20 Ma and 20-0 Ma. Both episodes were interpreted as reflecting exhumation with a basal heat flow similar to the present day, with around 2 km of section removed since the onset of exhumation. The estimated removed section is, however, reduced by about 500 m if the assumption of a constant surface temperature of 5°C (Green & Duddy 2010) is substituted by an end-Eocene surface temperature of 20°C. Green & Duddy (2010) also reported that similar results were obtained in a number of wells across the southwestern Barents Sea, while wells in the northeast of the region also showed an earlier cooling episode. Overall, results across the basin consistently define three episodes of cooling, in the intervals 65–55 Ma (Paleocene), 40–30 Ma (Eocene–Oligocene) and 10–5 Ma (Late Miocene).

Zattin *et al.* (2016) provided (U-Th-Sm)/He data in three wells from the western Barents Sea (although only one single grain age was obtained from one well). Ages were scattered from 1 to 50 Ma with no apparent relationship to either grain size or equivalent uranium, as required by current models of He-diffusion in apatite (Green & Duddy 2018). Zattin *et al.* (2016) interpreted their results as defining Miocene-Early Pliocene exhumation of the order of 1 km, but based on the scatter within the measured He-ages, any conclusion should be regarded with caution. The timing of their main phase of exhumation is consistent with the most recent episode defined by Green & Duddy (2010), and the failure by Zattin *et al.* (2016) to detect the earlier episode of cooing from higher temperatures can be explained by the use of apatite (U-Th-Sm)/He data alone, given the lower thermal sensitivity of the He-method. This emphasises the benefits to be gained from the application of multiple techniques.

4.5 Summary

While published studies are to some extent contradictory, the majority of published datasets are consistent with the conclusions of this study, namely that three dominant phases of cooling (each due dominantly to exhumation) have affected North Greenland, Svalbard, and Arctic Canada, in Late Cretaceous–Paleocene, end-Eocene and Miocene–Pliocene times.

However, further assessment of results presented here has resulted in tentative recognition that Late Cretaceous – Paleocene exhumation may represent the effects of two separate

episodes, a regional Maastrichtian episode of exhumation which affected much of Svalbard, and the Sverdrup Basin, and a more localised Paleocene episode recognised in North Greenland and most likely also in Arctic Canada (Pearya). It is quite possible that the regional Maastrichtian episode also affected North Greenland, although this remains uncertain at this stage. Similarly, localised Paleocene cooling may have affected regions of Svalbard that have not, as yet, been sampled.

One obstacle to clarifying these aspects is the lack of overlap in data coverage between different studies. For example, the lack of AFTA data from Prins Karls Forland precludes direct comparison with conclusions from zircon (U-Th)/He in that region. Given the nature of sample coverage, the conclusions of difference studies are considered to be quite consistent overall, despite some apparent anomalies. One particular anomaly in our results is the apparent lack of evidence for significant Eocene cooling between ~55 and 47 Ma, which is indicated as the timing of major Eurekan event in a number of studies. No explanation for this is available at present.

Table 4-01. Onset of cooling episodes defined from AFTA.

Wandel Sea Basin (Ma)	Svalbard (Ma)	Overlap (Ma)	Chronostratigraphy
326–320	326–269	326–320	Mid-Carboniferous
234–229	247–210	234–229	Late Triassic
173–150	195–143	173–150	Jurassic
138–91	118–95	118–95	Mid-Cretaceous
	72–65		Maastrichtian
60–57			Mid-Paleocene
~35	46–37	~35	End-Eocene
15–9	11–9	~10	Late Miocene

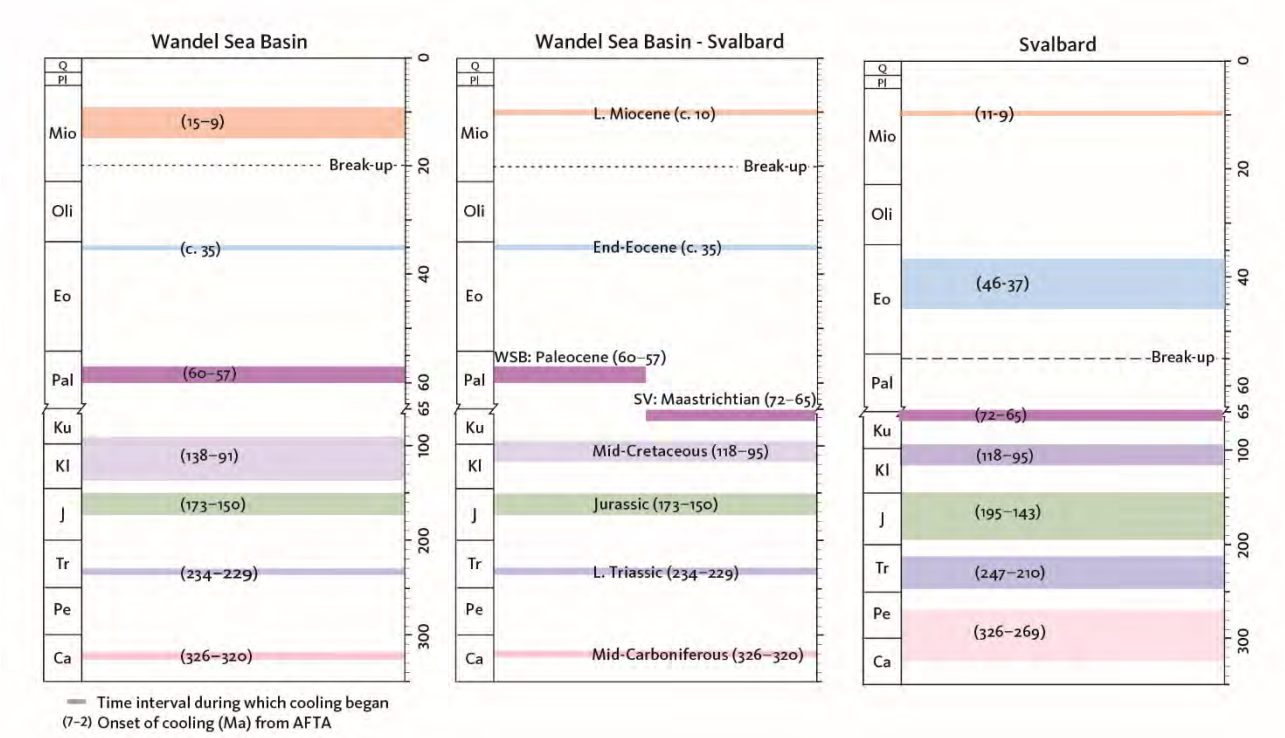

Figure 4-1. Onset of cooling episodes defined from AFTA. **Left**: Wandel Sea Basin (WSB). **Centre**: Overlap between the Wandel Sea Basin and Svalbard, **Right**: Svalbard (SV). See Table 4-01.

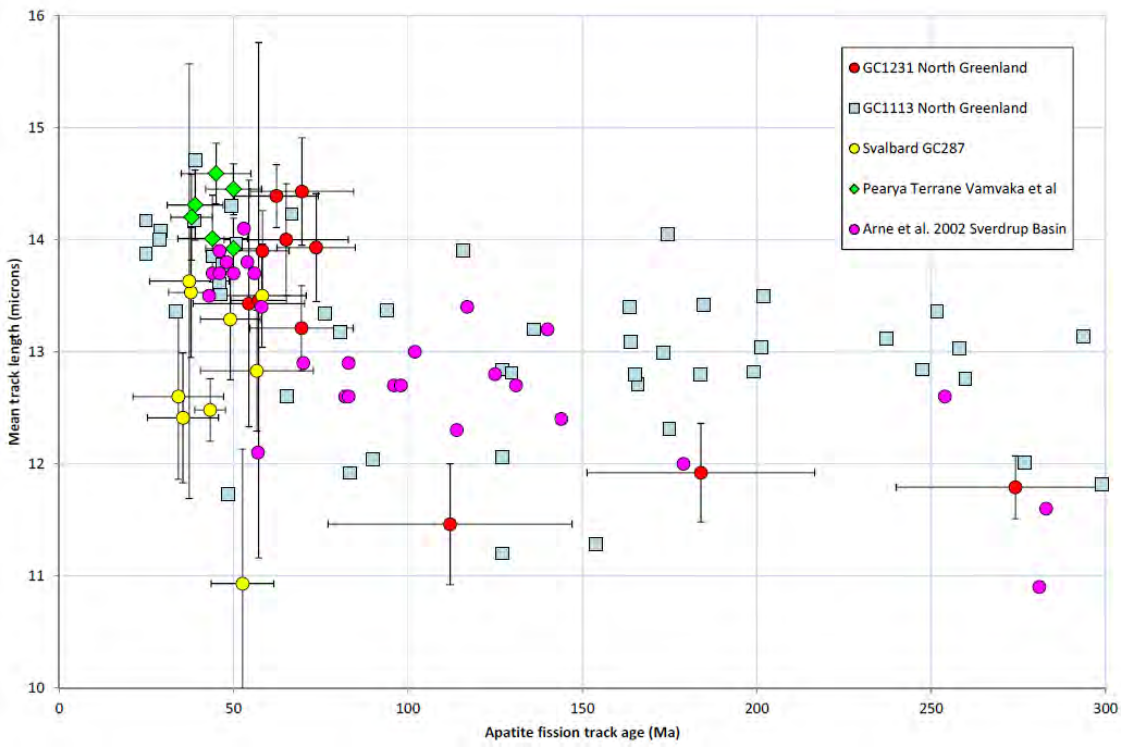

Figure 4-2. Comparison of apatite fission-track parameters from various sources from Arctic Canada, North Greenland and Svalbard. Ages around 50 Ma with mean track lengths around 14 µm are common to all areas and the three datasets show similar trends in terms of the variation of mean track length with fission-track age, suggesting a similar overall style of thermal history in all three regions.

5. Correlation of cooling episodes with the stratigraphic record

Here we compare the onset of cooling episodes (Table 4-01) with the stratigraphic record as outlined in Chapter 2 (Fig. 2-3). In both parts of the study area, six cooling episodes were identified in overlapping time intervals, while one episode was only identified in the Wandel Sea Basin and one only on Svalbard. Here we will refer to these episodes by the preferred chronostratigraphic timing for the onset of cooling (Fig. 5-1). Where the cooling episodes correlate with unconformities, we conclude that they represent periods of exhumation.

Mid-Carboniferous cooling (onset 326–320 Ma) correlates with unconformities in both Svalbard and North Greenland, between the lower Carboniferous Billefjorden and the lower Carboniferous – lower Permian Gipsdalen Groups at ~325 Ma in Svalbard (Dallmann *et al.* 2015, p. 107) and between the lower Carboniferous Sortebakker and the upper Carboniferous Kap Jungersen Formations in North Greenland. The unconformable contact between the Billefjorden and Gipsdalen Groups reflects major regional uplift by rifting along pre-existing fault zones, accompanied by a relatively abrupt climatic shift from humid to warm but arid conditions (Worsley 2008). We therefore consider it likely that cooling in this episode corresponds to denudation which led to formation of these unconformities.

Late Triassic cooling (onset 234–229 Ma) correlates with base-Carnian (~235 Ma) unconformities in Svalbard and North Greenland. In Svalbard, this timing corresponds to the transition between the Sassendalen and Kap Toscana Groups (Dallmann *et al.* 2015, p. 115), corresponding to a hiatus that Harland (1997, p. 347) dated as mid-Ladinian (~240 Ma). The transition between the Sassendalen and Kap Toscana Groups records a drastic change in the sedimentary environment from a marine basin to a shallow-marine to deltaic setting. In North Greenland, there is a marked erosional, base-Carnian (~235 Ma) unconformity with associated marine channel deposits of massive sandstones and conglomerates up to 50 m thick, which belong to the lower part of the Storekløft Formation on Peary Land (Bjerager *et al.* 2019). This unconformity is time-equivalent to abundant channelised sandy units in the lower part of the Kapp Toscana Group in the eastern part of Svalbard (De Geerdalen Formation).

Jurassic cooling (onset 173–150 Ma) overlaps with a well-defined hiatus in the stratigraphic record in both regions. On Svalbard, it corresponds to the regional hiatus of Aalenian–Bajocian age, near the top of the Kapp Toscana Group (174–168 Ma; Dallmann *et al.* 2015, p. 119). In North Greenland, this hiatus overlaps with that observed at the base of the Middle Jurassic Mågensfjeld Formation on Kronprins Christian Land and with the long hiatus at the base of the Upper Jurassic to Lower Cretaceous Ladegårdsåen Formation in Peary Land. There is thus good evidence to support an interpretation that the Jurassic cooling episode represents denudation reflected in the regional hiatus near the transition between the Early and the Middle Jurassic beginning at ~175 Ma. Dallmann *et al.* (2015) also noted that Middle Jurassic uplift affected Svalbard and the Barents Sea. In the south-western

Barents Sea, there is a major, Middle Jurassic hiatus between the Kapp Toscana and Adventdalen Groups (Henriksen *et al.* 2011).

Mid-Cretaceous cooling (onset 118–95 Ma) overlaps with the late Albian – Maastrichtian gap in the stratigraphic record on Svalbard (separating the Adventdalen Group from the Paleocene–Eocene Van Mijenfjorden Group) and with the Aptian – mid-Turonian gap in North Greenland at the base of the Upper Cretaceous Herlufsholm Stand Formation on Peary Land. Assuming that this cooling episode affected both parts of the study area, this information from the stratigraphic record thus implies that the time interval when the exhumation took place can be narrowed to late Albian – mid-Turonian (about 105 – 92 Ma) which overlaps with the constraints on the cooling episode. The Loppa High area, southwestern Barents Sea, underwent inversion in an overlapping time interval (Barremian–mid-Albian, 131–105 Ma; Indrevær *et al.* 2016), but an unconformity is also present between Cenomanian and Campanian strata on the Barents Shelf (Worsley 2008).

Maastrichtian cooling (onset 72–65 Ma), recognized in AFTA data from samples across a wide part of Svalbard, corresponds to the base-Paleocene unconformity in the CTB which ranges from the Albian to the mid-Paleocene. This unconformity has previously been suggested to be the product of Late Cretaceous uplift (Atkinson 1963; Nøttvedt 1985). Atkinson (1985), for example, found that the pattern of sub-outcrop below the base-Paleocene unconformity indicates that the Late Cretaceous deformation involved tilting of up to two degrees about an east-northeast axis. As discussed in Chapter 2, late Maastrichtian uplift and erosion followed by Paleocene subsidence and burial was widespread across the Canadian Arctic as well as much of the North American Arctic and the Barents Shelf (Ricketts 1994). Embry *et al.* (2018) dated the unconformity to 68 Ma in the Beaufort-Mackenzie Basin of Arctic Canada (Fig. 2-7). We therefore conclude that Maastrichtian exhumation affected Svalbard and the Canadian Arctic.

The AFTA data from North Greenland do not resolve definite evidence of Maastrichtian cooling. However, a significant hiatus separates the youngest, well-dated Upper Cretaceous sediments of Santonian age from late Paleocene deposits in Kronprins Christian Land (Lyck & Stemmerik 2000; Hovikoski *et al.* 2018), so Maastrichtian exhumation could also have affected this region. Further west, the presence of the Kap Washington volcanics and interbedded shales, of Maastrichtian in age (Tegner *et al.* 2011), suggests that Maastrichtian exhumation may not have been pronounced in this region.

Paleocene cooling (onset 60–57 Ma) is documented by the AFTA data from the Wandel Sea Basin, based on samples that are localised within the fault zones in a belt along the coastlines from Kap Washington through Herluf Trolle Land to Nakkehoved and Kilen. Examination of AFTA and VR data along these fault zones led Japsen *et al.* (2020a) to conclude that exhumation during this episode defines the timing of the compressional event that caused folding and thrusting of Upper Cretaceous and older sediments within these fault zones.

As pointed out in Chapter 4, the onset of cooling in this episode is based on samples which cooled below a certain limiting palaeotemperature at that time, corresponding to the onset of track retention. The cooling from the maximum palaeotemperature may thus have begun

earlier, i.e. prior to 60 Ma. Samples that cooled from a finite range of palaeotemperatures during this episode began to cool after 69 Ma, and therefore an alternative range for the onset of cooling and exhumation along these faults could be between 69 and 57 Ma, which overlaps with the timing of Maastrichtian cooling in Svalbard. However, the physical expression of the exhumation around the Maastrichtian–Paleocene boundary in Svalbard and North Greenland are distinctly different (Fig. 3-13A,B). As explained above, Maastrichtian exhumation was widespread on Svalbard and across wide areas in the Arctic, whereas the exhumation in North Greenland is focussed in inverted fault zones. We therefore conclude that the AFTA data provide evidence for two distinct episodes of exhumation, Maastrichtian in Svalbard and Paleocene in North Greenland.

The results of this study therefore support the interpretation of Japsen *et al.* (2020a), that the inversion of the fault zones in the Wandel Sea Basin represents the onset of the Eurekan Orogeny caused by the mid-Paleocene onset of seafloor spreading west of Greenland. The AFTA data from Svalbard do not provide evidence for Paleocene cooling and exhumation (see further discussion in Chapter 6).

End-Eocene cooling (onset ~35 Ma) is documented by the AFTA data from the Palaeogene successions on Svalbard (e.g. early Eocene sediments from the Sysselmannbreen borehole) and in North Greenland (the upper Paleocene – mid-Eocene Thyra Ø Formation), as well as in older units. Cooling at this time correlates with the post-Eocene unconformity in both areas. Evidence of end-Eocene exhumation also suggests that the age of the youngest part of the Palaeogene succession in these areas is older than 35 Ma, since a considerable amount of Eocene section must have been removed during this cooling episode. As pointed out by Dallmann *et al.* (2015, p. 127), the ages of the formation boundaries in the Van Mijenfjorden Group are not well defined (Helland-Hansen & Grundvåg 2020), so we suggest that the exhumation that began at ~35 Ma defines the age of the youngest Palaeogene sediments on Svalbard (e.g. the Aspelintoppen Formation) to be Priabonian or older.

Late Miocene cooling (~10 Ma) corresponds to the wide hiatus between Palaeogene and glacial sedimentary units exposed in both parts of the study area. Furthermore, the late Miocene cooling episode correlates closely with the age of the late Miocene basalts (Seidfjellet Formation) dated to 8.7–11.5 Ma that occur on northern Spitsbergen (Harland 1997, p. 423; Dallmann *et al.* 2015, p. 214; Dörr *et al.* 2019). The temporal overlap between the eruption of the basalts and the onset of cooling and exhumation at this time, provide evidence for significant tectonic activity.

Figure 5-1. Comparison between the regional cooling episodes from AFTA (Table 4-01) and the stratigraphy for the Wandel Sea Basin and Svalbard (Fig. 2-3). The vertical extent of the horizontal, coloured bars indicates the uncertainty for the onset of the cooling episode.
(Next page)

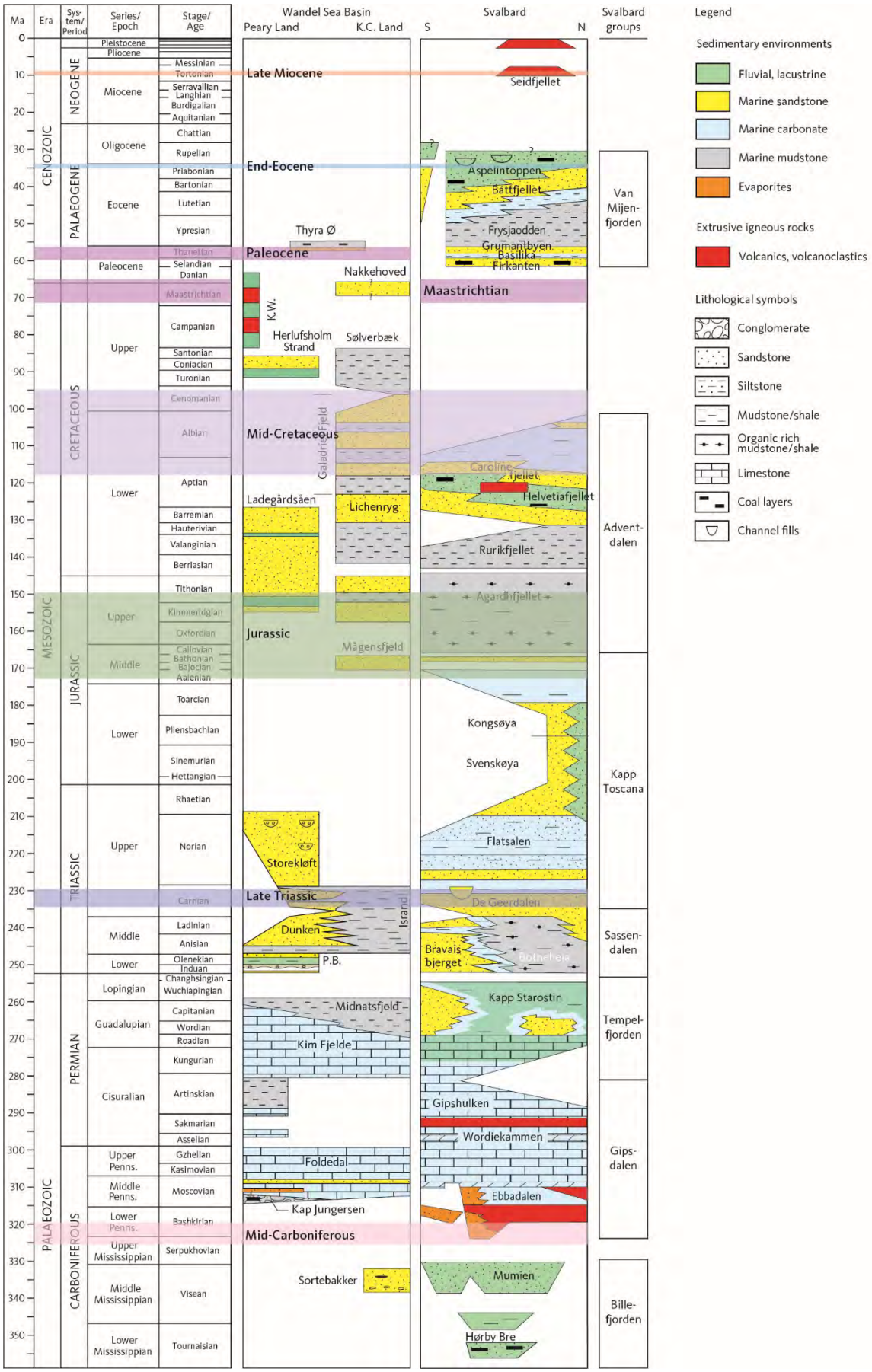
Ma
Era
System/ Period
Series/ Epoch
Stage/ Age
Wandel Sea Basin
Peary Land
K.C. Land
Svalbard
S
N
Svalbard groups
Legend
Sedimentary environments
Fluvial, lacustrine
Marine sandstone
Marine carbonate
Marine mudstone
Evaporites
Extrusive igneous rocks
Volcanics, volcanoclastics
Lithological symbols
Conglomerate
Sandstone
Siltstone
Mudstone/shale
Organic rich mudstone/shale
Limestone
Coal layers
Channel fills
CENOZOIC
MESOZOIC
PALAEOZOIC
NEOGENE
PALAEOGENE
CRETACEOUS
JURASSIC
TRIASSIC
PERMIAN
CARBONIFEROUS
Pleistocene
Pliocene
Miocene
Oligocene
Eocene
Paleocene
Upper
Lower
Middle
Messinian
Tortonian
Serravallian
Langhian
Burdigalian
Aquitanian
Chattian
Rupelian
Priabonian
Bartonian
Lutetian
Ypresian
Thanetian
Selandian
Danian
Maastrichtian
Campanian
Santonian
Coniacian
Turonian
Cenomanian
Albian
Aptian
Barremian
Hauterivian
Valanginian
Berriasian
Tithonian
Kimmeridgian
Oxfordian
Callovian
Bathonian
Bajocian
Aalenian
Toarcian
Pliensbachian
Sinemurian
Hettangian
Rhaetian
Norian
Carnian
Ladinian
Anisian
Olenekian
Induan
Lopingian
Changhsingian
Wuchiapingian
Guadalupian
Capitanian
Wordian
Roadian
Cisuralian
Kungurian
Artinskian
Sakmarian
Asselian
Upper Penns.
Gzhelian
Kasimovian
Middle Penns.
Moscovian
Lower Penns.
Bashkirian
Upper Mississippian
Serpukhovian
Middle Mississippian
Visean
Lower Mississippian
Tournaisian
Late Miocene
End-Eocene
Paleocene
Mid-Cretaceous
Jurassic
Late Triassic
Mid-Carboniferous
Thyra Ø
Nakkehoved
K.W.
Herlufsholm Strand
Sølverbæk
Galadriel fjeld
Ladegårdsåen
Lichenryg
Mågensfjeld
Storekløft
Dunken
Israndsbjerget
P.B.
Midnatsfjeld
Kim Fjelde
Foldedal
Kap Jungersen
Sortebakker
Seidfjellet
Aspelintoppen
Battfjellet
Frysjaodden
Grumantbyen
Basilika
Firkanten
Maastrichtian
Caroline fjellet
Helvetiafjellet
Rurikfjellet
Agardhfjellet
Kongsøya
Svenskøya
Flatsalen
De Geerdalen
Bravaisbjerget
Botneheia
Kapp Starostin
Gipshulken
Wordiekammen
Ebbadalen
Mumien
Hørby Bre
Van Mijen-fjorden
Advent-dalen
Kapp Toscana
Sassen-dalen
Tempel-fjorden
Gips-dalen
Bille-fjorden

6. Implications for the Eurekan Orogeny

6.1 A Maastrichtian precursor to the Eurekan Orogeny?

In Svalbard, our AFTA data define Maastrichtian cooling and exhumation beginning in the interval between 72 and 65 Ma across a wide part of Svalbard, correlating with the pronounced base-Paleocene unconformity that defines the base of the CTB (Figs 3-14B, 5-1). We therefore interpret this event as representing regional km-scale exhumation resulting in formation of this unconformity. However, in the Wandel Sea Basin, the AFTA data do not define a regional Maastrichtian cooling episode, possibly because any such effects were overprinted by the high palaeotemperatures during mid-Paleocene and/or end-Eocene palaeo-thermal episodes. There is a significant Santonian–Paleocene hiatus across most of the Wandel Sea Basin. However, on the northern tip of Kronprins Christian Land, the poorly dated Upper Cretaceous Nakkehoved Formation may overlap with this hiatus. The presence of the Maastrichtian Kap Washington volcanics and associated clastics, suggests that Maastrichtian exhumation may not have been pronounced in western Peary Land.

As discussed in Chapter 4, apatite fission-track data from the Sverdrup Basin (Arne *et al.* 2002) define regional cooling in the latest Cretaceous, and we regard this event as representing the creation of the Maastrichtian unconformity across Arctic Canada. In contrast, evidence for more localised cooling of Paleocene age in the Sverdrup Basin (Arne *et al.* 2002) and Pearya (Vamvaka *et al.* 2019) is interpreted as representing the onset of the Eurekan Orogeny, similar to more localised events in North Greenland and Svalbard (see below).

How this regional Maastrichtian exhumation relates to the Eurekan Orogeny is not clear, but since it pre-dates the onset of break-up in the Labrador Sea it clearly pre-dates the onset of the Eurekan Orogeny proper. There is, however, an overlap between the Arctic areas affected by the Maastrichtian event and those affected by the Eurekan Orogeny, even though the Maastrichtian event appears to have affected a much wider region. Furthermore, as the Maastrichtian unconformity in the Sverdrup Basin is more profound in directions towards Baffin Bay, we suggest that it may represent a precursor event prior to the onset of the more focused effects of the Eurekan Orogeny related to the Palaeogene convergence between Greenland, the Canadian Arctic and Svalbard (see below).

6.2 Mid-Paleocene onset of Eurekan Orogeny

We have demonstrated that the cooling and exhumation in the Wandel Sea Basin along the HFFZ and the TLFZ began during the mid-Paleocene episode (~60 Ma), and a similar timing is also likely for the region between the KCFZ and HFFZ. This episode therefore defines the onset of compression along these fault zones. We follow the interpretation of Pedersen *et al.* (2018), that the high palaeotemperatures in the southern part of Kilen were reached during maximum burial prior to basin inversion during a strong compressional event, that we thus date as mid-Paleocene in age. A cover of more than 3 km of Upper

Cretaceous to Paleocene sediments was present on the north coast of Kronprins Christian Land prior to the Paleocene exhumation (Japsen *et al.* 2020a). The onset of compression in the Wandel Sea Basin coincides with the mid-Paleocene onset of seafloor spreading in the Labrador Sea and thus with the movement of Greenland towards east-northeast (Oakey & Chalmers 2012). This implies that the mid-Paleocene compression happened during the first stage of the Eurekan Orogeny.

The relation between the undeformed Palaeogene strata and the heavily deformed Upper Cretaceous strata in the fault zones is not well defined from outcrops in the Wandel Sea Basin (Pedersen & Håkansson 2001; von Gosen & Piepjohn 2003). It is thus possible that the deformation continued in the fault zones during the deposition of the Palaeogene sediments. It has been suggested that the deformation at Kap Washington in the western part of the Wandel Sea Basin continued into the Eocene, as the Ar-Ar system of the Kap Washington Group was partially reset in the early Eocene (~47 Ma; Tegner *et al.* 2011), although AFTA data show no evidence for any paleo-thermal effects at this time. But the Ar-Ar age spectra do not show well-defined plateaus, and the resulting ages should perhaps be treated with caution.

The AFTA data from Svalbard provide no evidence of mid-Paleocene cooling and exhumation. Instead, subsidence and burial of the CTB began in the mid-Paleocene (~62 Ma; Jones *et al.* 2017), most likely coincident with the inversion of the fault zones in the Wandel Sea Basin. According to Jones *et al.* (2017), the sustained subsidence of the CTB took place in response to compression between Greenland and Svalbard induced by the onset of seafloor spreading in the Labrador Sea. In contrast, Steel *et al.* (1985) suggested that the initial formation of the CTB during the Paleocene took place during extension (possibly transtension), in particular, because these authors found no evidence for compression in the west at this time. However, subsidence in the initial phase of formation of the CTB was increasingly asymmetrical and greatest towards the De Geer line. This suggests that the relative movement between Greenland and Svalbard along this structure provided the overall control, and thus that the initial basin formation on Svalbard had much in common with the foredeep-like basin that developed in the eastern Sverdrup Basin, related to compressional loading driven by the onset of sea-floor spreading west of Greenland (Ricketts 1994; Embry & Beauchamp 2019). Sediment supply during the Paleocene to the CTB was primarily from eastern source areas, but in the earliest Eocene this changed to a western source area due to the emerging West Spitsbergen Fold Belt (Fig. 2-4; Dallmann *et al.* 2015; Elling *et al.* 2016; Petersen *et al.* 2016; Schneider *et al.* 2018).

The mid-Paleocene timing of the compressional event in the Wandel Sea Basin is consistent with the conclusion of Håkansson & Pedersen (2015 and previous papers), that the compressional tectonics, the Kronprins Christian Land Orogeny, occurred around the Cretaceous–Palaeogene boundary. However, the mid-Paleocene timing for the onset of compression there differs from the Eocene timing suggested by von Gosen & Piepjohn (2003, who stressed that an Eocene N-S compression of the Wandel Sea Basin would fit into a unified timing of Eurekan deformation extending from the Canadian Arctic islands over North Greenland to Svalbard. However, it is important to note that the Eurekan deformation took place in two stages (Fig. 1-2; Section 2.3.2). During the first, Paleocene Eurekan stage, the SSW-NNE movement of Greenland relative to Svalbard gave rise to compres-

sion that caused exhumation in the Wandel Sea Basin and subsidence of the CTB during its formation as a foreland basin. During the second, Eocene stage, compression continued, but the changed trajectory of the Greenland plate caused sinistral strike-slip movement between Greenland and Svalbard - i.e. sinistral transpression. The dominant feature of what can be seen today in the field is the final result of Eocene N-S transpression.

Corroborating evidence for Paleocene compression between the eastern part of North Greenland and Svalbard is provided by the shutdown of the Kap Washington volcanics around this time, whereas an increase in activity might be expected if there had been extension between these regions (Jones *et al.* 2017; their figure 5). The observations presented by Jones *et al.* (2017) thus support the idea that the formation of the CTB began at the same time as the compression of the Wandel Sea Basin, slightly prior to 60 Ma.

Other lines of evidence support our interpretation of a mid-Paleocene onset of the Eurekan Orogeny. According to Embry & Beauchamp (2019), the Sverdrup Basin was transgressed in the Paleocene and parts of the eastern portion of the basin underwent rapid subsidence, interpreted to be related to compressional loading driven by the onset of seafloor spreading west of Greenland. The mid-Paleocene cooling in Pearya required to explain the data of Vamvaka *et al.* (2019) as discussed in Chapter 4 may also represent this event.

We conclude that the mid-Paleocene episode of exhumation of the major fault zones in the Wandel Sea Basin as well as the onset of sediment accumulation during subsidence of the CTB represent the first stage of the Eurekan Orogeny induced by the onset of seafloor spreading west of Greenland that caused convergence between Greenland and the Barents margin (Dallmann *et al.* 2015; De Paor *et al.* 1989; Embry & Beauchamp 2019; Gaina *et al.* 2017; Gion *et al.* 2016; Jones *et al.* 2017; Oakey & Chalmers 2012).

6.3 End-Eocene tectonics in relation to the Eurekan Orogeny

Regional exhumation of the Wandel Sea Basin began at the end of the Eocene after the deposition of the Thyra Ø Formation. A wide area from Herluf Trolle Land to Kronprins Christian Land cooled from an end-Eocene palaeo-thermal maximum, when maximum palaeotemperatures in rocks now at outcrop were around 80–90°C across most of the region. These palaeotemperatures reflect burial below a cover of about 2.5 km of the Thyra Ø Formation and younger Eocene sediments (assuming a palaeogeothermal gradient of 30°C/km and palaeosurface temperature of 10°C) which has been subsequently eroded away. Large parts of the basin were thus subsiding during most of the Eocene.

Regional end-Eocene exhumation of the CTB and surrounding parts of Svalbard began after the deposition of the Aspelintoppen Formation, and a considerable amount of Eocene section must have been removed during this episode. Therefore, the age of youngest part of the Palaeogene succession preserved in the CTB must be older than 35 Ma. For example, our data from the Sysselmannbreen borehole show that the youngest Eocene sediments penetrated by that well reached a palaeotemperature of ~80–90°C prior to end-Eocene exhumation, therefore about 2 km of Eocene sediments must have been deposited

and then removed at this location (assuming a palaeogeothermal gradient of 35°C/km and palaeosurface temperature of 10°C).

In North Greenland, there is a clear offset in the end-Eocene palaeotemperatures across the HFFZ (Fig. 3-15A). Typical palaeotemperatures correspond to burial below a cover of ~3.5 km and ~2.5 km a.s.l. on the northern and the southern side of the fault, respectively (~110°C and 85°C at sea level; 30°C/km, 10°C at the surface). This implies that the rocks on the northern side of fault were more deeply buried by about 1 km, compared to those south of the fault, prior to the exhumation that began at the end of the Eocene. As we argue in Section 6.3, there is evidence to suggest that there was no significant vertical movement along the fault during the Miocene tectonic episode, which suggests that the offset of end-Eocene palaeotemperatures are due to differential vertical movement across the HFFZ that took place by the end of the Eocene.

N-S compression affected northern Peary Land in post-late Santonian times, with reverse faulting at the HFFZ and thrusting along the KCTZ (Piepjohn & von Gosen 2001). Piepjohn & von Gosen (2001) interpreted this compression to be part of the Eurekan Orogeny, but they also argued that the Eurekan compression along the HFFZ was terminated by the change in plate-tectonic configuration at C13 time (~35 Ma). They argued that Greenland had become part of the American Plate at this time and, consequently, that the compressive structures along the HFFZ must have formed prior to ~35 Ma.

Our AFTA data document km-scale, reverse movements along the HFFZ, which are consistent with the N-S reverse and thrust faults observed by Piepjohn & von Gosen (2001). However, our results show that the inversion of the HFFZ took place in two episodes; one that began during the Paleocene (~60 Ma) and at the other which began at the end of the Eocene (~35 Ma). Unlike the first episode that represents the onset of Eurekan Orogeny, the second episode represents post-Eurekan tectonics. Seafloor spreading west of Greenland had ceased by the end of the Eocene, such that the Greenland Plate finally became a part of the North American plate. Consequently, the Eurekan Orogeny had terminated by the end of the Eocene as also pointed out by Piepjohn & von Gosen (2001).

While the end-Eocene cooling and exhumation coincides with the termination of spreading in the Labrador Sea (and hence the end of the Eurekan Orogeny), it also coincides with an important phase of plate reorganization in North-East Atlantic (Gaina *et al.* 2009; 2017), suggesting control by more regional processes. Regional uplift and erosion in North Greenland and on Svalbard that began at the end of the Eocene is synchronous with episodes of exhumation that affected East and West Greenland, far from the Eurekan Orogen (Fig. 6-1). Many other observations show that significant tectonic changes affected Arctic regions around the Eocene–Oligocene transition. For example, late Eocene magmatic activity affected the East Greenland margin (Larsen *et al.* 2014), and uplift of the inner margin of SE Greenland resulted in a strong flux of coarse clastic turbidites during the late Oligocene on the shelf, above a middle Eocene to upper Oligocene hiatus (Larsen *et al.* 1994). Exhumation beginning at the end of the Eocene affected Arctic regions beyond Greenland; e.g. the Sverdrup Basin as well as the Barents Sea, Svalbard and the north slope of Alaska (Embry & Beauchamp 2019; Green & Duddy 2010). All these observations indicate that a deep-

rooted, tectonic process began in the NE Atlantic at the end of the Eocene and subsequent to the Eurekan Orogeny.

The AFTA data from Svalbard reveal major end-Eocene cooling in and around the CTB, but no cooling at that time is detected in samples along the northern coast of Svalbard. Given the small number of samples analysed from Svalbard, the present data coverage is too sparse to make any further conclusions regarding the end-Eocene exhumation.

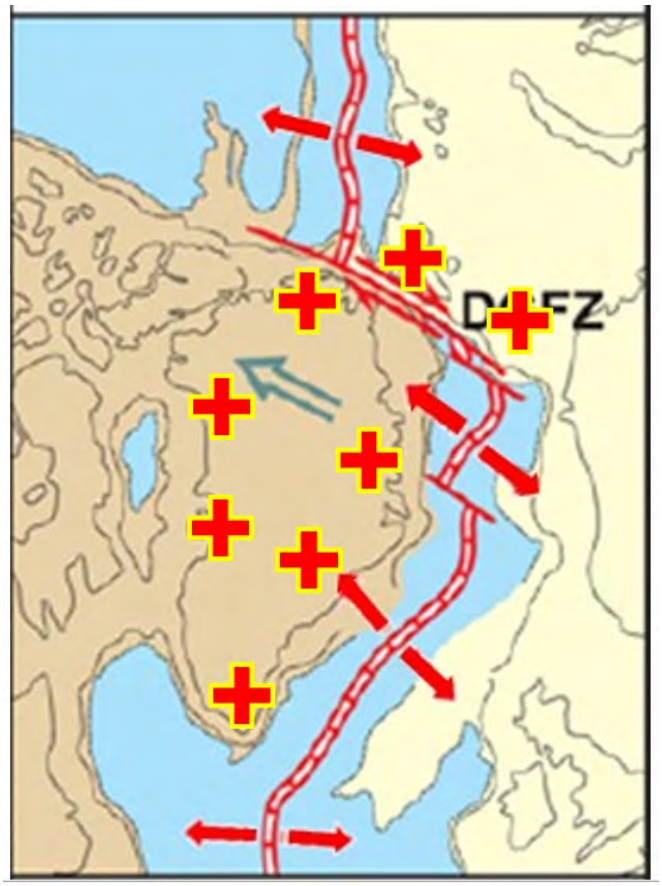

Figure 6-1. Evidence for end-Eocene (~35 Ma) uplift and erosion from AFTA in Greenland, Svalbard and the Barents Sea (crosses). This phase of exhumation coincides with the termination of spreading in the Labrador Sea (and hence the end of the Eurekan Orogeny) and with an important phase of plate reorganization in North-East Atlantic (Gaina *et al.* 2009; 2017). Based on Green & Duddy (2010), Green *et al.* (2014), Japsen *et al.* (2005, 2006, 2014, 2020b) and this study. Map from Fig. 1-2 illustrating the situation at chron C13 when Greenland had become attached to North America.

7. Pre-Eurekan tectonic evolution of the North-East Atlantic region

7.1. Pre-Eurekan palaeo-thermal episodes

This study has resulted in definition of a number of regional cooling episodes in late Paleozoic to late Mesozoic times, with a marked correlation in the timing of events in both North Greenland and Svalbard (Fig. 5-1). Here we compare the timing of these episodes with similar events in North-East Greenland and southern Scandinavia (Fig. 7-1; Japsen *et al.* 2007, 2016, 2018, 2020b).

The constraints on the onset of the **mid-Carboniferous** episode (326–320 Ma) defined in this study are close to those defined for the late Carboniferous episodes in North-East Greenland and southern Scandinavia (320–300 and 314–307 Ma, respectively; Fig. 7-1). It does, however, seem likely that the earlier timing defined in this study represents a tectonic difference between the northern and the southern regions (Fig. 7-2). The mid-Carboniferous episode defined here correlates with the unconformity (~325 Ma; Serpukhovian age) between the Billefjorden and Gipsdalen Groups on Svalbard which reflects major regional uplift (Worsley 2008). In contrast, the timing of the late Carboniferous episode defined in North-East Greenland correlates with a mid-Permian peneplain there that cuts across the late Carboniferous sediments of the Traill Ø Group (>310 Ma; Moscovian age; Stemmerik 2000; Japsen *et al.* 2020b). This unconformity marks the most profound change in tectonic style and overall depositional environment in the post-Caledonian development of East Greenland (Surlyk 1990). In the Oslo Rift, a 'pre-Upper Carboniferous peneplain' separates Upper Carboniferous sediments from folded Cambro-Silurian strata (Larsen *et al.* 2008).

The constraints on the onset of the **Late Triassic** episode (234–229 Ma) defined in this study are slightly younger than those defined for the Middle Triassic episodes in North-East Greenland and southern Scandinavia (~240 and 245–243 Ma, respectively). Again, it is possible that the difference can be attributed to the uncertainty in the definition of these episodes, but a distinct time lag seems likely. On Svalbard, the onset of exhumation corresponds to the base-Carnian unconformity that separates the Sassendalen and Kapp Toscana Groups, reflecting a change in the sedimentary environment from fully marine to near-coastal conditions (Harland 1997; Dallmann *et al.* 2015). Japsen *et al.* (2020b) suggested that the onset of the Middle Triassic exhumation in North-East Greenland and in southern Scandinavia represents manifestations of a common tectonic event at about 245 Ma (Anisian) that resulted in deposition of coarse-grained siliciclastic sediments: the Middle Triassic Pingo Dal Formation in North-East Greenland and the Middle–Upper Triassic Skagerrak Formation (or Hegre Formation) around southern Scandinavia (Berthelsen 1980; Clemmensen 1980; Goldsmith *et al.* 2003). The changes in the depositional systems in the more southernly regions are more drastic than further north and appear not to have a time equivalent counterpart in our study area. Therefore, we suggest that north-south time lag is real, but it is not clear whether the exhumation that affected the study area simply is a delayed

effect of the uplift further south or whether it is a manifestation of a different tectonic process.

Jurassic cooling (beginning 173–150 Ma) in the study area correlates well with Early and Middle Jurassic cooling in North-East Greenland and southern Scandinavia (~180 and 171–154 Ma, respectively). On Svalbard, the onset of this cooling episode corresponds to the regional hiatus of Aalenian–Bajocian age near the top of the Kapp Toscana Group that Dallmann *et al.* (2015) related to a phase of uplift that affected Svalbard and the Barents Sea. This hiatus has counterparts in the Wandel Sea Basin. Japsen *et al.* (2020b) concluded that these southern areas were affected by major uplift and erosion that began at the Early–Middle Jurassic boundary, in agreement with a comparison of the main tectonic events and stratigraphic trends of the same areas (Surlyk & Ineson 2003). We therefore suggest that major uplift and erosion at the Early-Middle Jurassic boundary (~175 Ma) also affected this study area.

The onset of **mid-Cretaceous** cooling (118–95 Ma) in the study area overlaps with similar episodes in North-East Greenland and southern Scandinavia (95–90 and 107–92 Ma, respectively) in the earliest Late Cretaceous, around 95 Ma (Cenomanian–Turonian). This episode corresponds to the earlier part of the base-Paleocene hiatus (late Albian – Maastrichtian) on Svalbard and with the Aptian – mid-Turonian gap at the base of the Upper Cretaceous Herlufsholm Stand Formation on Peary Land. Taken together, these hiati define a common late Albian – mid-Turonian (about 105 – 92 Ma) gap which overlaps with the constraints on the cooling episodes in all three areas illustrated in Fig. 7-1. In North-East Greenland, this episode represents regional exhumation that led to removal of much of post-rift succession that had accumulated above the rift and its margins in North-East Greenland after the rift climax at the Jurassic–Cretaceous transition (Japsen *et al.* 2020b). This phase of uplift and erosion most likely corresponds to the mid-Turonian, erosional base of the Jackson Ø Group that records a phase of basin reorganization (Bjerager *et al.* 2020). In southern Scandinavia, the inversion of the Sorgenfrei-Tornquist Zone began during the mid-Cretaceous episode (Japsen *et al.* 2007).

7.2. Discussion

Japsen *et al.* (2016) provided a synthesis of stratigraphic landscape analysis and AFTA data from the southern Baltic Shield and highlighted the importance of late Carboniferous, Middle Triassic and mid-Jurassic events of uplift and exhumation in this region. But these episodes also affected wide areas beyond the Baltic Shield, and are interpreted as epeirogenic uplifts accompanying fragmentation of Pangaea, caused by accumulation of mantle heat beneath the supercontinent (Nance et al. 2014). Japsen *et al.* (2020b) provided a similar synthesis for North-East Greenland and showed that three episodes of uplift and erosion there were almost synchronous with those defined in southern Scandinavia in agreement with a large body of geological evidence. The observations from North-East Greenland and southern Scandinavia thus point to common tectonic events beginning at ~310, 245 and 175 Ma.

However, the episodes of cooling and exhumation at about these times that affected North Greenland and Svalbard show some variation in timing compared to those further south; i.e. the mid-Carboniferous, Late Triassic and Jurassic episodes (Table 4-01). Evidence from the stratigraphic record indicate that these episodes most likely began at ~325, 235 and 175 Ma. Whereas the mid-Jurassic episode appear to have affected the entire region from Svalbard to southern Sweden simultaneously, there are time lags for the two earlier episodes across the region as discussed in the previous Section. Mid-Carboniferous exhumation affected the northern part of the region about 15 Myr earlier than the late Carboniferous episode in the south, and Late Triassic exhumation affected the northern region about 10 Myr later than the Middle Triassic episode further south. It is, however, not clear whether the time lag from north to south between these earlier episodes of exhumation reflects propagation of the underlying processes or a whether it is a manifestation of different tectonic processes.

As discussed in the previous Section, the onset of the mid-Cretaceous episode in this study area correlates closely with episodes in North-East Greenland and southern Scandinavia, indicating that they all reflect a common episode in the earliest Late Cretaceous, around 95 Ma (Cenomanian–Turonian). In North-East Greenland, this episode corresponds to an important phase of basin reorganization (Bjerager *et al.* 2020; Japsen *et al.* 2020b), and in southern Scandinavia, it represents the inversion of the Sorgenfrei-Tornquist Zone (Japsen *et al.* 2007). This phase of inversion fits into a pattern of intraplate basin inversion and basement thrusting in central Europe that occurred in response to an important change in relative motion between the European and African plates that took place at ~90 Ma (Kley & Voigt 2008). It is possible that these events are related to a global-scale, mid-Cretaceous phase of plate reorganization (105–100 Ma) as suggested by Matthews *et al.* 2012.

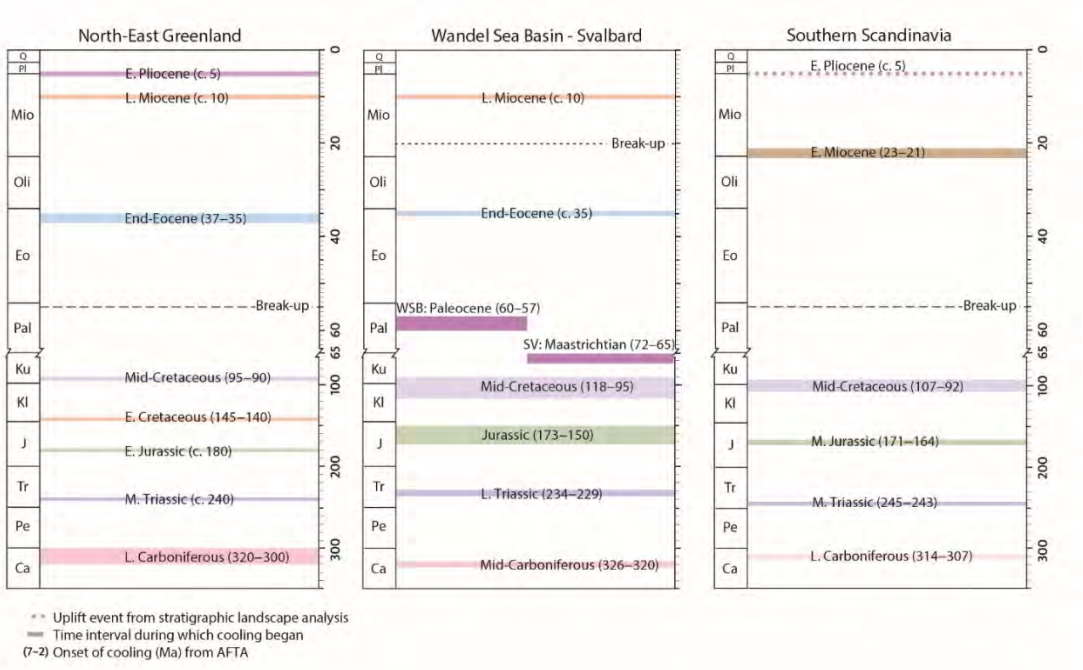

Figure 7-1. Comparison of the timing of regional, post-Devonian episodes of uplift and erosion estimated from AFTA data. **Left**: North-East Greenland (Japsen *et al.* 2020b). **Centre**: Wandel Sea Basin and Svalbard (Table 4-01). **Right**: Southern Scandinavia (Japsen *et al.* 2007, 2016, 2018). Break-up west of Greenland took place in mid-Paleocene (~62 Ma), but sea-floor spreading ceased there by the end of the Eocene in contrast to the opening of the NE Atlantic, east of Greenland, which began at the Paleocene–Eocene transition (~56 Ma) and is still ongoing (Chalmers and Pulvertaft 2001; Oakey and Chalmers 2012; Gaina *et al.* 2017). The Fram Strait between Greenland and Svalbard opened in early Miocene (~20 Ma; Jokat *et al.* 2016; Dumas *et al.* (2020). **L**: Late. **E**: Early. **M**: Mid. **C**: Carboniferous. **Pe**: Permian. **Tr**: Triassic. **J**: Jurassic. **Kl**: Lower Cretaceous. **Ku**: Upper Cretaceous. **Pal**: Paleocene. **Eo**: Eocene. **Oli**: Oligocene. **Mio**: Miocene. **Pl**: Pliocene. **Q**: Quaternary. **SV**: Svalbard. **WSB**: Wandel Sea Basin.

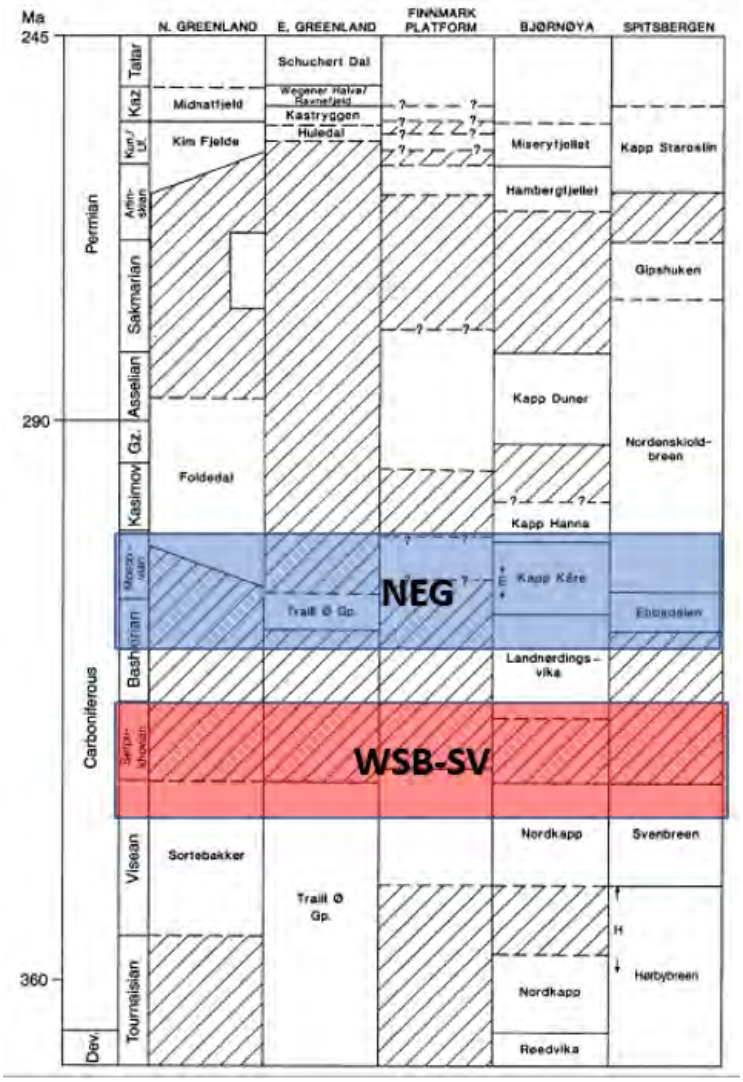

Figure 7-2. Comparison between (1) the major lithostratigraphic units in the North Greenland–Barents Sea–East Greenland (Stemmerik 2000) and (2) the constraints on the onset of the mid-Carboniferous episode (326–320 Ma; red rectangle marked ‘WSB-SV’) defined in this study and those defined for the late Carboniferous episodes in North-East Greenland (320–300 Ma; blue rectangle marked ‘NEG’. See also Figure 7-1.

8. Late Neogene tectonic evolution of the North-East Atlantic region

8.1 North Greenland and Svalbard

The present-day maximum summit level on both sides of the HFFZ is about 1.8 km a.s.l., corresponding broadly to the thickness of the cover needed to explain Miocene palaeotemperatures of ~60°C at sea level on both sides of the fault, as defined by AFTA data from the high mountains north of the fault zone and samples from Herluf Trolle Land. We suggest that the summit level may represent the remnants of a peneplain that was graded to near sea level after end-Eocene exhumation and then uplifted to the level of the present-day summits after ~10 Ma, similar to our interpretation of the landscape development in North-East Greenland (Japsen *et al.* 2020b). If this is so, then the present-day relief must have been shaped by differential uplift and subsequent incision below this peneplain since the late Miocene (Fig. 3-15A illustrates the differential uplift across south-eastern Peary Land). The constant summit level across the HFFZ implies that there was no significant vertical movement along the fault during and after the Miocene tectonic episode, and thus that the offset of end-Eocene palaeotemperatures is due to differential vertical movement across the HFFZ that took place prior to the Miocene erosion that created the peneplain. The most likely time for this offset is the end-Eocene exhumation episode.

Elevated plateaus characterize much of the landscape on Svalbard (Fjellanger & Sørbel 2005; Dallmann *et al.* 2015; Dörr *et al.* 2019). The plateaus occur throughout northern, central and eastern Spitsbergen, as well as on many eastern islands. The plateaus cut across sedimentary rocks of Palaeogene and older age as well as across metamorphic rocks. On northern Spitsbergen, the plateaus are at ~1 km a.s.l., and truncates Devonian sandstones and Precambrian basement below remnants of a once coherent cover of late Miocene lavas (~10 Ma; the Seidfjellet Fm). The lava flows occasionally fill minor river valleys of tens of metres depth, and therefore a low-relief surface with shallow valleys had developed prior to basalt extrusion (Dörr *et al.* 2019). Post-basalt incision up to 800 m deep cuts into the plateau surface and the Miocene volcanics.

The presence of Miocene volcanics on these plateaus on Svalbard, is thus comparable to the extensive elevated planation surfaces in East Greenland, where mid-Miocene basalts rest on the Upper Planation Surface (~2.8 km a.s.l.; 69.2ºN; Storey *et al.* 2004; Bonow *et al.* 2014). This observation thus implies that the Upper Planation Surface in East Greenland had been formed by mid-Miocene times. According to Japsen *et al.* (2014), the Upper Planation Surface was graded to the baselevel of the Atlantic Ocean after end-Eocene uplift and erosion and subsequently raised to its present elevation after uplift that began in the late Miocene at ~10 Ma. Given the synchroneity of uplift episodes in North and East Greenland and Svalbard at 35 and 10 Ma, it therefore seems possible that a similar sequence of events could have shaped the basalt-covered plateau in northern Svalbard. This is supported by the geological observations from Svalbard that the plateaus cut across the Palaeogene sediments in the CTB and that late Miocene lavas rest on the plateaus in northern Svalbard. Accepting this scenario, it appears that the volcanic eruptions are broadly syn-

chronous with uplift of the plateau surface. Dörr *et al.* (2019) also concluded that the present-day elevation of the plateau on northern Svalbard was reached after extrusion of the basalts in the late Miocene. They argued that the surface itself was shaped during early Palaeogene and Miocene stages of exhumation.

In summary, there appear to be a striking similarity between the late Neogene development in North and East Greenland and in Svalbard. Not only in terms of synchronous end-Eocene and late Miocene episodes of uplift and erosion but also in terms of the formation of peneplains graded to the baselevel of the adjacent ocean and their subsequent rise to their present elevation in both regions.

8.2 Morris Jesup Rise and Yermak Plateau

The continental outliers at the Morris Jesup Rise and the Yermak Plateau most likely experienced the phase of uplift and erosion that affected Peary Land at ~35 Ma as they were located north of Peary Land at the end of the Eocene (Fig. 2-5; Kristoffersen *et al.* 2020). As the Fram Strait most likely opened in the early Miocene (Jokat *et al.* 2016; Dumais *et al.* 2020), it is therefore possible that there was sufficient time available for the development of an erosion surface across these continental outliers, similar to the elevated plateaus in North-East Greenland and on Svalbard (Bonow *et al.* 2020; Dörr *et al.* 2019). Such a series of events may explain the flat topography across these features, with the notable difference that the erosion surface across Morris Jesup Rise and the Yermak Plateau subsided below sea level after its formation, whereas the correlative surfaces in Greenland and Svalbard were uplifted after 10 Ma.

8.3 Late Neogene landscape development in the North-East Atlantic region

The late Miocene uplift and erosion (~10 Ma) began at the same time in the study area as in North-East Greenland as well as in other parts of Greenland (Japsen *et al.* 2005, 2006, 2014; Green *et al.* 2014). On both sides of Greenland, this event initiated the formation of the present relief with incision below the uplifted Upper Planation Surface leading to the development of the Lower Planation Surface (Bonow & Japsen 2020). Accordingly, it seems likely that a common process was responsible on both margins. Similarly, Green & Duddy (2010) reported widespread evidence from AFTA for late Neogene cooling over a wide Arctic region.

Japsen *et al.* (2020b) suggested that uplift of onshore Greenland and the subsequent progradation offshore, began during the late Miocene. In support of this, Døssing *et al.* (2016) demonstrated that the onset of mid-late Miocene uplift of North-East Greenland led to formation of a regional, intra-Miocene unconformity offshore North-East Greenland and to massive progradation on the shelf. They found that the correlation between margin uplift and plate motion changes (e.g. accelerated opening of the Fram Strait) indicated that the uplift was triggered by plate tectonic forces. It is therefore, not surprising that the late Mio-

cene episode affected the American and the Eurasian Plates on both sides of the Fram Strait.

Numerical modelling has shown that no ice could build in East Greenland up on the low-lying and almost flat landscape defined by the Upper Planation Surface prior to the late Miocene uplift (Solgaard *et al.* 2013), whereas large amounts of ice may have formed after the late Miocene uplift. This can explain the occurrence of ice-rafted debris in the late Neogene deposits off East Greenland (Larsen *et al.* 1994; Jansen *et al.* 1996). The pronounced late Neogene progradation along the East Greenland margin has been documented by many studies (Clausen 1998; Larsen *et al.* 1994; Hamann *et al.* 2005; Berger & Jokat 2008, 2009; Petersen 2019).

In North-East Greenland, an early Pliocene (~5 Ma) episode of cooling and exhumation has been defined by AFTA data (Japsen *et al.* 2020b). This phase of uplift initiated the formation of the present-day landscape through fluvial and glacial erosion. The mountains of North-East Greenland were therefore formed during three episodes of uplift, end-Eocene, late Miocene and early Pliocene. Knies *et al.* (2014) showed that Pliocene uplift also affected the northern Svalbard based on sedimentological and geochemical data from the Yermak Plateau.

In southern Scandinavia Neogene uplift and erosion began in the early Miocene (23–21 Ma; Japsen *et al.* 2007, 2016, 2018), distinctly earlier than in Greenland (~10 Ma). The mountains of southernmost Norway formed during two steps. First, early Miocene uplift and erosion to the base level led to formation of a peneplain that included the present-day Hardangervidda plateau. Second, early Pliocene uplift raised this peneplain to their present elevation. It is thus possible that the final phase of uplift, in the early Pliocene, affected both Greenland and Scandinavia at about the same time, implying that this phase was caused by the same process(es), of which dynamic support from the Iceland Plume may be one component. In contrast, earlier Cenozoic episodes are out of phase across the Atlantic Ocean (Fig. 7-1). In Greenland, the formation of the dominant peneplain began after uplift in the late Eocene, whereas it began in the early Miocene in southern Norway, and the uplift of these peneplains, which led to the formation of the present-day relief, began in the late Miocene and in the early Pliocene, respectively. In Greenland, the modern relief was formed during late Miocene and early Pliocene uplift, whereas the present-day relief in Norway is the result of early Pliocene uplift and later events (with remnants of older relief above the dominant Miocene peneplain; e.g. Jotunheimen).

8.4 Speculations about the underlying processes

The correlation – and lack of correlation – of uplift events across the North-East Atlantic (Fig. 7-1), invites some speculations about the underlying processes. As noted by Japsen *et al.* (2014), synchroneity between changes in plate motion and uplift events along conjugate margins is suggestive of rapid, far-field transmission of momentum through the upper mantle by viscous stresses (Colli *et al.* 2018), whereas uplift events that have no counterpart on the conjugate margin may be related to transmission of stress within the crust (Cloetingh & Burov 2010).

1) End-Eocene exhumation affected Arctic regions from the Sverdrup Basin to Svalbard and the Barents Sea, and coincides with the cessation of sea-floor spreading west of Greenland and with a major plate reorganization in the North-East Atlantic that was preceded by a significant drop in spreading rates (Gaina *et al.* 2009, 2017; Green & Duddy 2010). Whereas the effects of this phase of uplift and erosion is focussed in and around Greenland, they were only minor in southern Scandinavia (Japsen *et al.* 2018). It is thus possible that the forces driving the uplift were linked with the stress that prevented further movements of the Greenland plate.
2) Regional early Miocene uplift only affected the European side of the North-East Atlantic, and this basic observation led Japsen *et al.* (2016) to suggest that the forces driving the uplift most likely originated from stress transmitted from orogenies elsewhere on the Eurasian plate (Cloetingh & Burov 2010). A possible source for such stress could be the early Miocene–Present Neohimalayan orogenic phase in Himalaya and southern Tibet (Hodges 2000; Jiang & Li 2014). The 'hard' India–Asia collision that occurred around 25–20 Ma initiated this phase and coincides with far-field deformation in central Asia (van Hinsbergen *et al.* 2012). An alternative source for the stress could be the collision between Africa and Eurasia. DeMets *et al.* (2015) estimated that Nubia-Eurasia plate motion decreased by ~50% between 20–18 Ma and 13 Ma.
3) Major late Miocene uplift affected West and East Greenland but not southern Scandinavia. The uplift was triggered by plate tectonic forces (Døssing *et al.* 2016), and we speculate that late Neogene changes in the absolute motion of the North American plate may explain this asymmetric behaviour across the North-East Atlantic. Eurasia/North America and Nubia/North America seafloor spreading rates varied moderately from 20 to ~8 Ma but slowed down by ~20% between 8 and 5 Ma and have remained remarkably steady since then (Merkouriev & DeMets 2008; DeMets *et al.* 2015; Iaffaldano & DeMets 2016). These changes in relative motions were related to a change in the absolute motion of North America and Antarctica, and they might be linked to the late Neogene dynamics of the Pacific plate (Iaffaldano & DeMets 2016).
4) Early Pliocene uplift appear to have affected West and East Greenland as well as southern Scandinavia. In Scandinavia, the magnitude of rock uplift is about 1 km in southern Norway but only 150 m in southern Sweden (Lidmar-Bergström *et al.* 2013; Japsen *et al.* 2016, 2018). In West and East Greenland, the magnitude is typically about 1 km and in central Greenland it is likely to be minimal (Solgaard *et al.* 2013). However, it is about 2 km along Blosseville Kyst, where Greenland is closest to Iceland, and this may indicate support from the Iceland Plume (Rickers *et al.* 2013; Bonow *et al.* 2014; Japsen *et al.* 2014; Steinberger *et al.* 2015). The observation that the margins at both sides of the North-East Atlantic were affected by early Pliocene uplift indicates that this phase may be driven by far-field transmission of momentum through the upper mantle related to the Iceland Plume (Colli *et al.* 2018).

9. Concluding remarks

9.1 Implications for hydrocarbon exploration in the Barents Sea

9.1.1 Review of previous work

It is well known that the Barents Sea has undergone significant amounts of exhumation during Cenozoic times, as evidenced by the lack of post-Cretaceous cover over much of the basin, although debate continues regarding the magnitude and timing of the main phases; see reviews by Cavanagh *et al.* (2006) and Henriksen *et al.* (2011). This is perhaps not surprising because few studies have actually measured the timing of exhumation, relying instead on inference from geological observations such tracing prograding sediment wedges on basin margins. Many studies have also assumed a single dominant episode of exhumation, with most favouring a late Pliocene – Pleistocene timing based on the presence of marginal sedimentary wedges and the common assumption that glaciation could provide a convenient mechanism for exhumation (e.g. Nyland *et al.* 1992; Riis & Fjeldskaar 1992; Cavanagh *et al.* 2006). These issues are of major importance for hydrocarbon exploration, as exhumation can cause breach of seals, loss of charge and remigration (e.g. Doré *et al.* 2002), although uplift, erosion, and pressure release are not necessarily devastating for oil accumulations (Ohm *et al.* 2008).

Geotrack have performed a large number of studies (both proprietary and non-exclusive) of wells from the Barents Sea using AFTA and vitrinite reflectance to directly determine both the timing of exhumation (cooling) and the magnitude of the section removed. Green & Duddy (2010) provided a review of results available at that time. Subsequent work has confirmed the general pattern reported by Green & Duddy (2010) (albeit with some local differences) and the description below is based on their summary illustration, reproduced here as Figure 9-1.

Green & Duddy (2010) reported three major episodes of Cenozoic exhumation which began in the intervals 65 to 55 Ma, 40 to 30 Ma and 10 to 5 Ma. While the two most recent episodes appear to have affected much (if not all) of the basin, the earliest episode was recognized only in wells located in the north-eastern part of the Barents Sea. However, the presence of a major pre-Paleocene unconformity in the Hammerfest Basin in the south-west (Henriksen *et al.* 2011) suggests that the earliest episode also affected that region, but any palaeo-thermal effects were overprinted by the two more recent episodes.

In all cases where palaeotemperature constraints defined from the AFTA and VR data were available over a significant depth interval, the ranges of palaeogeothermal gradients required to explain those constraints were consistent with values similar to present-day values, showing that cooling was due predominantly to exhumation (combined with some degree of climate-related surface cooling).

The case study of Hammerfest Basin well 7120/9-2 reported by Green & Duddy (2010) showed that around 2 km of section had been deposited and removed above the early Paleogene section preserved in this well since the onset of exhumation around the end of the Eocene (although as discussed in Section 4.4.4, this could be decreased by about 500 m if climate cooling is allowed for). Around 1 km was removed during the late Miocene phase of exhumation. Because both phases of exhumation took place within the single unconformity separating Paleogene and Quaternary units in this well, it is not possible to determine how much section was removed in each phase of exhumation, as the amount of reburial, if any, between each phase is not known (Fig. 3-20). This aspect of the results is more pronounced in those north-eastern wells showing all three phases of exhumation, all within a single unconformity.

9.1.2 Comparison with this study

The timing of the three phases of exhumation defined from AFTA in Barents Sea wells are clearly very similar to the phases of exhumation defined in North Greenland and Svalbard in this study. Exhumation beginning at 40–30 Ma and between 10 and 5 Ma closely match the end-Eocene (~35 Ma) and Miocene (11–9 Ma) episodes listed in Table 4-01. Since these episodes are regarded as affecting a very wide area of the North-East Atlantic and Arctic region, we conclude that these exhumation episodes in the Barents Sea also represent manifestations of these mega-regional events.

Recognition of these three episodes highlights the limitations of attempting to define the timing of exhumation from geological evidence alone (see Section 9.1.1), because the sediment packages from earlier episodes will have been disrupted and possibly removed during later phases.

In previous studies, we have assumed that the earliest of the three Cenozoic episodes of exhumation in the Barents Sea represented a similar regional event at ~60 Ma, synchronous with other events around this time in other areas (Green & Duddy 2010). However, based on the results of this study it seems more likely that this episode in the Barents Sea represents the effects of the event responsible for the base-Paleocene unconformity on Svalbard, that is attributed to regional Maastrichtian exhumation.

The scale of all three events defined across Svalbard and the Barents Sea suggests that they are controlled by plate tectonic forces, although as yet a detailed explanation of these events has not been produced. This is important in basin modelling studies that attempts to predict patterns of hydrocarbon prospectivity etc. Studies of this nature tend to seek local influences on thermal history related to well-understood processes (e.g. localized inversion) and may drastically underestimate the amount of heating and cooling which have affected the section.

The occurrence of multiple episodes of exhumation within the last 70 Myr or so is a factor that is not well understood. Current geodynamic models attempt to explain uplift and erosion within the paradigm of dynamic topography related to mantle circulation and plume activity (Wilson *et al.* 2014; Richards *et al.* 2016), but multiple episodes cannot be accom-

modated in such models. This problem is compounded by the realization that prior to the onset of exhumation, the section that was removed must previously have been deposited. Thus, the controlling processes produce both positive and negative vertical motions, and this aspect has not yet been considered in attempts to explain such processes.

9.2 Regional episodes of exhumation and plate-tectonic process

This study has resulted in definition of a series of episodes of km-scale exhumation, which appear to be broadly synchronous, not only between North Greenland and Svalbard but also across a much wider region of the North-east Atlantic and Arctic. The processes responsible are not well understood at present, but a control by plate tectonic processes, including stress build up at plate boundaries during the onset of the Eurekan Orogeny, is well supported by the observations presented here. Late Paleozoic and early Mesozoic events may be related to the break-up of Pangea (Japsen *et al.* 2016).

We interpret Maastrichtian, mid-Paleocene and end-Eocene phases of exhumation, identified in Arctic Canada, North Greenland and Svalbard, as representing events prior to, at the initiation of and following the termination of the Eurekan Orogeny, respectively. No effects can be defined related to the widely accepted times of major phases of the orogeny at 55 Ma and 47 Ma. We suspect that this is because effects at these times are more local and involve smaller amounts of denudation compared to the three phases defined here. The pre- and post-Eurekan events (Maastrichtian and end-Eocene, respectively) are detected over a much wider region compared to the effects of the Eurekan Orogeny itself and appear to share aspects in common with the mega-regional, late Paleozoic and early Mesozoic events mentioned above.

Late Miocene cooling and exhumation defined in North Greenland and Svalbard is regarded as related to the development of the modern-day topography in these areas. Studies in West and East Greenland show that end-Eocene exhumation resulted in peneplains graded to sea level (Bonow *et al.* 2006a,b, 2014; Japsen *et al.* 2006, 2014). These peneplains were uplifted in late Miocene and early Pliocene times and led to the formation of the present-day landscape with elevated plateaus similar to those on northern Svalbard. However, since Miocene cooling is also detected in samples from Barents Sea wells, the situation must be more complicated, since this region has subsided once more following this most recent episode of exhumation. End-Eocene exhumation may explain the flat topography across the continental outliers at the Morris Jesup Rise and the Yermak Plateau that subsided below sea level after 10 Ma, whereas the correlative surfaces in Greenland and Svalbard were uplifted after 10 Ma.

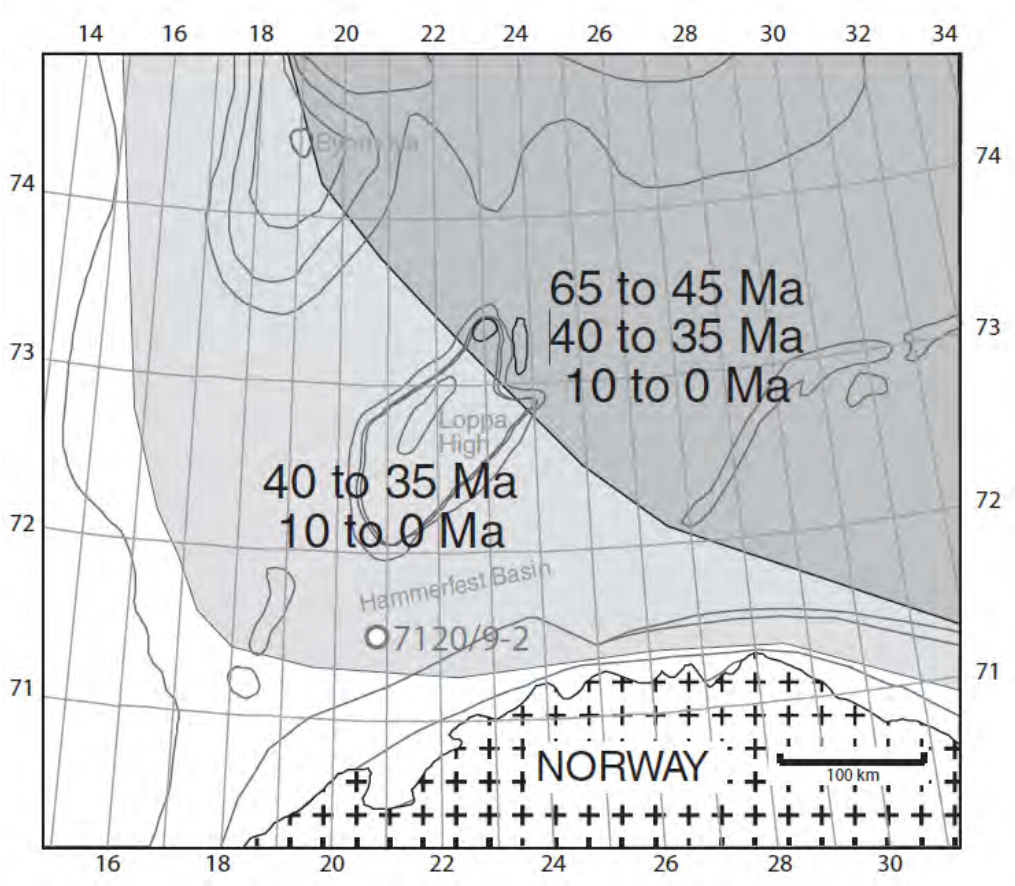

Figure 9-1. Summary of areas of the Barents Sea dominated by different Cenozoic exhumation episodes. From Green & Duddy (2010).

10. References

Abay, T.B., Karlsen, D.A., Pedersen, J.H., Olaussen, S. & Backer-Owe, K. 2017: Thermal maturity, hydrocarbon potential and kerogen type of some Triassic–Lower Cretaceous sediments from the SW Barents Sea and Svalbard. Petroleum Geoscience **24**, 349-373.

Alsen, P., McRoberts, C., Svennevig, K., Bojesen-Koefoed, J., Hovikoski, J. & Piasecki, S. 2017: The Israd Formation: a Middle Triassic Daonella-bearing, black shale unit in Kilen, North Greenland (with a note on the Triassic in Amdrup Land). Newsletters on Stratigraphy 50, 31–46.

Arne, D., Zentilli, M., Grist, A. & Collins, M. 1998: Constraints on the timing of thrusting during the Eurekan orogeny, Canadian Arctic Archipelago: an integrated approach to thermal history analysis. Canadian Journal of Earth Sciences **35**, 30-38.

Arne, D., Grist, A., Zentilli, M., Collins, M., Embry, A. & Gentzis, T. 2002: Cooling of the Sverdrup Basin during Tertiary basin inversion: implications for hydrocarbon exploration. Basin Research 14, 183–205.

Atkinson, D.J. 1963: Tertiary Rocks of Spitsbergen. AAPG Bulletin **47**, 302-323.

Baig, I., Faleide, J.I., Jahren, J. & Mondol, N.H. 2016: Cenozoic exhumation on the southwestern Barents Shelf: Estimates and uncertainties constrained from compaction and thermal maturity analyses. Marine and Petroleum Geology.

Barnes, C.J. & Schneider, D.A. 2019: Late Cretaceous− Paleogene burial and exhumation history of the Southwestern Basement Province, Svalbard, revealed by zircon (U-Th)/He thermochronology. Circum-Arctic Structural Events: Tectonic Evolution of the Arctic Margins and Trans-Arctic Links with Adjacent Orogens **541**, 131.

Berger, D. & Jokat, W. 2008: A seismic study along the East Greenland margin from 72 degrees N to 77 degrees N. Geophysical Journal International **174**, 733-748.

Berger, D. & Jokat, W. 2009: Sediment deposition in the northern basins of the North Atlantic and characteristic variations in shelf sedimentation along the East Greenland margin. Marine and Petroleum Geology **26**, 1321-1337.

Bertelsen, F. 1980: Lithostratigraphy and depositional history of the Danish Triassic: DGU Ser B. **4**. Geological Survey of Denmark Series B. Copenhagen: Geological Survey of Denmark, 1-59.

Bjerager, M., Alsen, P., Hovikoski, J., Lindström, S., Stemmerik, L. & Therkelsen, J. 2019: Triassic lithostratigraphy of the Wandel Sea Basin, North Greenland. Bulletin of the Geological Society of Denmark 67, 83–105.

Bjerager, M., Alsen, P., Bojesen-Koefoed, J., Fyhn, M.B., Hovikoski, J., Ineson, J., Nøhr-Hansen, H., Nielsen, L.H., Piasecki, S. & Vosgerau, H. 2020: Cretaceous lithostratigraphy of North-East Greenland. Bulletin of the Geological Society of Denmark **68**, 37-93.

Blythe, A.E. & Kleinspehn, K.L. 1998: Tectonically versus climatically driven Cenozoic exhumation of the Eurasian plate margin, Svalbard: Fission track analyses. Tectonics **17**, 621-639.

Bonow, J.M. & Japsen, P 2020: Peneplains and tectonics in North-East Greenland after opening of the North-East Atlantic. Geological Survey of Denmark and Greenland Bulletin (*accepted*).

Bonow, J.M., Japsen, P., Lidmar-Bergström, K., Chalmers, J.A., & Pedersen A.K. 2006a: Cenozoic uplift of Nuussuaq and Disko, West Greenland - elevated erosion surfaces as uplift markers of a passive margin. Geomorphology **80**, 325–337.

Bonow, J.M., Lidmar-Bergström, K., & Japsen, P. 2006b: Palaeosurfaces in central West Greenland as reference for identification of tectonic movements and estimation of erosion. Global and Planetary Change **50**, 161–183.

Bonow, J.M., Japsen, P. & Nielsen, T.F.D. 2014: High-level landscapes along the margin of East Greenland – a record of tectonic uplift and incision after breakup in the North-East Atlantic. Global and Planetary Change **116**, 10–29.

Boyd, A. 1990: The Thyra Ø flora: Toward an understanding of the climate and vegetation during the early tertiary in the high arctic. Review of Palaeobotany and Palynology 62, 189–203.

Boyd, A., Håkansson, E. & Stemmerik, L. 1994: Preliminary age considerations and descriptions of the Early Tertiary Thyra Ø flora from eastern North Greenland. Wandel Sea Basin: Basin Analysis, Completion Report to the Ministry of Energy, Scientific Report 15, 32 pp.

Brozena, J., Childers, V., Lawver, L., Gahagan, L., Forsberg, R., Faleide, J. & Eldholm, O. 2003: New aerogeophysical study of the Eurasia Basin and Lomonosov Ridge: Implications for basin development. Geology **31**, 825-828.

Bruhn, R. & Steel, R. 2003: High-resolution sequence stratigraphy of a clastic foredeep succession (Paleocene, Spitsbergen): An example of peripheral-bulge-controlled depositional architecture. Journal of Sedimentary Research **73**, 745-755.

Burden, E.T. & Langille, A. 1990: Stratigraphy and sedimentology of Cretaceous and Paleocene strata in half-grabens on the southeast coast of Baffin Island, Northwest Territories. Bulletin of Canadian Petroleum Geology **38**, 185-196.

Burnham, A.K. and Sweeney, J.J., 1989. A chemical kinetic model of vitrinite reflectance maturation. Geochimica et Cosmochimica Acta. 53, 2649–2657.

Cavanagh, A.J., di Primio, R., Scheck-Wenderoth, M. & Horsfield, B. 2006: Severity and timing of Cenozoic exhumation in the southwestern Barents Sea. Journal of the Geological Society, London **163**, 761-774.

Chalmers, J.A. & Pulvertaft, T.C.R. 2001: Development of the continental margins of the Labrador Sea: a review. In: Wilson, R.C.L., Withmarsh, R.B., Taylor, B. & Froitzheim, N. (eds): Non-volcanic Rifting of Continental Margins: A Comparison of Evidence from Land and Sea. Geological Society Special Publication 187, 77–105.

Cloetingh, S. & Burov, E. 2010: Lithospheric folding and sedimentary basin evolution: a review and analysis of formation mechanisms. Basin Research **23**, 1–34.

Colli, L., Ghelichkhan, S., Bunge, H.-P. & Oeser, J. 2018: Retrodictions of Mid Paleogene mantle flow and dynamic topography in the Atlantic region from compressible high resolution adjoint mantle convection models: Sensitivity to deep mantle viscosity and tomographic input model. Gondwana Research **53**, 252–272.

Clausen, L. 1998: Late Neogene and Quaternary sedimentation on the continental slope and upper rise offshore Southeast Greenland: Interplay of contour and turbidity processes In: Saunders, A.D., Larsen, H.C. & Wise, S.W. (eds): Proceedings of the Ocean Drilling Program, Scientific Results **152**, 3-18.

Clemmensen, L.B. 1980: Triassic rift sedimentation and palaeogeography of central East Greenland. Bull. Grønlands Geol. Unders. **136**.

Croxton, C.A., Dawes, P.R., Soper, N.J. & Thomsen, E. 1980: An occurrence of Tertiary shales from the Harder Fjord Fault, North Greenland fold belt, Peary Land. Rapport Grønlands Geologiske Undersøgelse 101, 61–64.

Dam, G., Pedersen, G.K., Sønderholm, M., Midtgaard, H.H., Larsen, L.M., Nøhr-Hansen, H. & Pedersen, A.K. 2009: Lithostratigraphy of the Cretaceous–Paleocene Nuussuaq Group, Nuussuaq Basin, West Greenland. Geological Survey of Denmark and Greenland Bulletin **19**, 171 pp.

Dallmann, W.K., Andresen, A., Bergh, S.G., Maher jr, H.D. & Ohta, Y. 1993: Tertiary fold-and-thrust belt of Spitsbergen, Svalbard. Norsk Polarinstitut Meddelelser 128, 48 pp, 3 maps.

Dallmann, W., Ohta, Y., Elvevold, S. & Blomeier, D. 2002: Bedrock map of Svalbard and Jan Mayen, Norsk Polarinstitutt Temakart 33. Norwegian Polar Institute, Tromsø.

Dallmann, W. 2015: Geoscience Atlas of Svalbard: Norsk polarinstitutt, 292 pp.

de Paor, D.G., Bradley, D.C., Eisenstadt, G. & Phillips, S.M. 1989: The Arctic Eurekan orogen: A most unusual fold-and-thrust belt. Geological Society of America Bulletin **101**, 952-967.

DeMets, C., Iaffaldano, G. & Merkouriev, S. 2015: High-resolution Neogene and Quaternary estimates of Nubia-Eurasia-North America Plate motion. Geophysical Journal International **203**, 416-427.

Dimakis, P., Braathen, B.I., Faleide, J.I., Elverhøi, A. & Gudlaugsson, S.T. 1998: Cenozoic erosion and preglacial uplift of the Svalbard-Barents Sea region. Tectonophysics **300**, 311-327.

Dixon, J. 1986: Cretaceous to Pleistocene stratigraphy and paleogeography, northern Yukon and northwestern District of Mackenzie. Bulletin of Canadian Petroleum Geology **34**, 49-70.

Doré, A.G., Corcoran, D.V. & Scotchman, I.C. 2002: Prediction of the hydrocarbon system in exhumed basins, and application to the NW European margin. In: Doré, A.G., Cartwright, J.A., Stoker, M.S., Turner, J. & White, N. (eds): Exhumation of the North Atlantic Margin: Timing, Mechanisms and Implications for Petroleum Explorations **196**, 401-429. Geological Society.

Dörr, N., Clift, P.D., Lisker, F. & Spiegel, C. 2012: Why is Svalbard an island? Evidence for subsidence and mantle thermal anomalies. Tectonics.

Dörr, N., Lisker, F., Jochmann, M., Rainer, T., Schlegel, A., Schubert, K. & Spiegel, C. 2018: Subsidence, rapid inversion and slow erosion of the Central Tertiary Basin of Svalbard: Evidence from the thermal evolution and basin modelling. Circum-Arctic Structural Events: Tectonic evolution of the Arctic margins and Trans-Arctic links with adjacent orogens **541**.

Dörr, N., Lisker, F., Piepjohn, K. & Spiegel, C. 2019: Cenozoic development of northern Svalbard based on thermochronological data. Terra Nova **31**, 306-315.

Døssing, A., Stemmerik, L., Dahl-Jensen, T. & Schlindwein, V. 2010: Segmentation of the eastern North Greenland oblique-shear margin — Regional plate tectonic implications. Earth and Planetary Science Letters 292, 239–253.

Døssing, A., Jackson, H.R., Matzka, J., Einarsson, I., Rasmussen, T.M., Olesen, A.V. & Brozena, J.M. 2013: On the origin of the Amerasia Basin and the High Arctic Large Igneous Province-Results of new aeromagnetic data. Earth and Planetary Science Letters **363**, 219-230.

Døssing, A., Japsen, P., Watts, A.B., Nielsen, T., Jokat, W., Thybo, H. & Dahl-Jensen, T. 2016: Miocene uplift of the NE Greenland margin linked to plate tectonics: Seismic evidence from the Greenland Fracture Zone, NE Atlantic. Tectonics **35**, 26 pp.

Dumais, M.A., Olesen, O., Gernigon, L., Johansen, S. & Brönner, M. 2020: Delineating the geological settings of the southern Fram Strait with state-of-the-art aeromagnetic data. NGF Abstracts and Proceedings **2020**, 51.

Elling, F.J., Spiegel, C., Estrada, S., Davis, D.W., Reinhardt, L., Henjes-Kunst, F., Allroggen, N., Dohrmann, R., Piepjohn, K. & Lisker, F. 2016: Origin of bentonites and detrital zircons of the Paleocene Basilika Formation, Svalbard. Frontiers in Earth Science **4**, 73.

Embry, A. & Beauchamp, B. 2019: Sverdrup Basin. In: The Sedimentary Basins of the United States and Canada, 559-592. Elsevier.

Embry, A., Beauchamp, B., Dewing, K. & Dixon, J. 2018: Episodic tectonics in the Phanerozoic succession of the Canadian High Arctic and the “10-million-year flood”. In: Tectonic Evolution of the Arctic Margins and Trans-Arctic Links with Adjacent Orogens. GSA Special Publication **541.**

Engen, Ø., Faleide, J.I. & Dyreng, T.K. 2008: Opening of the Fram Strait gateway: A review of plate tectonic constraints. Tectonophysics **450**, 51-69.

Escher, J.C. & Pulvertaft, T.C.R. 1995: Geological map of Greenland, 1:2 500 000. Copenhagen: Geological Survey of Denmark.

Faleide, J.I., Tsikalas, F., Breivik, A.J., Mjelde, R., Ritzmann, O., Engen, O., Wilson, J. & Eldholm, O. 2008: Structure and evolution of the continental margin off Norway and the Barents Sea. Episodes **31**, 82-91.

Fjellanger, J. & Sorbel, L. 2005: Long-term landscape development of the Coloradofjella plateau, central Spitsbergen, Svalbard. Polar Research **24**, 17-31.

Gaina, C., Gernigon, L. & Ball, P. 2009: Paleocene-Recent plate boundaries in the NE Atlantic and the formation of the Jan Mayen microcontinent. Journal of the Geological Society **166**, 601-616.

Gaina, C., Nasuti, A., Kimbell, G.S. & Blischke, A. 2017: Break-up and seafloor spreading domains in the NE Atlantic. In: Péron-Pinvidic, G., Hopper, J.R., Stoker, M.S., Gaina, C., Doornenbal, J.C., Funck, T. & Arting, U.E. (eds): The NE Atlantic Region: A Reappraisal of Crustal Structure, Tectonostratigraphy and Magmatic Evolution **447**, SP447. 12.

Galbraith, R.F. 2005: Statistics for Fission Track Analysis, 192. Boca Raton, FL, USA: Chapman and Hall/CRC. 192 pp.

Gallagher, K., Hawkesworth, C.J. & Mantovani, M.S.M. 1995: Denudation, fission track analysis and the long-term evolution of passive margin topography: application to the southeast Brazilian margin. Journal of South American Earth Sciences **8**, 65–77.

Gautier, D.L., Stemmerik, L., Christiansen, F.G., Sørensen, K., Bidstrup, T., Bojesen-Koefoed, J.A., Bird, K.J., Charpentier, R.R., Houseknecht, D.W., Klett, T.R., Scheck, C.J. & Tennyson, M.E. 2011: Assessment of NE Greenland: prototype for development of Circum-Arctic Resource Appraisal methodology. In: Spencer, A.M., Embry, A.F., Gautier, D.L., Soupakova, A.V. & Sørensen, K. (eds): Arctic Petroleum Geology Memoirs **35**, 663–672. London: Geological Society.

Gion, A.M., Williams, S.E. & Mueller, R.D. 2017: A reconstruction of the Eurekan Orogeny incorporating deformation constraints. Tectonics **36**, 304–320.

Goldsmith, P., Hudson, G. & Van Veen, P. 2003: Triassic. In: Evans, D., Graham, C., Armour, A. & Bathurst, P. (eds): The millennium atlas: Petroleum geology of the central and northern North Sea: Geological Society (London) **105**, 105-127.

Green P.F. 1986. On the thermo-tectonic evolution of Northern England: evidence from fission track analysis. Geological Magazine **123**, 493 – 506.

Green, P.F. & Duddy, I.R. 2010: Synchronous exhumation events around the Arctic including examples from Barents Sea and Alaska North Slope. In: Vining, B.A. & Pickering, S.C. (eds): Petroleum Geology: From Mature Basins to New Frontiers – Proceedings of the 7th Petroleum Geology Conference, 633-644. London: Geological Society.

Green, P.F. & Duddy, I.R. 2012: Thermal history reconstruction in sedimentary basins using apatite fission-track analysis and related techniques. In: Analyzing the Thermal History of Sedimentary Basins: Methods and Case Studies 103, 65–104.

Green, P. & Duddy, I. 2018: Apatite (U-Th-Sm)/He thermochronology on the wrong side of the tracks. Chemical Geology **488**, 21-33.

Green, P.F., Lidmar-Bergström, K., Japsen, P., Bonow, J.M. & Chalmers, J.A. 2013: Stratigraphic landscape analysis, thermochronology and the episodic development of elevated passive continental margins. Geological Survey of Denmark and Greenland Bulletin **2013/30**, 150 pp.

Green, P.F., Japsen, P., Guarnieri, P. & Nielsen, T.F.D. 2014: Thermal history of outcrop samples from South-East Greenland based on apatite fission-track analysis. In: Stensgaard, B.M. (ed.): South-East Greenland Mineral Endowment Task (SEGMENT), 2014 Workshop Abstract Volume and Status Primo-2014 Abstract Volume (preliminary version). South-East Greenland Workshop, March 27–28 2014, GEUS Copenhagen, 21–25. GEUS.

Green, P.F., Japsen, P., Chalmers, J.A., Bonow, J.M. & Duddy, I.R. 2018: Post-breakup burial and exhumation of passive continental margins: Seven propositions to inform geodynamic models. Gondwana Research 53, 58–81.

Guenthner, W.R., Reiners, P.W., Ketcham, R.A., Nasdala, L. & Giester, G. 2013: Helium diffusion in natural zircon: Radiation damage, anisotropy, and the interpretation of zircon (U-Th)/He thermochronology. American Journal of Science **313**, 145-198.

Håkansson, E. & Pedersen, S.A.S. 1982: Late Paleozoic to Tertiary tectonic evolution of the continental margin in North Greenland. Canadian Society of Petroleum Geologist Memoir **8**, 331–348.

Håkansson, E. & Pedersen, S.A.S. 2001: The Wandel Hav Strike-Slip Mobile Belt — A Mesozoic plate boundary in North Greenland. Bulletin of the Geological Society of Denmark 48, 149–158.

Håkansson, E. & Pedersen, S.A.S. 2015: A healed strike-slip plate boundary in North Greenland indicated through associated pull-apart basins. In: Gibson, B.S., Roure, F. & Manatschal, G. (eds): Sedimentary Basins and Crustal Processes at Continental Margins: From Modern Hyper-extended Margins to Deformed Ancient Analogues 413, 27 pp. London: Geological Society.

Håkansson, E. & Stemmerik, L. 1989: Wandel Sea basin — A new synthesis of the late Paleozoic to Tertiary accumulation in North Greenland. Geology **17**, 683-686.

Håkansson, E., Heinberg, C. & Stemmerik, L. 1991: Mesozoic and Cenozoic history of the Wandel Sea Basin area. North Greenland. Bulletin Grønlands Geologiske Undersøgelse 160, 153–164.

Hamann, N.E., Whittaker, R.C. & Stemmerik, L. 2005: Geological development of the Northeast Greenland Shelf. In: Doré, A.G. & Vining, B. (eds): Petroleum Geology: North-West Europe and Global Perspectives-Proceedings of the 6th Petroleum Geology Conference 887-902. Geological Society, London.

Harland, W.B. 1997: Svalbard. Geological Society, London, Memoirs **17**.

Harrison, J. 2008: Regional variation in structural style, deformation kinematics, and summary of tectonic history, northeast Ellesmere Island. Geological Survey of Canada Bulletin **592**, 245-284.

Harrison, J.C., Mayr, U., McNeil, D.H., Sweet, A.R., McIntyre, D.J., Eberle, J.J., Harington, C.R., Chalmers, J.A., Dam, G. & Nøhr-Hansen, H. 1999: Correlation of Cenozoic sequences of the Canadian Arctic region and Greenland; implications for the tectonic history of northern North America. Bulletin of Canadian Petroleum Geology **47**, 223-254.

Helland-Hansen, W. & Grundvåg, S.A. 2020: The Svalbard Eocene-Oligocene (?) Central Basin succession: Sedimentation patterns and controls. Basin Research.

Henriksen, E., Bjørnseth, H., Hals, T., Heide, T., Kiryukhina, T., Kløvjan, O., Larssen, G., Ryseth, A., Rønning, K. & Sollid, K. 2011: Uplift and erosion of the greater Barents Sea: impact on prospectivity and petroleum systems. Geological Society, London, Memoirs **35**, 271-281.

Hodges, K.V. 2000: Tectonics of the Himalaya and southern Tibet from two perspectives. Geological Society of America Bulletin **112**, 324–350.

Holford, S.P., Green, P.F., Hillis, R.R., Underhill, J.R., Stoker, M. & Duddy, I.R. 2010: Multiple post-Caledonian exhumation episodes across NW Scotland revealed by apatite fission-track analysis. Journal of the Geological Society, London **167**, 675-694.

Hopper, J.R., Funck, T., Stoker, M., Arting, U., Peron-Pinvidic, G., Doornenbal, H. & Gaina, C. (eds). 2014: Tectonostratigraphic Atlas of the North-East Atlantic Region, Geological Survey of Denmark and Greenland. Copenhagen, Denmark.

Hovikoski, J., Pedersen, G.K., Alsen, P., Lauridsen, B.W., Svennevig, K., Nøhr-Hansen, H., Sheldon, E., Dybkjær, K., Bojesen-Koefoed, J. & Piasecki, S. 2018: The Jurassic–Cretaceous lithostratigraphy of Kilen, Kronprins Christian Land, eastern North Greenland. Bulletin of the Geological Society of Denmark, 66, 61–112.

Iaffaldano, G. & DeMets, C. 2016: Late Neogene changes in North America and Antarctica absolute plate motions inferred from the Mid-Atlantic and Southwest Indian Ridges spreading histories. Geophysical Research Letters **43**, 8466–8472.

Indrevær, K., Gabrielsen, R.H. & Faleide, J.I. 2016: Early Cretaceous synrift uplift and tectonic inversion in the Loppa High area, southwestern Barents Sea, Norwegian shelf. Journal of the Geological Society **174**, 242-254.

Jansen, E., Raymo, M. & Blum, P. 1996: Proceedings, initial reports, Ocean Drilling Program, Leg 162, North Atlantic-Arctic gateways II. In, 345-387. College Station: ODP Texas A and M University.

Japsen, P., Green, P.F. & Chalmers, J.A. 2005: Separation of Palaeogene and Neogene uplift on Nuussuaq, West Greenland. Journal of the Geological Society, London **162**, 299-314.

Japsen, P., Bonow, J.M., Green, P.F., Chalmers, J.A. & Lidmar-Bergström, K. 2006: Elevated, passive continental margins: Long-term highs or Neogene uplifts? New evidence from West Greenland. Earth and Planetary Science Letters 248, 315–324.

Japsen, P., Green, P.F., Nielsen, L.H., Rasmussen, E.S. & Bidstrup, T. 2007: Mesozoic-Cenozoic exhumation events in the eastern North Sea Basin: a multi-disciplinary study based on palaeothermal, palaeoburial, stratigraphic and seismic data. Basin Research **19**, 451-490.

Japsen, P., Green, P.F., Bonow, J.M., Nielsen, T.F.D. & Chalmers, J.A. 2014: From volcanic plains to glaciated peaks: Burial and exhumation history of southern East Greenland after opening of the North-East Atlantic. Global and Planetary Change **116**, 91–114.

Japsen, P., Green, P.F., Bonow, J.M. & Erlström, M. 2016: Episodic burial and exhumation of the southern Baltic Shield: Epeirogenic uplifts during and after break-up of Pangea. Gondwana Research **35**, 357-377.

Japsen, P., Bonow, J.M. & Green, P.F. 2017: Burial, uplift and exhumation history of the continental margins onshore and offshore of Labrador and Newfoundland. Final report. GEUS Report **2017/23**.

Japsen, P., Green, P.F., Chalmers, J.A. & Bonow, J.M. 2018: Mountains of southernmost Norway: uplifted Miocene peneplains and re-exposed Mesozoic surfaces. Journal of the Geological Society, London **157**, 721-741.

Japsen, P., Green, P.F. & Chalmers, J.A. 2020a: Thermo-tectonic history of the Wandel Sea Basin, North Greenland. GEUS Bulletin.

Japsen, P., Green, P.F., Bonow, J.M., Bjerager, M. & Hopper, J.R. 2020b: Episodic burial and exhumation in North-East Greenland before and after opening of the North-East Atlantic. GEUS Bulletin.

Japsen, P., Green, P.F. & Chalmers, J.A: 2020c: Thermo-tectonic development of the Wandel Sea Basin, North Greenland. Nordic Geological Winter Meeting, Oslo, 8-10 January 2020.

Jiang, X.-D. & Li, Z.-X. 2014: Seismic reflection data support episodic and simultaneous growth of the Tibetan Plateau since 25 Myr. Nature Communications, DOI: 10.1038/ncomms6453.

Jokat, W., Lehmann, P., Damaske, D. & Nelson, J.B. 2016: Magnetic signature of North-East Greenland, the Morris Jesup Rise, the Yermak Plateau, the central Fram Strait: constraints for the rift/drift history between Greenland and Svalbard since the Eocene. Tectonophysics **691**, 98-109.

Jones, M. T., L. E. Augland, G. E. Shephard, S. D. Burgess, G. T. Eliassen, M. M. Jochmann, B. Friis, D. A. Jerram, S. Planke and H. H. Svensen 2017: Constraining shifts in North Atlantic plate motions during the Palaeocene by U-Pb dating of Svalbard tephra layers. Scientific reports **7**. DOI:10.1038/s41598-017-06170-7

Kley, J. & Voigt, T. 2008: Late Cretaceous intraplate thrusting in central Europe: Effect of Africa-Iberia-Europe convergence, not Alpine collision. Geology **36**, 839-842.

Knies, J., Mattingsdal, R., Fabian, K., Grøsfjeld, K., Baranwal, S., Husum, K., De Schepper, S., Vogt, C., Andersen, N., Matthiessen, J., Andreassen, K., Jokat, W., Nam, S.-I. & Gaina, C. 2014: Effect of early Pliocene uplift on late Pliocene cooling in the Arctic–Atlantic gateway. Earth and Planetary Science Letters **387**, 132-144.

Knudsen, C., Hopper, J.R., Bierman, P.R., Bjerager, M., Funck, T., Green, P.F., Ineson, J.R., Japsen, P., Marcussen, C., Sherlock, S.C. & Thomsen, T.B. 2017: Samples from the Lomonosov Ridge place new constraints on the geological evolution of the Arctic Ocean. Geological Society, London, Special Publications **460**.Kristoffersen, Y., Otha, Y. & Hall, J. 2020: On the origin of the Yermak Plateau north of Svalbard, Arctic Ocean. NORWEGIAN JOURNAL OF GEOLOGY.

Kristoffersen, Y., Otha, Y. & Hall, J. 2020: On the the origin of the Yermak Plateau north of Svalbard, Arctic Ocean. Norwegian Journal of Geology.

Ktenas, D., Henriksen, E., Meisingset, I., Nielsen, J.K. & Andreassen, K. 2017: Quantification of the magnitude of net erosion in the southwest Barents Sea using sonic velocities and compaction trends in shales and sandstones. Marine and Petroleum Geology **88**, 826-844.

Larsen, B.T., Olaussen, S., Sundvoll, B. & Heeremans, M. 2008: The Permo-Carboniferous Oslo Rift through six stages and 65 million years. Episodes **31**, 52.

Larsen, H.C., Saunders, A.D., Clift, P.D., Beget, J., Wei, W. & Spezzaferri, S. 1994: Seven million years of glaciation in Greenland. Science **264**, 952-955.
Lidmar-Bergström, K., Bonow, J.M. & Japsen, P. 2013: Stratigraphic landscape analysis and geomorphological paradigms: Scandinavia as an example of Phanerozoic uplift and subsidence. Global and Planetary Change **100**, 153-171.
Løseth, H., Lippard, S.J., Saettem, J., Fanavoll, S., Fjerdingstad, V., Leith, T.L., Ritter, U., Smelror, M. & Sylta, O. 1993: Cenozoic uplift and erosion of the Barents Sea; evidence from the Svalis Dome area. In, 643-664.
Lüthje, C.J., Milàn, J. & Hurum, J.r.H. 2010: Paleocene tracks of the mammal pantodont genus Titanoides in coal-bearing strata, Svalbard, Arctic Norway. Journal of Vertebrate Paleontology **30**, 521-527.
Lyck, J.M. & Stemmerik, L. 2000: Palynology and depositional history of the Paleocene? Thyra Ø Formation, Wandel Sea Basin, eastern North Greenland. Geology of Greenland Survey Bulletin 187, 21–49.
Maher, H.D., Braathen, A., Bergh, S., Dallmann, W. & Harland, W.B. 1995: Tertiary or Cretaceous age for Spitsbergen's fold-thrust belt on the Barents Shelf. Tectonics 14, 1321–1326.
Maher, J., Harmon D 2001: Manifestations of the Cretaceous High Arctic large igneous province in Svalbard. The Journal of Geology **109**, 91-104.
Manum, S.B. & Throndsen, T. 1977: Rank of coal and dispersed organic matter and its geological bearing in the Spitsbergen Tertiary. Norsk Polarinstitutt Årbok **1977**, 159-177.
Marshall, C., Uguna, J., Large, D.J., Meredith, W., Jochmann, M., Friis, B., Vane, C., Spiro, B.F., Snape, C.E. & Orheim, A. 2015: Geochemistry and petrology of Paleocene coals from Spitzbergen—Part 2: Maturity variations and implications for local and regional burial models. International Journal of Coal Geology **143**, 1-10.
Matthews, K.J., Seton, M. & Müller, R.D. 2012: A global-scale plate reorganization event at 105−100 Ma. Earth and Planetary Science Letters **355–356**, 283-298.
McWhae, J. 1981: Structure and spreading history of the northwestern Atlantic region from the Scotian Shelf to Baffin Bay. In: Geology of the North Atlantic Borderlands Canadian Society of Petroleum Geologists Memoir, 299-332.
Merkouriev, S. & DeMets, C. 2008: A high-resolution model for Eurasia–North America plate kinematics since 20 Ma. Geophysical Journal International **173**, 1064-1083.
Miall, A.D. 1986: The Eureka Sound Group (Upper Cretaceous - Oligocene), Canadian arctic islands. Bulletin of Canadian Petroleum Geology **34**, 240-270.
Nance, R.D., Murphy, J.B. & Santosh, M. 2014: The supercontinent cycle: A retrospective essay. Gondwana Research **25**, 4-29.
Nøhr-Hansen, H., Nielsen, L.H., Sheldon, E., Hovikovski, J. & Alsen, P. 2011: Palaeogene deposits in north-east Greenland. Geological Survey of Denmark and Greenland Bulletin **23**, 61–64.
Nøttvedt, A. 1985: Askeladden Delta Sequence (Palaeocene) on Spitsbergen—sedimentation and controls on delta formation. Polar Research **3**, 21-48.
Nyland, B., Jensen, L.N., Skagen, J.I., Skarpnes, O. & Vorren, T.O. 1992: Tertiary uplift and erosion in the Barents Sea; magnitude, timing and consequences. In: Larsen, R.M., Brekke, H., Larsen, B.T. & Telleraas, E. (eds): Structural and tectonic modelling and its application to petroleum geology **1**, 153-162. Amsterdam: Elsevier.
Oakey, G.N. & Chalmers, J.A. 2012: A new model for the Paleogene motion of Greenland relative to North America: Plate reconstructions of the Davis Strait and Nares Strait regions between Canada and Greenland. Journal of Geophysical Research-Solid Earth 117, 1–28.
Ohm, S.E., Karlsen, D.A. & Austin, T.J.F. 2008: Geochemically driven exploration models in uplifted areas: Examples from the Norwegian Barents Sea. AAPG Bulletin **92**, 1191-1223.
Okulitch, A. & Trettin, H. 1991: Late Cretaceous–Early Tertiary deformation, Arctic Islands. Geology of the Innuitian Orogen and Arctic Platform of Canada and Greenland. Geological Survey of Canada, Geology of Canada 3, 469–490.

Paech, H.-J. & Estrada, S. 2018: Coal rank data and tectonic structure of Mesozoic and Paleogene sediments in North Greenland. In: Piepjohn, K., Strauss, J.V., Reinhardt, L. & McClelland, W.C. (eds): Tectonic Evolution of the Arctic Margins and Trans-Arctic Links with Adjacent Orogens 541: Geological Society of America.

Pedersen, G.K., Lauridsen, B.W., Svennevig, K., Bojesen-Koefoed, J.A., Nøhr-Hansen, H. & Alsen, P. 2018: Burial history of a folded cretaceous succession–A case study from the southern part of Kilen, eastern north Greenland. Cretaceous Research 89, 22–35.

Petersen, T.G., Thomsen, T., Olaussen, S. & Stemmerik, L. 2016: Provenance shifts in an evolving Eurekan foreland basin: the Tertiary Central Basin, Spitsbergen. Journal of the Geological Society **173**, 634-648.

Petersen, T.G. 2019: Seismic stratigraphy of the post-breakup succession offshore Northeast Greenland: Links to margin uplift. Marine and Petroleum Geology.

Piasecki, S., Nøhr-Hansen, H. & Dalhoff, F. 2018: Revised stratigraphy of Kap Rigsdagen beds, Wandel Sea Basin, North Greenland. Newsletters on Stratigraphy 51, 411–425.

Piepjohn, K. & von Gosen, W. 2001: Polyphase deformation at the Harder Fjord Fault Zone (North Greenland). Geological Magazine 138, 407–434.

Piepjohn, K., von Gosen, W., Tessensohn, F., Reinhardt, L., McClelland, W.C., Dallmann, W., Gaedicke, C. & Harrison, J.C. 2015: Tectonic map of the Ellesmerian and Eurekan deformation belts on Svalbard, north Greenland, and the Queen Elizabeth Islands (Canadian Arctic). arktos **1**, 12.

Piepjohn, K., von Gosen, W. & Tessensohn, F. 2016: The Eurekan deformation in the Arctic: an outline. Journal of the Geological Society, London 173, 1007–1024.

Praeg, D., Stoker, M.S., Shannon, P.M., Ceramicola, S., Hjelstuen, B.O., Laberg, J.S. & Mathiesen, A. 2005: Episodic Cenozoic tectonism and the development of the NW European 'passive' continental margin. Marine and Petroleum Geology **22**, 977-1005.

Richards, F., Hoggard, M. & White, N. 2016: Cenozoic epeirogeny of the Indian peninsula. Geochemistry, Geophysics, Geosystems.

Richardsen, G., Vorren, T.O. & Torudbakken, B.O. 1993: Post-Early Cretaceous uplift and erosion in the southern Barents Sea – A discussion based on analysis of seismic interval velocities. Norsk Geologisk Tidsskrift **73**, 3-20.

Rickers, F., Fichtner, A. & Trampert, J. 2013: The Iceland–Jan Mayen plume system and its impact on mantle dynamics in the North Atlantic region: Evidence from full-waveform inversion. Earth and Planetary Science Letters **367**, 39-51.

Ricketts, B.D. 1994: Basin analysis, Eureka Sound Group, Axel Heiberg and Ellesmere Islands, Canadian Arctic archipelago. Geological Survey of Canada Memoir 439.

Riis, F. & Fjeldskaar, W. 1992: On the magnitude of the late Tertiary and Quaternary erosion and its significance for the uplift of Scandinavia and the Barents Sea. In: Larsen, R.M., Brekke, H., Larsen, B.T. & Telleraas, E. (eds): Structural and tectonic modelling and its application to petroleum geology 1, 163-185. Amsterdam: Elsevier.

Ritter, U., Duddy, I.R., Mork, A., Johansen, H. & Arne, D.C. 1996: Temperature and uplift history of Bjørnoya (Bear Island), Barents Sea. Petroleum Geoscience **2**, 133-144.

Sætre, C. 2011: Development of Hollendardalen Formation (Svalbard); with emphasis on sedimentological and petrographical analysis, PhD. Thesis, University of Oslo.

Schneider, D.A., Faehnrich, K., Majka, J. & Manecki, M. 2018: 40Ar/39Argeochronologic evidence of Eurekan deformation within the West Spitsbergen Fold and Thrust Belt. Circum-Arctic Structural Events: Tectonic Evolution of the Arctic Margins and Trans-Arctic Links with Adjacent Orogens **541**.

Skilbrei, J.R. 1998: On the late Cenozoic uplift of Svalbard. Global and Planetary Change.

Solgaard, A.M., Bonow, J.M., Langen, P., Japsen, P. & Hvidberg, C. 2013: Mountain building and the initiation of the Greenland ice sheet. Palaeogeography Palaeoclimatology Palaeoecology **392**, 161-176.

Steel, R., J. Gjelberg, W. Helland-Hansen, K. Kleinspehn, A. Nøttvedt and M. Rye-Larsen (1985). The Tertiary strike-slip basins and orogenic belt of Spitsbergen. In: Biddle, K.T. & Christle-Blick. K. (eds) Strike-Slip Deformation, Basin Formation, and Sedimentation, The Society of Economic Paleontologists and Mineralogists (SEPM). SP37: 339–359.

Steinberger, B., Spakman, W., Japsen, P. & Torsvik, T.H. 2015: The key role of global solid-Earth processes in preconditioning Greenland's glaciation since the Pliocene. Terra Nova **27**, 1–8.

Stemmerik, L. 2000: Late Palaeozoic evolution of the North Atlantic margin of Pangea. Palaeogeography, Palaeoclimatology, Palaeoecology 161, 95–126.

Stemmerik, L. & Worsley, D. 2005: 30 years on-Arctic Upper Palaeozoic stratigraphy, depositional evolution and hydrocarbon prospectivity. Norwegian Journal of Geology/Norsk Geologisk Forening 85, 151–168.

Stemmerik, L., Dalhoff, F., Larsen, B.D., Lyck, J.M., Mathiesen, A. & Nilsson, I. 1998: Wandel Sea Basin, eastern North Greenland. Geology of Greenland Survey Bulletin **180**, 55–62.

Stoker, M.S., Praeg, D., Shannon, P.M., Hjelstuen, B.O., Laberg, J.S., Nielsen, T., van Weering, T.C.E., Sejrup, H.P. & Evans, D. 2005: Neogene evolution of the Atlantic continental margin of NW Europe Lofoten Islands to SW Ireland: anything but passive. In: Doré, A.G. & Vining, B.A. (eds.). Petroleum geology: North-West Europe and global perspectives. Proceedings of the 6th Petroleum Geology Conference, 1057–1076. London. Geological Society.

Storey, M., Pedersen, A.K., Stecher, O., Bernstein, S., Larsen, H.C., Larsen, L.M., Baker, J.A. & Duncan, R.A. 2004: Long-lived postbreakup magmatism along the East Greenland margin: Evidence for shallow-mantle metasomatism by the Iceland plume. Geology **32**, 173–176.

Surlyk, F. 1990: Timing, style and sedimentary evolution of Late Palaeozoic - Mesozoic extensional basins in East Greenland. In: Hardman, R.F.P. & Brooks, J. (eds): Tectonic Events Responsible for Britain's Oil and Gas Reserves **55**, 107-125.

Surlyk, F. & Ineson, J. 2003: The Jurassic of Denmark and Greenland: key elements in the reconstruction of the North Atlantic Jurassic rift system. In: Ineson, J. & Surlyk, F. (eds): The Jurassic of Denmark and Greenland **1**, 9-20.

Svennevig, K., Guarnieri, P. & Stemmerik, L. 2016: Tectonic inversion in the Wandel Sea Basin: A new structural model of Kilen (eastern North Greenland). Tectonics 35, 2896–2917. doi:10.1002/2016TC004152.

Svennevig, K., Guarnieri, P. & Stemmerik, L. 2017: 3D restoration of a Cretaceous rift basin in Kilen, eastern North Greenland. Norwegian Journal of Geology/Norsk Geologisk Forening 97, 21–32. https://dx.doi.org/10.17850/njg97-1-02.

Svennevig, K., Alsen, P., Guarnieri, P., Hovikoski, J., Lauridsen, B.W., Pedersen, G.K., Nøhr-Hansen, H. & Sheldon, E. 2018: Descriptive text to the Geological map of Greenland, 1: 100 000, Kilen 81 Ø. 1 Syd. Geological Survey of Denmark and Greenland Map Series 8, 29 pp + map.

Tegner, C., Storey, M., Holm, P.M., Thorarinsson, S.B., Zhao, X., Lo, C.H. & Knudsen, M.F. 2011: Magmatism and Eurekan deformation in the High Arctic Large Igneous Province: 40Ar-39Ar age of Kap Washington Group volcanics, North Greenland. Earth and Planetary Science Letters 303, 203–214.

Tessensohn, F. & Piepjohn, K. 2000: Eocene compressive deformation in Arctic Canada, North Greenland and Svalbard and its plate tectonic causes. Polarforschung **68**, 121-124.

Thorarinsson, S.B., Holm, P.M., Tappe, S., Heaman, L.M. & Tegner, C. 2011: Late Cretaceous-Palaeocene continental rifting in the High Arctic: U-Pb geochronology of the Kap Washington Group volcanic sequence, North Greenland. Journal of the Geological Society, London **168**, 1093-1106.

Underhill, J.R. & Partington, M.A. 1993: Jurassic thermal doming and deflation in the North Sea: implications of the sequence stratigraphic evidence. In: Parker, J.R. (ed.): Pe-

troleum Geology of North West Europe, Proceedings of the 4th Conference, 337-345. London: Geological Society.
Vågnes, E., Faleide, J.I. & Gudlaugsson, S.T. 1992: Glacial erosion and tectonic uplift in the Barents Sea. Norsk Geologisk Tidsskrift 72, 333-338.
Vamvaka, A., Pross, J., Monien, P., Piepjohn, K., Estrada, S., Lisker, F. & Spiegel, C. 2019: Exhuming the top end of North America: episodic evolution of the Eurekan belt and its potential relationships to North Atlantic plate tectonics and Arctic climate change. Tectonics.
van Hinsbergen, D.J.J., Lippert, P.C., Dupont-Nivet, G., McQuarrie, N., Doubrovine, P.V., Spakman, W. & Torsvik, T.H. 2012: Greater India Basin hypothesis and a two-stage Cenozoic collision between India and Asia. Proceedings of the National Academy of Sciences of the United States of America **109**, 7659–7664.
von Gosen, W. & Piepjohn, K. 2003: Eurekan transpressive deformation in the Wandel Hav Mobile Belt (northeast Greenland). Tectonics 22, 28 pp. doi:10.1029/2001TC901040,
Vorren, T.O., Richardsen, G., Knutsen, S.M. & Henriksen, E. 1991: Cenozoic erosion and sedimentation in the western Barents Sea. Marine and Petroleum Geology **8**, 317-340.
Wilson, J.W.P., Roberts, G.G., Hoggard, M.J. & White, N.J. 2014: Cenozoic epeirogeny of the Arabian Peninsula from drainage modeling. Geochemistry, Geophysics, Geosystems **15**, 3723-3761.
Worsley, D. 2008: The post-Caledonian development of Svalbard and the western Barents Sea. Polar Research **27**, 298-317.
Zattin, M., Andreucci, B., de Toffoli, B., Grigo, D. & Tsikalas, F. 2016: Thermochronological constraints to late Cenozoic exhumation of the Barents Sea Shelf. Marine and Petroleum Geology **73**, 97-104.